

Conditional Guide RNAs: Programmable Conditional
Regulation of CRISPR/Cas Function via Dynamic RNA
Nanotechnology

Thesis by
Mikhail Henning Hanewich-Hollatz

In Partial Fulfillment of the Requirements for the
Degree of
Doctor of Philosophy

The logo for the California Institute of Technology (Caltech), featuring the word "Caltech" in a bold, orange, sans-serif font.

CALIFORNIA INSTITUTE OF TECHNOLOGY
Pasadena, California

2020
Defended June 19, 2019

© 2020

Mikhail Henning Hanewich-Hollatz

ORCID: 0000-0002-5369-3846

All rights reserved except where otherwise noted

ACKNOWLEDGEMENTS

I would like to thank my advisor, Niles Pierce, for his support and guidance since joining his group in 2013. Throughout my tenure, Niles has taught me by example that taking on a difficult challenge is worthwhile in the pursuit of a powerful idea, and that being meticulous in the understanding and framing of a problem deserves the time it takes. I would also like to thank my thesis committee, Erik Winfree, Richard Murray, Michael Elowitz, and Mikhail Shapiro, for their thoughts on the present and future of conditional guide RNAs. My time in the Pierce Lab would not have been the same without the intelligent and kind people I have had the opportunity to work with; thank you to Lisa Hochrein for her mentorship when I first joined the lab, to Naeem Husain for his friendship and guidance, to Nick Porubsky for his patience in helping me to get the most out of NUPACK, to my coauthors Zhewei Chen and Jining Huang, and to all of the other members of the Pierce Lab.

On my path to graduate school, I have had the good fortune of encountering several people who took the time to mentor me, without whom I would not have found myself at Caltech. Thank you especially to Santiago Faucher, Suman Bose, Pedro Valencia, Rohit Karnik, and Paul Rothemund for teaching me how to carry out the day to day of experimental research, and for serving as exemplary role models for how science should be carried out.

The friends at Caltech who have grown with me, helped me through, or otherwise made my time here worthwhile are too many to adequately acknowledge, but here are a few of their names: Arash, Brett, Dan, Eduardo, Ingmar, Jacques, Jee, Jeff, Lincoln, Lorinda, Luke, Marilena, Matt, Michael, Naeem, Nathan, Rachel, Sarah, Stefan, Teddy, Thom, Vanessa, Vatsal, Will. Thank you.

I thank my brother Andreas for leading the way, and for being a reliable source of compelling conversation and lateral thinking.

Finally, I would like to thank my parents, Kim Hanewich and Henning Hollatz. They taught me to love the world I see, inspiring a keen interest in a mechanistic understanding of minutia and an appreciation for the beauty that emerges. My upbringing provided important lessons in self-reliance and a confidence in my ability to take on whatever comes my way, traits that have certainly been essential (and thoroughly tested) in my graduate school experience. Perhaps most importantly, my parents were uncompromising in their encouragement and support of my pursuing

all that fascinated me, which (it turns out) can be an awful lot, and for that I am immensely grateful.

ABSTRACT

A guide RNA (gRNA) directs the function of a CRISPR protein effector to a target gene of choice, providing a versatile programmable platform for engineering diverse modes of synthetic regulation (edit, silence, induce, bind). However, the fact that gRNAs are constitutively active places limitations on the ability to confine gRNA activity to a desired location and time. To achieve programmable control over the scope of gRNA activity, here we apply principles from dynamic RNA nanotechnology to engineer conditional guide RNAs (cgRNAs) whose activity is dependent on the presence or absence of an RNA trigger. These cgRNAs are programmable at two levels, with the trigger-binding sequence controlling the scope of the effector activity and the target-binding sequence determining the subject of the effector activity. There are two possible logical directions for single-input cgRNAs: constitutively active cgRNAs that are conditionally inactivated by an RNA trigger (ON→OFF logic) and constitutively inactive cgRNAs that are conditionally activated by an RNA trigger (OFF→ON logic). Using an in vitro assay for cgRNA activity with synthetic trigger, in vitro transcribed cgRNA, and recombinant dCas9, we observe a conditional (ON→OFF logic) response for a set of four allosteric constitutively active cgRNAs with a median $\approx 6\%$ crosstalk between noncognate cgRNA/trigger pairs. Motivated by the observed lack of conditional response of this mechanism when ported to *E. coli*, we describe a systematic study of unstructured sequence inserts into the standard gRNA structure and report the conditional response of a set of 34 candidate cgRNAs in living cells. Molecular mechanisms for both ON→OFF and OFF→ON cgRNAs are demonstrated in *E. coli*. For each mechanism, automated sequence design is performed using the reaction pathway designer within NUPACK to produce an orthogonal library of cgRNAs that respond to different RNA triggers. In *E. coli* expressing cgRNAs, triggers, and silencing dCas9 as the protein effector, we observe a median conditional response of ≈ 15 -fold for a library of three orthogonal ON→OFF “splinted switch” cgRNA/trigger pairs, and ≈ 3 -fold for a library of three orthogonal OFF→ON “toehold switch” cgRNA/trigger pairs; the median crosstalk within each library is $< 2\%$ and $\approx 20\%$ for the two mechanisms, respectively. By providing programmable control over both the scope and target of protein effector function, cgRNA regulators offer a promising platform for conditional gene regulation and synthetic biology.

PUBLISHED CONTENT AND CONTRIBUTIONS

1. Hanewich-Hollatz, M. H., Chen, Z., Hochrein, L. M., Huang, J. & Pierce, N. A. Conditional Guide RNAs: Programmable Conditional Regulation of CRISPR/Cas Function in Bacterial and Mammalian Cells via Dynamic RNA Nanotechnology. *ACS Cent. Sci.* doi:10 . 1021 / acscentsci . 9b00340 (2019).

M.H.H.-H. participated in cgRNA mechanism invention, exploratory mechanism studies, experimental design, and developing the data presentation approach, and performed computational sequence design for all splinted switch and toehold switch mechanisms, computational sequence design for mammalian terminator switch mechanism, splinted switch and toehold switch mechanism prototyping and optimization in bacteria, and all final data collection in bacteria. Paper written by M.H.H.-H. and N.A.P. Supplementary information written by M.H.H.-H., L.M.H. and N.A.P.

TABLE OF CONTENTS

Acknowledgements	iii
Abstract	v
Published Content and Contributions	vi
Table of Contents	vii
List of Illustrations	ix
List of Tables	xii
Chapter I: Introduction	1
1.1 Nucleic acid nanotechnology through the rational design of sequence and structure	1
1.2 Small conditional RNAs for programmable conditional regulation . .	2
1.3 Programmable regulation with CRISPR/Cas	4
1.4 Conditional guide RNAs	7
1.5 Thesis outline	8
Chapter II: Engineering orthogonal constitutively active cgRNAs in vitro via hybridization of target sequence-independent modifications	9
Chapter III: Study of domain dimensioning for constitutively active sequence- independent cgRNAs in <i>E. coli</i>	19
Chapter IV: Engineering orthogonal constitutively active cgRNAs in <i>E. coli</i> via hybridization of target sequence-independent modifications	27
4.1 Automated sequence design of orthogonal constitutively active splinted switch cgRNAs using NUPACK	27
4.2 Performance of orthogonal constitutively active splinted switch cgR- NAs in <i>E. coli</i>	34
4.3 Increasing fractional dynamic range of splinted switch cgRNAs . . .	36
4.4 Characterization of cgRNA temporal response with induction of cog- nate trigger	38
Chapter V: Engineering orthogonal constitutively inactive cgRNAs in <i>E. coli</i> via sequestration of the target binding region	41
Chapter VI: Conclusions and future directions	48
6.1 Developing cgRNA mechanisms with improved dynamic range	48
6.2 Detection of endogenous mRNA inputs with cgRNAs	51
6.3 Mechanism engineering for versatile constitutively inactive (OFF→ON) cgRNAs	52
6.4 Future applications for cgRNAs	52
Bibliography	54
Appendix A: Materials and methods	63
A.1 Rational design of libraries of orthogonal cgRNAs using NUPACK .	63
A.2 In vitro assay of gRNA/cgRNA activity with catalytically active Cas9	65
A.3 Methods for bacterial studies in <i>E. coli</i>	65

A.4 Part sequences for cgRNA, trigger, and control gRNA	72
A.5 Plasmids	83
A.6 Sequences for dsDNA target	91
Appendix B: Supplementary figures and data for Chapter 2	93
Appendix C: Supplementary figures and data for Chapter 3	96
Appendix D: Supplementary figures and data for Chapter 4	104
Appendix E: Supplementary figures and data for Chapter 5	107

LIST OF ILLUSTRATIONS

<i>Number</i>	<i>Page</i>
1.1 Programmable conditional regulation	4
1.2 Conditional guide RNA (cgRNA)	5
2.1 In vitro assay of guide RNA (gRNA) activity	10
2.2 Constitutively active cgRNAs (ON→OFF logic) with catalytically active Cas9	10
2.3 Target test tubes for sequence design of splinted switch cgRNAs with 15 nt sequence inserts	12
2.4 Study of the effect of 15 nt 5' extension and handle loop sequence inserts on guide RNA activity in vitro	13
2.5 Programmable conditional function of four orthogonal splinted switch cgRNAs in vitro	14
2.6 In vitro cgRNA mechanism function with Cas9 pre-incubation	16
2.7 Programmable conditional function of four orthogonal 15 nt insert splinted switch cgRNAs with silencing dCas9 in <i>E. coli</i>	18
3.1 Logic and schematic for single and double sequence inserts for construction of allosteric cgRNAs in <i>E. coli</i>	19
3.2 Target test tubes for sequence design of candidate single and double sequence insert cgRNAs	21
3.3 Performance of single and double sequence inserts for construction of allosteric cgRNAs in <i>E. coli</i>	23
3.4 Fractional dynamic range vs predicted $\Delta\Delta G$ of trigger binding for candidate cgRNAs with handle loop insert	26
4.1 Constitutively active splinted switch cgRNAs (ON→OFF logic) with silencing dCas9 in <i>E. coli</i>	28
4.2 Target structure definition and nucleotide defect weights for sequence design of splinted switch cgRNAs	30
4.3 Target test tubes for sequence design of orthogonal splinted switch cgRNAs	32
4.4 Analysis of design quality by equilibrium pair probability	33
4.5 Computational orthogonality study for splinted switch design.	34

4.6	Characterization of ON state of four orthogonal splinted switch cgRNAs in <i>E. coli</i>	35
4.7	Programmable conditional function of three orthogonal splinted switch cgRNAs (ON→OFF logic) with silencing dCas9 in <i>E. coli</i>	36
4.8	Characterization of splinted switch performance with lacI-regulated expression of no-target gRNA competitor	38
4.9	Characterization of splinted switch response to lacI-regulated trigger expression in <i>E. coli</i>	40
5.1	Constitutively inactive toehold switch cgRNAs (ON→OFF logic) with silencing dCas9 in <i>E. coli</i>	42
5.2	Target test tubes for sequence design of orthogonal toehold switch cgRNAs	43
5.3	Characterization of ON state of four orthogonal toehold switch cgRNAs in <i>E. coli</i>	44
5.4	Programmable conditional function of three orthogonal toehold switch cgRNAs (OFF→ON logic) with silencing dCas9 in <i>E. coli</i>	45
5.5	Characterization of toehold switch cgRNA with varied trigger domain dimensions	46
A.1	Example plasmid map for splinted switch in <i>E. coli</i>	84
A.2	Example annotated plasmid sequence for splinted switch in <i>E. coli</i>	85
A.3	Example plasmid map for toehold switch in <i>E. coli</i>	87
A.4	Example annotated plasmid sequence for toehold switch in <i>E. coli</i>	88
A.5	Plasmid map for pdCas9+lacI in <i>E. coli</i>	89
A.6	Annotated plasmid sequence for expression of pdCas9+lacI in <i>E. coli</i>	90
B.1	Quantifying in vitro cgRNA insert study (cf. Figure 2.4)	93
B.2	Additional reaction conditions and quantification of in vitro cgRNAs	94
C.1	Fractional dynamic range vs predicted $\Delta\Delta G$ of trigger binding for all single and double insert candidate cgRNAs	103
D.1	Analysis of design quality by equilibrium pair probability for splinted switch cgRNA:trigger X_A duplex	104
D.2	Flow cytometry replicates for splinted switch ON state, OFF state, and conditional response in <i>E. coli</i>	105
D.3	Flow cytometry replicates for splinted switch orthogonal response in <i>E. coli</i>	106
E.1	Flow cytometry replicates for toehold switch ON state, OFF state, and conditional response in <i>E. coli</i>	107

E.2 Flow cytometry replicates for toehold switch orthogonal response in
E. coli 108

LIST OF TABLES

<i>Number</i>	<i>Page</i>
A.2 Splinted switch sequences for in vitro studies (Chapter 2)	73
A.4 Candidate cgRNA/trigger sequences for insert studies in <i>E. coli</i> (Chapter 3)	79
A.5 Splinted switch sequences for studies in <i>E. coli</i> (Chapter 4)	80
A.6 Toehold switch sequences for studies in <i>E. coli</i> (Chapter 5)	81
A.7 Control gRNA sequences	81
A.8 Transcriptional promoter and terminator sequences	82
A.9 Plasmids used with splinted switch cgRNAs in <i>E. coli</i>	83
A.10 Plasmids used with toehold switch cgRNAs in <i>E. coli</i>	86
C.1 Quantifying ON state, OFF state, fold change, and dynamic range for gRNA insert studies, 0.2 nM aTc	97
C.2 Quantifying ON state, OFF state, fold change, and dynamic range for gRNA insert studies, 2 nM aTc	99
C.3 Quantifying ON state, OFF state, fold change, and dynamic range for gRNA insert studies, 20 nM aTc	101
C.4 Free energy of cgRNA/trigger complexes and trigger hybridization for candidate cgRNAs with single and double inserts predicted via NUPACK analysis	102
D.1 Quantifying ON state, OFF state, fold change, and dynamic range for splinted switch cgRNA in <i>E. coli</i>	105
D.2 Quantifying crosstalk for cognate and non-cognate splinted switch cgRNA/trigger pairs in <i>E. coli</i>	106
E.1 Quantifying ON state, OFF state, fold change, and dynamic range for toehold switch cgRNA in <i>E. coli</i>	107
E.2 Quantifying crosstalk for cognate and non-cognate toehold switch cgRNA/trigger pairs in <i>E. coli</i>	108

Chapter 1

INTRODUCTION

The nucleic acids DNA and RNA are central to the function of all known forms of life. In their information-bearing role, DNA and RNA serve to store and transmit the genetic information characteristic of a particular cell. The information encoded in these nucleic acids also directs the fate of the individual cell, as both the template for gene expression and, for RNA, through the control of gene expression via various regulatory pathways. In this way, the identity of the nucleic acid species within a cell is both indicative of its current state and a determinant of its future. To have at our disposal a general and versatile means for the coupled detection of intracellular nucleic acids and generation of biologically active nucleic acid species is to be fluent in the language of the cell's internal environment. The motivating goal of the work presented here is to contribute to the development of such a means, leveraging recent progress in the engineering of dynamic nucleic acid nanotechnology through rational design and our ability to affect gene expression using CRISPR/Cas technology.

1.1 Nucleic acid nanotechnology through the rational design of sequence and structure

The same information-bearing capacity and reliable base-pairing essential to the natural biological role of nucleic acids have been essential to the field of nucleic acid nanotechnology, in which these properties are exploited to precisely engineer the structure and dynamics of RNA and DNA. Rational design of DNA sequence has enabled the sequence-guided self-assembly of static 2- and 3-dimensional DNA nanostructures, based on the hierarchical assembly of small DNA tiles¹⁻⁵ or the sequence-guided folding of much larger DNA scaffolds into DNA origami structures on the scale of 100 nanometers,⁴⁻⁷ the latter providing addressability of specific sites on structures of arbitrary geometry with sub-nanometer resolution in some cases.^{8,9} The relatively diverse set of RNA secondary and tertiary structural motifs has provided a basis for the design of self-assembled static 2D and 3D RNA architectures,¹⁰⁻¹⁴ including the cotranscriptional folding of RNA tiles for higher-order assembly¹⁵ and the *in vivo* production of RNA nanostructures^{16,17} which highlight the ability to transcribe RNA within a cell as a potential advantage of engineered RNA structures for *in vivo* applications. Dynamic interactions of nu-

cleic acid species have also been engineered, largely based on strand displacement via toehold-mediated branch migration.^{18–20} Examples include DNA motors,^{21–23} computation with DNA logic gates,^{24–26} and signal amplification via programmed polymerization,^{27–29} among others.^{19,20,30,31}

The rational design of nucleic acid structure and dynamics has been facilitated by advancements in algorithms for the prediction and design of DNA and RNA secondary structure. Dynamic programming algorithms have been developed for the calculation of the partition function of a given sequence over all secondary structures, and hence the equilibrium base pairing probabilities for a single strand^{32,33} and, further, complexes of interacting strands^{34,35} and test tubes of interacting strands^{36,37} using a physical model based on experimentally derived energy parameters.^{38–40} These same *in silico* analytical methods can be extended to the design of *de novo* nucleic acid sequence to adopt a particular target structure within a structural ensemble.^{33,35} Design algorithms have subsequently been extended to the design of a test tube of complexes with specified target concentrations³⁶ and, most recently, the ability to design nucleic acid reaction pathways with a set of target test tubes, each with their own target structures and concentrations and subject to diverse sequence constraints.³⁷ This paradigm of sequence optimization through prediction of nucleic acid secondary structure has been implemented for the design of a number of dynamic RNA structures, including riboswitches,⁴¹ sets of orthogonal conditional activators of transcription⁴² and translation⁴³ in bacteria, and partially chemically modified RNA mechanisms for the conditional generation of Dicer substrates.^{44,45}

1.2 Small conditional RNAs for programmable conditional regulation

To date, dynamic DNA nanotechnology in a test tube^{19,30} has received far more research emphasis than dynamic RNA nanotechnology in the cell,^{42,46–48} although it is the latter that has the greatest potential for introducing synthetic regulatory links into living cells and organisms. We envision small conditional RNAs (scRNAs) that, upon detection of a programmable nucleic acid input, change conformation to produce a programmable output that up-regulates or down-regulates the activity of a biological pathway. In this scenario, the input controls the scope of regulation and the output controls the target of regulation, with the scRNA performing signal transduction to create a logical link between the two. Any pathway that recognizes RNA is a potential candidate for conditional regulation by scRNAs (e.g., RNA interference, RNase H, PKR, RIG-1, endosomal TLRs, CRISPR/Cas), as these pathways provide a built-in infrastructure for producing the downstream biological effect for which we

can potentially engineer a conditionally active substrate. Several groups have made contributions toward the goal of conditional regulation via the RNA interference pathway, with demonstrations of nucleic acid-triggered conditional generation of siRNAs⁴⁹ and Dicer substrates.^{44,45,50–52} scRNA mechanisms developed in our lab toward the goal of conditional RNA interference (RNAi) have been demonstrated in buffer⁴⁴ and human cell lysate,⁴⁵ the simplest consisting of a dimer scRNA that conditionally generates a monomer Dicer substrate anti-Y upon detection of mRNA X. CRISPR/Cas9 is another RNA-recognizing pathway which has seen significant recent development and broad application,⁵³ and as such is an attractive candidate for the implementation of conditional regulation.

With the ubiquity of nucleic acid species as potential inputs and the diversity of downstream biological effects of RNA-recognizing pathways, the potential applications of a robust and versatile scRNA implementation would be far-reaching. Existing methods for programmable regulation of gene expression (e.g., CRISPR/Cas, RNAi) enable the selection of gene target Y as the sequence-specific target of a regulatory pathway, but lack a general means to restrict regulation to a desired location and time (Figure 1.1, top arrow; all cells are subject to the same downstream regulation of target Y). In principle, scRNAs could restrict activity of a regulatory pathway to a desired cell type, tissue, or organ by selecting an endogenous RNA trigger X with the desired spatial and temporal expression profile (Figure 1.1, bottom arrow), independent of the downstream target Y. To shift conditional regulation to a different tissue or developmental stage, the scRNA would simply be reprogrammed to recognize a different trigger sequence, providing a powerful tool for fundamental biological study. This same approach to signal transduction would also have attractive therapeutic potential, with trigger X as a programmable disease marker and target Y as an independent programmable therapeutic target, enabling selective treatment of diseased cells. Synthetic biology provides another attractive arena for use of scRNAs. Traditional synthetic biology regulators have relied on protein:protein and protein:DNA interactions mined from existing genomes, placing limits on scalability due to crosstalk and the limited number of available regulators.^{54,55} With powerful tools for rational design and a large sequence space for the design of orthogonal libraries of interoperable parts, scRNA regulators offer a promising platform for scalable synthetic biology.

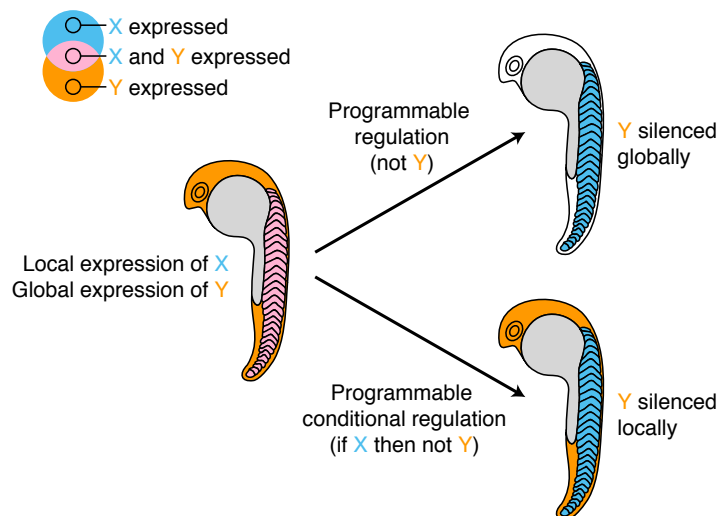


Figure 1.1: Programmable conditional regulation. Molecular logic of programmable regulation using a standard programmable regulator, such as CRISPR/Cas gRNA (“not Y,” top arrow) vs programmable conditional regulation using a small conditional RNA, such as a cgRNA (“if X, then not Y,” bottom arrow). In this conceptual illustration, the standard programmable regulator silences Y in all tissues, while the programmable conditional regulator silences Y only in tissues where and when X is expressed, exerting spatiotemporal control over regulation.

1.3 Programmable regulation with CRISPR/Cas

CRISPR/Cas systems exist in nature as a prokaryotic immune system, enabling nucleic acid sequence-specific acquired immunity to foreign genetic elements.^{56–58} Although varied in their mechanisms of adaptation, guide RNA (gRNA) structure and biogenesis, and the identity of their interference proteins, the foundation of all CRISPR/Cas interference is the targeting of foreign nucleic acids by RNA-guided CRISPR nucleases.^{57–59} The specificity of the interaction between the guide RNA/CRISPR effector complex and the nucleic acid target is dependent on the variable sequence of nucleotides in the gRNA target-binding region and on the presence of a protospacer adjacent motif⁶⁰ (PAM, or, alternatively, a protospacer flanking site⁶¹), a short CRISPR effector-specific sequence adjacent to the target sequence in the nucleic acid target⁵⁸ (Figure 1.2a). The gRNA may be a single strand or complex of strands, with a programmable target binding region and a CRISPR effector-specific structure and sequence preference.^{58,60}

The repurposing of RNA-guided CRISPR effectors through the development of modified gRNAs and CRISPR-associated (Cas) proteins has yielded a suite of powerful tools for biological research and synthetic biology.^{53,62} A notable property of

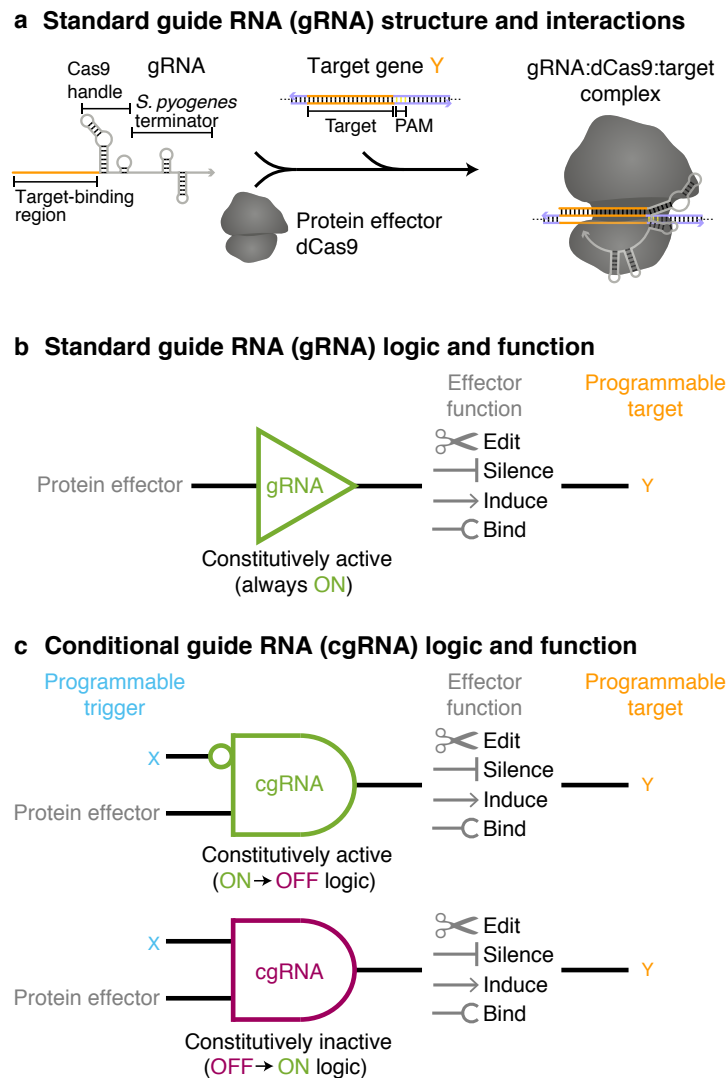


Figure 1.2: Conditional guide RNA (cgRNA). (a) A standard guide RNA (gRNA) directs the function of protein effector dCas9 to a target gene Y. (b) Standard guide RNAs are constitutively active, lacking a general means for spatiotemporal control; different dCas9 variants implement different functions (edit, silence, induce, bind). (c) A conditional guide RNA (cgRNA) changes conformation in response to a programmable trigger X to conditionally direct the activity of a protein effector to a programmable target Y. Top: a constitutively active cgRNA is conditionally inactivated by trigger X (ON→OFF logic). Bottom: a constitutively inactive cgRNA is conditionally activated by trigger X (OFF→ON logic).

Cas9, the most studied of the Class 2 CRISPR effectors,⁶³ is its portability between species, with the same basic architecture applied to gene editing in a diverse array of cell types and organisms.^{63,64} Precision genome editing has been achieved in a variety of organisms using gRNAs to direct the nuclease activity of Cas9 and Cas12a (Cpf1) to a target gene of choice.^{53,65–67} Mutation of the nuclease domains to produce a catalytically dead Cas9 (dCas9) has enabled silencing of genetic expression via inhibition of transcriptional elongation,^{68,69} or induction (or silencing) of genetic expression using dCas9 fusions that incorporate transcriptional regulatory domains.⁷⁰ Similarly, the function of several sub-types of the RNA-targeting CRISPR effector Cas13 (c2c2) has been demonstrated for the highly specific knock down of RNA in human and plant cells,^{71–74} and the development of catalytically dead Cas13 has enabled site-specific RNA editing⁷³ and modulation of RNA splicing.^{71,75,76} Other dCas9 fusions have mediated target-binding to enable visualization of genomic loci,^{77,78} epigenetic modification,⁷⁹ and single-base editing at a specific genomic locus.^{53,80} Hence, gRNA:effector complexes combine the benefits of the rich functional vocabulary of the protein effector (edit, silence, induce, bind) and the programmability of the gRNA in targeting effector activity to a gene of choice. The functional versatility, high regulatory dynamic range, and portability between species characteristic of the pathway^{53,68,70} position CRISPR/Cas9 as a particularly suitable regulatory motif for the development of novel and diverse modes of programmable conditional regulation in living organisms.

Because gRNAs are constitutively active (Figure 1.2b), additional measures are needed to restrict effector activity to a desired location and time.⁸¹ Temporal control can be achieved by small-molecule induction of gRNAs^{82,83} or Cas9,⁸⁴ but this comes with limitations in terms of multiplexing and spatial control. Spatiotemporal control has been achieved by regulation of Cas9 via photoactivation⁸⁵ or via tissue-specific promoters or microRNAs,^{86–88} which come with the unwelcome restriction that all gRNAs are subject to the same regulatory scope and lack the versatile programmability possible with the scRNA paradigm. Systematic mapping of the structure and sequence properties of functional gRNAs has revealed that Cas9 activity is tolerant to significant modifications to the standard gRNA structure,^{89,90} facilitating introduction of auxiliary domains that enable conditional control of gRNA activity via structural changes induced by small-molecules,^{91–93} protein-bound RNAs,⁹⁴ nucleases,⁹⁵ or nuclease-recruiting DNAs.⁹⁵ Alternatively, the activity of standard gRNAs has been modulated by antisense RNAs⁹⁶ or by photolysis of antisense DNAs incorporating photocleavable groups.⁹⁷ For generality,

it is highly desirable to control the regulatory scope in a manner that is both conditional and programmable, a tantalizing prospect central to the proposed scRNA paradigm based on dynamic RNA nanotechnology.

1.4 Conditional guide RNAs

With this paradigm for programmable conditional regulation in mind, we set out to engineer conditional guide RNAs (cgRNAs, a class of scRNA) that change conformation in response to an RNA trigger X to conditionally direct the function of dCas9 to a target gene Y (Figure 1.2c). Unlike a standard gRNA, a cgRNA is programmable at two levels, with the trigger-binding sequence (constrained by trigger X) controlling the scope of cgRNA activity and the target-binding sequence (constrained by target Y) determining the subject of effector activity. Functionally, the cgRNA must perform sequence transduction between X and Y as well as shape transduction between active/inactive conformations. In principle, the activity of a single-input cgRNA can be engineered to be toggled either OFF→ON (as was recently demonstrated by Siu and Chen with dCas9⁹⁸ and Oesinghaus and Simmel with dCas12a⁹⁹) or ON→OFF in response to a cognate RNA trigger X; this conditional control can be exerted over dCas9 variants that either edit, silence, induce, or bind the target Y, emphasizing the broad functional potential available via interplay between cgRNA logic and protein effector function (Figure 1.2c).

To implement the conditional logic of cgRNAs, it is essential to modify the sequence and structure of the standard guide RNA in a way that is well tolerated in the ON state (i.e., minimally disrupts the formation of the gRNA:dCas9 complex and downstream interaction with target Y when ON), and provides a basis for a clean OFF state (i.e., is structurally incompatible with the formation of the gRNA:dCas9 complex and/or downstream interaction with target Y when OFF). Prior to our lab's work on cgRNA engineering, there had been no literature reports of the systematic study of the sequence and structural modifications to the standard gRNA required for toggling CRISPR/Cas activity (ON→OFF or OFF→ON) in response to hybridization of a nucleic acid trigger. However, anecdotal reports of the incorporation of sequence domains to recruit various binding proteins^{66,100–104} and of aptamer modifications achieving a conditional response to the presence of small molecules^{91–93} provide us some insight into which regions of the gRNA might best tolerate the incorporation of new sequence (notably, the handle hairpin loop,^{100,102–106} the first terminator loop of the *S. pyogenes* terminator,^{100,102–106} and, in the mammalian setting, the 3' end of the gRNA^{66,91,100–102,105}). Partial tolerance of gRNA activity to target-mismatched

nucleotides in an extended target-binding region^{66,69} point to a 5' extension of the gRNA as another promising prospect. Crystal structures of the gRNA:Cas9 complex indicate that these same regions are solvent exposed,^{107–110} and as such are strong candidates for modifications tolerated in the ON state, as inserted nucleic acid sequence might minimally disrupt the structure of Cas9. Systematic study of the sequence and structural requirements for a functional guide RNA^{60,89,90,111–113} also provide us insight into the gRNA structural components most sensitive to disruption, and as such guide mechanism design for achieving the desired OFF state.

1.5 Thesis outline

The chapters that follow detail the work I have done toward the goal of implementing programmable conditional regulation using CRISPR/Cas9, both in vitro and in bacteria. Chapter 2 details the engineering of cgRNAs and the development of a set of sequence-independent ON→OFF orthogonal regulators in vitro. Chapter 3 describes a systematic study of the modification of gRNA sequence and structure motivated by the failure of the aforementioned in vitro cgRNAs when tested in *E. coli*. Chapter 4 describes the study of the constitutively active (ON→OFF) splinted switch cgRNA mechanism (identified through the systematic study of gRNA modification of Chapter 3) and the demonstration of a set of orthogonal constitutively active cgRNAs in *E. coli*, with a more detailed discussion of the tools used for cgRNA design. Chapter 5 introduces a cgRNA mechanism of the inverse logic (constitutively inactive, OFF→ON) and details the performance of an orthogonal set of these constitutively inactive cgRNAs in *E. coli*. Chapter 6 summarizes the major contributions of this work, and discusses future work that will be required to develop cgRNAs into a robust and versatile tool for programmable conditional regulation.

Materials and methods for Chapters 2–5 are provided in Appendix A. Supplementary figures and data for the results and discussion presented in Chapters 2–5 are included in Appendices B–E.

*Chapter 2***ENGINEERING ORTHOGONAL CONSTITUTIVELY ACTIVE
cgRNAs IN VITRO VIA HYBRIDIZATION OF TARGET
SEQUENCE-INDEPENDENT MODIFICATIONS**

To enable the study of candidate modifications to the sequence and structure of the standard Cas9 gRNA, and to subsequently demonstrate the conditional and orthogonal performance of the cgRNA mechanisms we design, we developed an assay for gRNA activity *in vitro* (Figure 2.1). Although removed from our ultimate goal of conditional regulation in living cells, an *in vitro* assay of gRNA activity provides the opportunity to study gRNA and cgRNA performance without the potentially confounding factors of metabolism, unknown absolute quantity of system components, and the influence of unintended off-target interactions. The reaction mixture contains only those components essential to the assay of gRNA activity—namely the gRNA itself (in *in vitro* transcribed and purified), recombinant Cas9 protein, and dsDNA target containing a single target binding site with adjacent PAM—and buffer. The activity of the gRNA can be assayed through the visualization and quantification of the dsDNA cleavage products via non-denaturing PAGE with a nucleic acid stain, as the sequence-guided cleavage of the dsDNA target (into two fragments of known size) reflects the capacity of the gRNA to mediate the interaction between catalytically active Cas9 and dsDNA target. This assay also enables visualization of nucleic acid interactions (hybridization states of nucleic acid species), such as the homodimer band visible in the gRNA+Cas9 lane of Figure 2.1, thereby enabling direct observation of both the mechanism of action of candidate cgRNAs (i.e., hybridization of cgRNA and trigger via the associated shift in mobility) and any unintended hybridization interactions or crosstalk.

Motivated by the reported tolerance gRNA activity to handle loop modifications^{100,102–106} and 5' extension^{66,69} *in vitro*, and the essential roles of the gRNA target binding region and handle region for gRNA interaction with target⁶⁰ and Cas9,^{89,107,109} respectively, we designed a constitutively active cgRNA mechanism for the conditional cleavage of dsDNA target Y by catalytically active Cas9 (Figure 2.2a). Compared to a standard gRNA (Figure 1.2a), this “splinted switch” mechanism has a rationally designed 15 nt 5' extension domain “d” and modified handle with a designed 15 nt extended loop domain “e” (Figure 2.2b). Hybridization of the RNA trigger X to

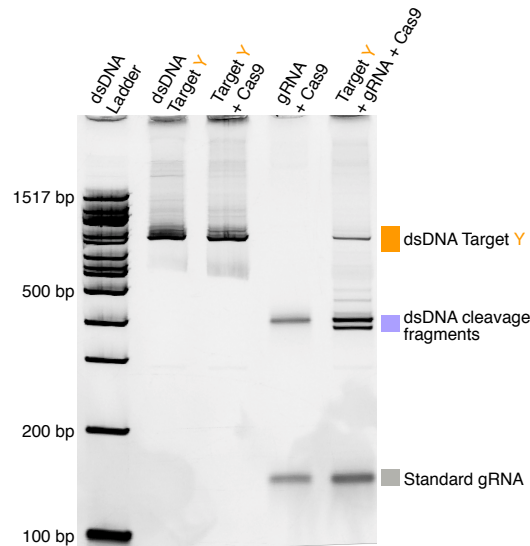
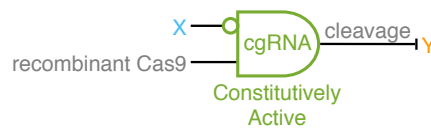


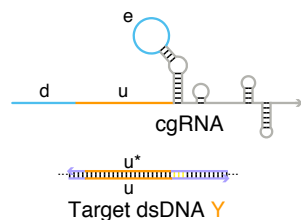
Figure 2.1: In vitro assay of guide RNA (gRNA) activity. Functional in vitro transcribed gRNA directs catalytically active recombinant Cas9 to a single target sequence within a purified dsDNA target, resulting in cleavage of the dsDNA. The extent of dsDNA target cleavage can be assayed via non-denaturing PAGE (4-20% 1xTBE polyacrilimide gel).

these modified domains is intended to form a structure incompatible with cgRNA mediation of Cas9 function by sequestering the target binding region of the gRNA and disrupting the handle structure.

a In vitro splinted switch cgRNA (ON→OFF logic)



b ON State



OFF State

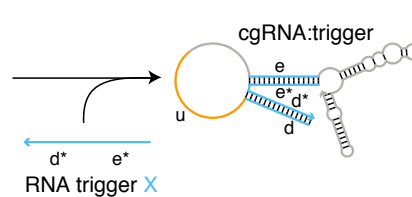


Figure 2.2: Constitutively active cgRNAs (ON→OFF logic) with catalytically active Cas9. (a) Conditional logic: if not X, then not Y. (b) cgRNA mechanism: the constitutively active cgRNA is inactivated by hybridization of RNA trigger X. Rational sequence design of the 15 nt 5' extension (domain “d”) and an extended 15 nt Cas9 handle loop (domain “e”).

A set of four orthogonal cgRNA/trigger sequences was designed using the reaction pathway designer within NUPACK.^{35,37} Sequence design was formulated as a multistate optimization problem using target test tubes to represent reactant and product states of cgRNA/trigger hybridization, as well as to model crosstalk between orthogonal cgRNA/trigger pairs (Figure 2.3). Note that the trigger target structure X_N contains a hairpin with sequence constrained by synthetic terminator at its 3' end; anticipating the potential for future implementation in living cells, cgRNAs were designed with a previously characterized⁶⁸ sfGFP target-binding region, and triggers designed with a synthetic transcriptional terminator for expression in *E. coli*. Each reactants tube (Figure 2.3, Step 0^G and Step 0^X) and products tube (Step 1) contains a set of desired “on-target” complexes (each with a target secondary structure and target concentration) corresponding to the on-pathway hybridization products for a given step, and a set of undesired “off-target” complexes (each with a target concentration of 0 nM) corresponding to on-pathway reactants and off-pathway hybridization crosstalk for a given step. Hence, these elementary step tubes are designed for full conversion of cognate reactants into cognate products and against local hybridization crosstalk between these same reactants. To simultaneously design N orthogonal systems, elementary step tubes are specified for each system (Figure 2.3; left). Note that for design of a library of N orthogonal cgRNA/trigger pairs, all N cgRNAs have the same on-target structure, and all N triggers have the same on-target structure; within a library, the only difference between cgRNA/trigger pairs is the designed sequence. To design against off-pathway interactions between systems, a set of crosstalk tubes are specified (Figure 2.3; right), with each noncognate pair defined explicitly as its own tube. This design used a version of NUPACK that did not yet support exclusion of a set of user-defined complexes from a target test tube ensemble; a more compact specification to design against off-pathway interactions between systems utilizing the exclusion of complexes with NUPACK 3.2 (as implemented by Wolfe et al.³⁷) is described in Chapter 3 and in Section 4.1.

As a first step to characterize this cgRNA mechanism, we sought to confirm that the designed 15 nt 5' extension and handle loop sequences were compatible with interactions between cgRNA, Cas9, and target in the cgRNA ON state (i.e., cgRNA in the absence of trigger). DNA templates were constructed for each 15 nt insert (viz. 5' extensions and handle loops A, B, C, and D) and each double-modification cgRNA (cgRNAs A, B, C, and D), and from these templates candidate cgRNAs were in vitro transcribed and PAGE purified. Assaying the activity of each of these

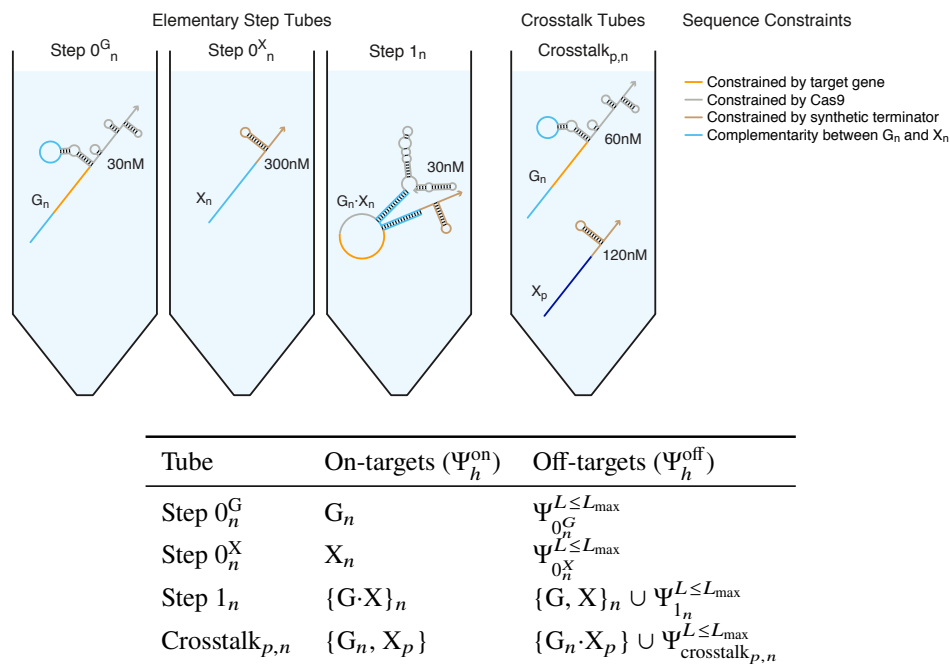


Figure 2.3: Target test tubes for sequence design of splinted switch cgRNAs with 15 nt sequence inserts. Top: Target test tube schematics. Bottom: Target test tube details. Each target test tube contains the depicted on-target complexes (each with the depicted target structure and target concentration) and the off-target complexes listed in the table (each with vanishing target concentration). The on-target structures depicted above are used in the mechanism schematic of Figure 2.2, with the addition of a short synthetic trigger terminator for future *E. coli* studies. To simultaneously design N orthogonal systems, the total number of target test tubes is $|\Omega| = N^2 + 2N$. $L_{\max} = 2$ for all tubes. Design conditions: RNA in 1 M Na^+ at 37 °C.³⁸

candidate cgRNAs in vitro, we observed cgRNA-mediated cleavage of dsDNA target by all single- and double-modified cgRNAs (Figure 2.4a), with yield comparable to that of the standard (unmodified) gRNA (Figure 2.4b).

To achieve the desired OFF state, we hope to observe a high yield of cgRNA:trigger duplex through hybridization of the cognate trigger with the designed sequence domains. An in vitro assay of cgRNA activity in the absence and presence of cognate trigger produced a visible shift in the cgRNA band with both a 2x (Figure B.2) and 10x (Figure 2.5a) excess of trigger, indicating formation of the cgRNA:trigger duplex as intended. Further, a significant reduction in cleavage is observed in the presence of cognate trigger (dark magenta boxes in Figure 2.5a), achieving a conditional ON→OFF response for each of the four cgRNAs, with OFF state comparable to the ideal OFF state given by a control reaction lacking gRNA (Figure 2.5b, left).

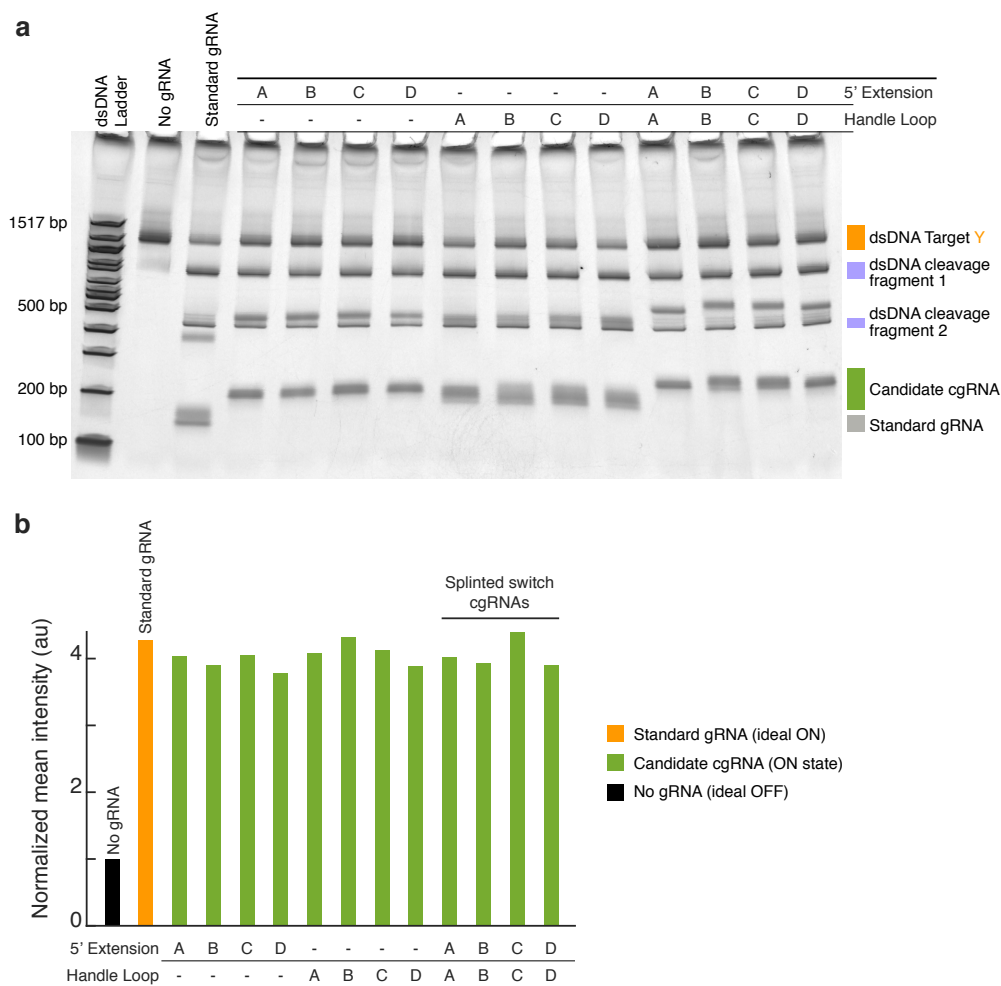


Figure 2.4: Study of the effect of 15 nt 5' extension and handle loop sequence inserts on guide RNA activity in vitro. (a) Non-denaturing PAGE (4-20% 1xTBE polyacrilimide gel) of reaction products for each of four sequences (A, B, C, and D) of 5' extension, handle loop insert, and combined 5' extension and handle loop insert (15 nt each). (b) Quantification of normalized mean pixel intensity for each candidate cgRNA (modified guide RNA) using dsDNA cleavage fragment 1. Normalized mean intensity = $[(\text{mean fragment 1 band intensity}) - \text{background}] / [(\text{no gRNA mean fragment 1 band intensity}) - \text{background}]$. Observed cleavage activity for each of the candidate cgRNAs tested is comparable to that of the standard gRNA, indicating all modifications are well tolerated in the ON state. dsDNA target contains a single 20 nt target binding sequence from sfGFP, and the adjacent PAM sequence [AGG].

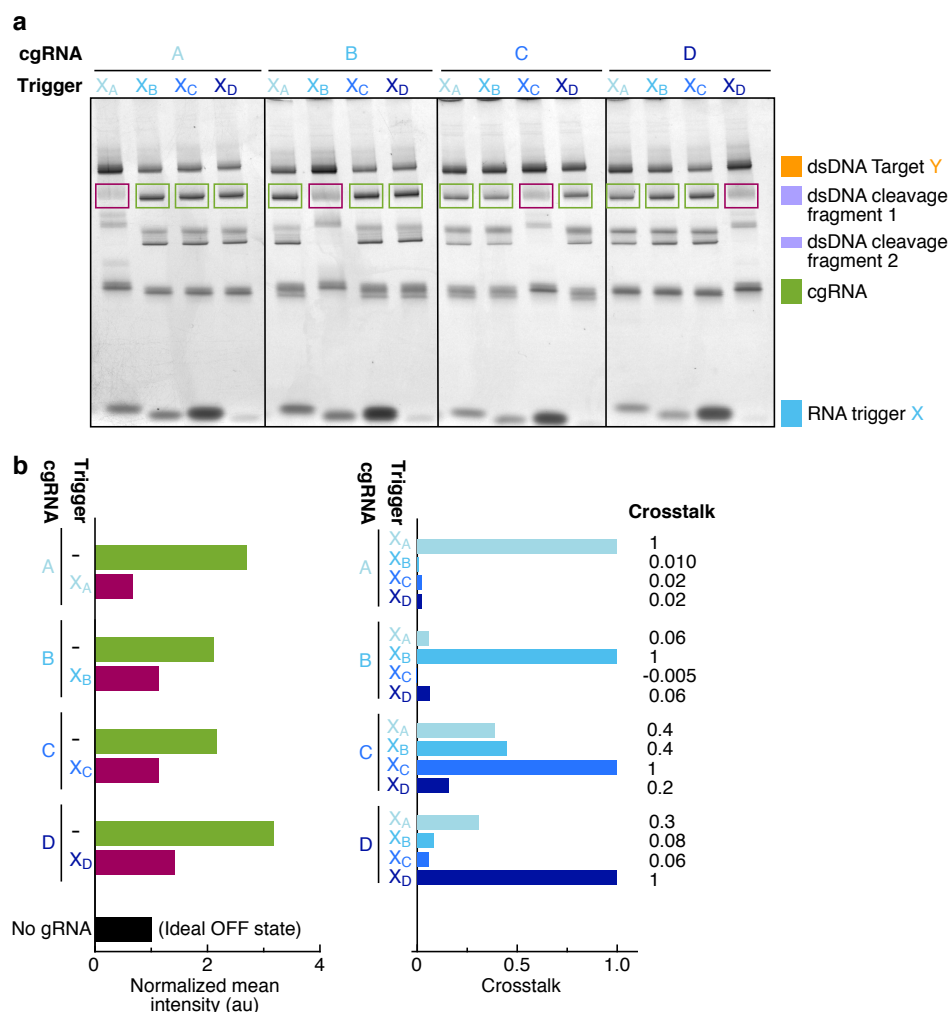


Figure 2.5: Programmable conditional function of four orthogonal splinted switch cgRNAs in vitro. (a) Non-denaturing PAGE (4-20% 1xTBE polyacrilimide gel) of reaction products for four cgRNAs (A, B, C, and D) with each of four synthetic RNA triggers (X_A , X_B , X_C , and X_D). cgRNA was snap-cooled with RNA trigger in buffer and pre-incubated with recombinant Cas9 (10 min) prior to addition of dsDNA target (final reaction concentrations: 30 nM cgRNA, 300 nM RNA trigger, 3 nM dsDNA cleavage target). Cleavage fragment with cognate trigger indicated by dark magenta boxes, cleavage fragment with noncognate trigger indicated by green boxes. All lanes include Cas9 and dsDNA target. (b) Left: Quantification of normalized mean pixel intensity for each cgRNA with and without RNA trigger (see full nucleic acid gels, Figure B.2) using dsDNA cleavage fragment 1. Normalized mean intensity = $[(\text{mean fragment 1 band intensity}) - \text{background}] / [(\text{no gRNA mean fragment 1 band intensity}) - \text{background}]$. Right: normalized intensity depicting orthogonality between noncognate cgRNA/trigger pairs (crosstalk = $[(\text{noncognate trigger}) - (\text{no trigger})] / [(\text{cognate trigger}) - (\text{no trigger})]$; crosstalk for cognate trigger = 1 by definition).

With this splinted switch mechanism, the sequences of the RNA trigger X and the silencing target Y are fully independent, with the cgRNA mediating allosteric regulation: the trigger down-regulates cgRNA:Cas9 activity not by sequestering the target-binding region (orange in Figure 2.2b), but by hybridizing to the distal trigger-binding regions (blue). Toward the goal of developing a versatile means of programmable conditional regulation, this sequence-independence of X and Y is a distinct asset for programmability, as trigger X and target Y can be selected and reassigned independently, improving potential outcomes for the design of orthogonal regulators and allowing the possibility to select X and/or Y from endogenous biological sequences. To test the programmability of this mechanism, we assayed the activity of each of the four cgRNAs with its cognate trigger and each of three noncognate triggers, achieving a median $\approx 6\%$ crosstalk for noncognate cgRNA/trigger combinations (Figure 2.5b, right). Although significant crosstalk is observed for cgRNA C with triggers X_A and X_B , the strong ON state, substantial ON \rightarrow OFF response in the presence of trigger, and low median crosstalk of this mechanism in vitro affirm its potential as a candidate for conditional programmable regulation in living cells.

At present, it is unclear if the OFF state is achieved by a cgRNA:trigger duplex incompatible with Cas9 binding, a cgRNA:trigger:Cas9 triplex incompatible with dsDNA target localization, or a cgRNA:trigger:Cas9:dsDNA quadruplex that disrupts the nuclease function of Cas9 (or a combination of partial contributions of the above). In working toward the implementation of cgRNAs for conditional regulation in living cells, in vitro study may prove useful in the elucidation of the structural details of the cgRNA OFF state, and the mechanism by which the cgRNA is toggled between states. It also remains to measure and optimize cgRNA conditional response times, which are expected to depend on a variety of factors, including whether trigger can toggle the state of both free cgRNA and cgRNA in complex with Cas9 (possibly a mechanism-specific property), and, in living cells, the production and degradation rates of the participating chemical species. As an initial effort to investigate the accessibility of the cgRNA to trigger when bound by Cas9 (i.e., in the cgRNA:Cas9 complex), and hence our ability to toggle the cgRNA from ON to OFF when already in the presence of effector, we assayed gRNA- and cgRNA-mediated cleavage of dsDNA target under a variety of conditions, varying the relative times at which Cas9, trigger, and dsDNA target were introduced into the reaction mixture (Figure 2.6). When a short target-binding region antisense trigger was annealed with a standard gRNA prior to the addition of Cas9 (Figure 2.6a, standard gRNA trigger

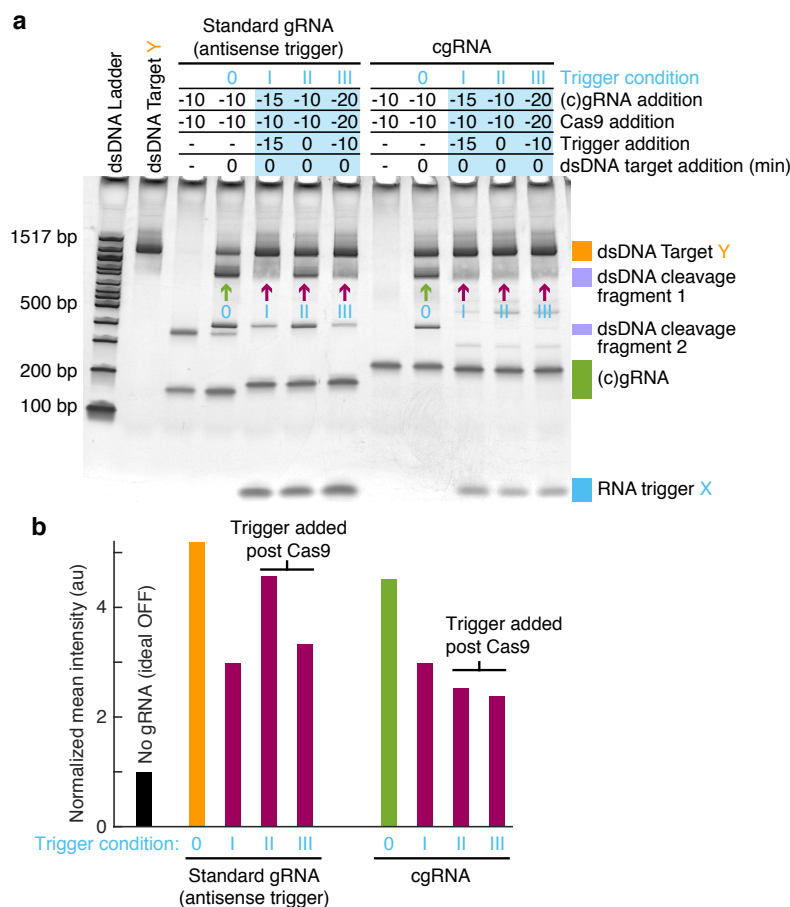


Figure 2.6: In vitro cgRNA mechanism function with Cas9 pre-incubation. (a) Non-denaturing PAGE (4-20% 1xTBE polyacrilimide gel) of reaction products for standard gRNA and cgRNA in the absence of trigger and with trigger added under varying conditions. Standard gRNA or cgRNA, recombinant Cas9, synthetic RNA trigger, and dsDNA target were added to the reaction mixture at the times specified, with $t = 0$ corresponding to the reaction start with dsDNA target addition (if applicable) and incubation at 37 °C. Trigger was either omitted (trigger condition 0), snap-cooled with (c)gRNA for 5 min prior to the addition of Cas9 (trigger condition I), added simultaneously with dsDNA target after a 10 min pre-incubation of (c)gRNA with Cas9 (trigger condition II), or added 10 min before dsDNA target after a 10 min pre-incubation of (c)gRNA with Cas9 (trigger condition III). A synthetic 20 nt RNA complement to the target-binding region was used as trigger for the standard gRNA. (b) Quantification of normalized mean pixel intensity for standard gRNA and cgRNA in the absence of trigger and with trigger added under varying conditions. Normalized mean intensity = [(mean fragment 1 band intensity) - background]/[(no gRNA mean fragment 1 band intensity) - background]. Addition of trigger to standard gRNA after incubation with Cas9 appears to reduce the efficacy of the trigger in producing the OFF state, whereas for cgRNA the trigger efficacy is unaffected by Cas9 pre-incubation.

condition I), we observed a significant decrease in target cleavage as compared to the gRNA-only condition (condition 0). With a 10 min pre-incubation of gRNA and Cas9, followed by the simultaneous addition of antisense trigger and dsDNA target (condition II), we observed a notable increase in cleavage, i.e., a reduced effect of the antisense trigger. When a 10-minute delay was introduced between the addition of trigger to pre-incubated gRNA+Cas9 and the addition of dsDNA target (condition III), this effect was partially mitigated. Unlike the standard gRNA, when a cgRNA was pre-incubated with Cas9, no reduction in trigger efficacy was observed (Figure 2.6b, cgRNA trigger conditions II, III). This suggests that cgRNA accessibility to trigger hybridization is not meaningfully impacted by its interaction with Cas9 in this setting, possibly due to the probable solvent exposure of the 5' extension and extended handle loop with cgRNA bound by Cas9,^{107,109} further suggesting the potential to achieve fast response times using this mechanism (on the timescale of hybridization, rather than degradation and expression, in vivo).

Having demonstrated the programmable conditional function and orthogonality for our library of four cgRNAs in vitro, we next investigated the function of this mechanism in living bacterial cells. We sought to validate the cgRNA mechanism in *E. coli* expressing a fluorescent protein reporter (mRFP) as the target gene for silencing via inhibition of transcriptional elongation by dCas9.⁶⁸ In this setting, an *E. coli* strain expressing the standard gRNA exhibits low fluorescence (ideal ON state) while a strain expressing a no-target gRNA lacking a target-binding region exhibits high fluorescence (ideal OFF state). For the cgRNAs in *E. coli*, we did not observe a consistent effect on fluorescence due to the presence or absence of a constitutively expressed cognate trigger (Figure 2.7, left), and there was no observed selectivity for cognate trigger (Figure 2.7, right). These data lead to the conclusion that in this in vivo setting, the set of four cgRNAs shown to function conditionally and orthogonally in vitro do not function as intended. There exist many plausible explanations for this difference in performance, including environmental differences (such as molecular crowding¹¹⁴ and salt conditions¹¹⁵) resulting in critically different binding energies for species involved, the unknown absolute quantity and unreliable stoichiometry of those species, and a fundamental difference in the downstream function of Cas9—namely, the difference between target cleavage by catalytically active dCas9 and inhibition of transcriptional elongation by catalytically dead dCas9, the former being more sensitive to the binding of the 5'-most bases of the target-binding region,^{116,117} suggesting potential for a “cleavage-only” cgRNA mechanism. The genesis of this discrepancy in performance between the

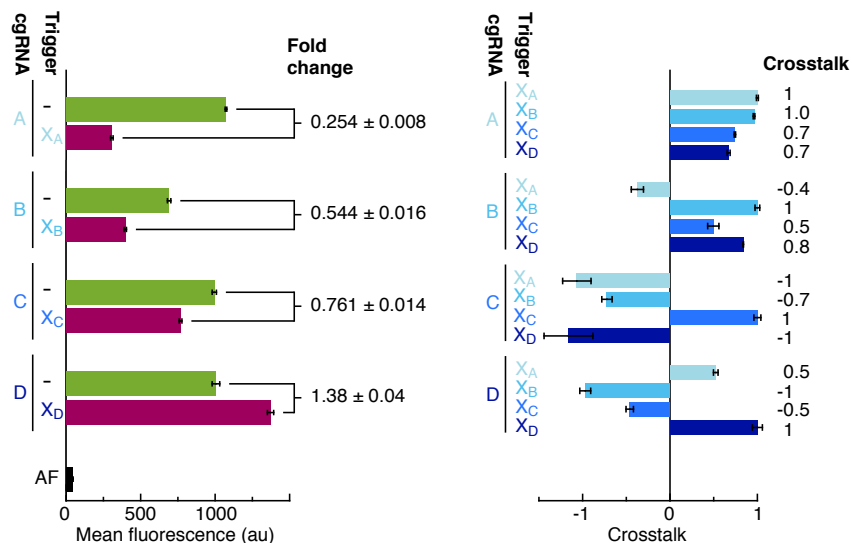


Figure 2.7: Programmable conditional function of four orthogonal 15 nt insert splinted switch cgRNAs with silencing dCas9 in *E. coli*. Expression of RNA trigger X (30 nt + synthetic terminator) is designed to toggle the cgRNA from ON→OFF, and is intended to result in an increase in fluorescence for functional cgRNAs. Left: Raw fluorescence depicting ON→OFF conditional response to cognate trigger (fold change = OFF/ON = [(cognate trigger)–AF]/[(no trigger)–AF]). Right: normalized fluorescence depicting orthogonality between noncognate cgRNA/trigger pairs (crosstalk = [(noncognate trigger) – (no trigger)]/[(cognate trigger) – (no trigger)]). Induced expression (aTc) of silencing dCas9 and constitutive expression of mRFP target gene Y. Autofluorescence (AF): cells with no mRFP. Single-cell fluorescence intensities via flow cytometry. Bar graphs depict mean ± estimated standard error calculated based on the mean single-cell fluorescence over 37,096–45,965 cells for each of $N = 3$ replicate wells (with the exception of cgRNA D + trigger D, which had $N = 2$ replicate wells; fold change and crosstalk calculated with uncertainty propagation).

in vitro setting and *E. coli* notwithstanding, this result underscores the need for systematic study of the tolerance of gRNA sequence and structure to modification for the production of both the ON state and the OFF state, specific to regulation via inhibition of transcriptional elongation in *E. coli*. A description of the study of domain dimensioning for engineering constitutively active sequence-independent cgRNAs in *E. coli* is provided in the next chapter.

Chapter 3

STUDY OF DOMAIN DIMENSIONING FOR CONSTITUTIVELY ACTIVE SEQUENCE-INDEPENDENT cgRNAs IN *E. COLI*

To elucidate the structure/function relationship of the gRNA through modification, and to establish the design space of allosteric ON→OFF cgRNAs (i.e., constitutively active cgRNAs with trigger X sequence-independent of output Y, Figure 3.1a), we undertook a systematic study of unstructured sequence inserts into the standard gRNA structure, seeking to identify inserts that satisfied two key properties:

- well-tolerated by dCas9, so that the ON state is similar to that of the standard gRNA, and
- upon hybridization to a cognate trigger, inactivates the cgRNA to permit a clean OFF state.

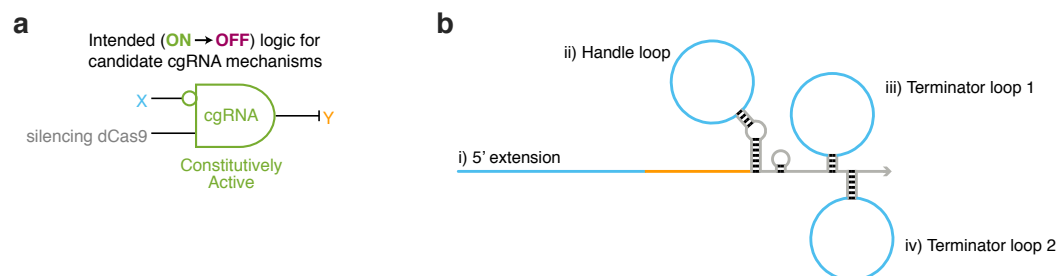


Figure 3.1: Logic and schematic for single and double sequence inserts for construction of allosteric cgRNAs in *E. coli*. (a) Intended (ON→OFF) conditional logic for candidate cgRNA mechanisms. (b) Schematic depicting sequence insert locations (blue). Designed sequences of 15, 25, and 35 nt were inserted into the standard gRNA sequence at either one or two of the four insert sites: i) 5' extension (sequence added to the 5' end of the gRNA; no other sequence replaced); ii) Cas9 handle loop (designed sequence replacing the 4 nt standard gRNA handle loop sequence [GAAA]); iii) Terminator loop 1 (designed sequence replacing the 4 nt standard gRNA sequence of the first *S. pyogenes* terminator loop [GAAA]); iv) Terminator loop 2 (designed sequence replacing the 3 nt standard gRNA sequence of the second *S. pyogenes* terminator loop [AGT]).

We tested candidate cgRNAs with designed unstructured sequence inserts of each of three lengths (15, 25, and 35 nt) at each of four insert sites (5'-extension, Cas9 handle loop, terminator loop 1, terminator loop 2; Figure 3.1b) or at pairwise combinations

of insert sites, with and without expression of a complementary cognate trigger (complementary to insert sequence for single inserts, or concatenated complement of two inserts for pairwise combinations). Insert sequences were designed for each of the candidate cgRNAs and their corresponding triggers using the reaction pathway engineering tools within NUPACK, employing a design formulation analogous to that of the in vitro splinted switch cgRNA (Chapter 2), but with an updated version of NUPACK (v3.2) enabling the use of the “minus” operator to enable a more compact specification with one Reactants tube for each of N candidate cgRNAs (rather than two reactants tubes per system) and a single Global Crosstalk tube (rather than one crosstalk tube per noncognate cgRNA/trigger pair, Figure 3.2). Shorter inserts at each site were designed to be subsequences of longer inserts (e.g., 35 nt handle loop sequence \equiv 25 nt handle loop sequence + 10 additional nucleotides, 25 nt handle loop sequence \equiv 15 nt handle loop sequence + 10 additional nucleotides, etc.). The set of cognate interactions excluded from the Global Crosstalk tube in this case is the set of all cgRNA:trigger complexes with intended complementarity, including cases where there is only partial intended complementarity (e.g., the complex of the candidate cgRNA with a single 35 nt handle loop insert and the 25 nt handle loop trigger is excluded from the Global Crosstalk tube).

To determine an upper bound for ON state performance of candidate cgRNAs in *E. coli* expressing silencing dCas9, the low fluorescence ideal ON state was measured using the standard gRNA with genomically incorporated sfGFP as the target Y. To check whether the inserts in a given candidate cgRNA are tolerated by both dCas9 and downstream interaction with target, we measured fluorescence for a cgRNA-only strain (ON state) for each of the 34 candidate cgRNAs. To check for conditional inactivation of the cgRNA by the cognate trigger, we measure fluorescence for a cgRNA + trigger strain (OFF state). The ideal OFF state is measured for a strain expressing a no-target gRNA lacking the target-binding region. Autofluorescence (AF) is measured for a strain expressing no fluorescent protein reporters. A total of 71 strains were used to quantify performance of single and double inserts: AF, no-target gRNA, standard gRNA, 16 single-insert cgRNA-only (no trigger), 16 single-insert cgRNA + cognate trigger, 18 double-insert cgRNA-only (no trigger), and 18 double-insert cgRNA + cognate trigger.

The raw data are displayed for all insert combinations in Figure 3.3a-c with moderate induction of dCas9 (2 nM aTc). For the cgRNA without trigger, all modifications appear well-tolerated by dCas9, with strong ON state silencing activity comparable

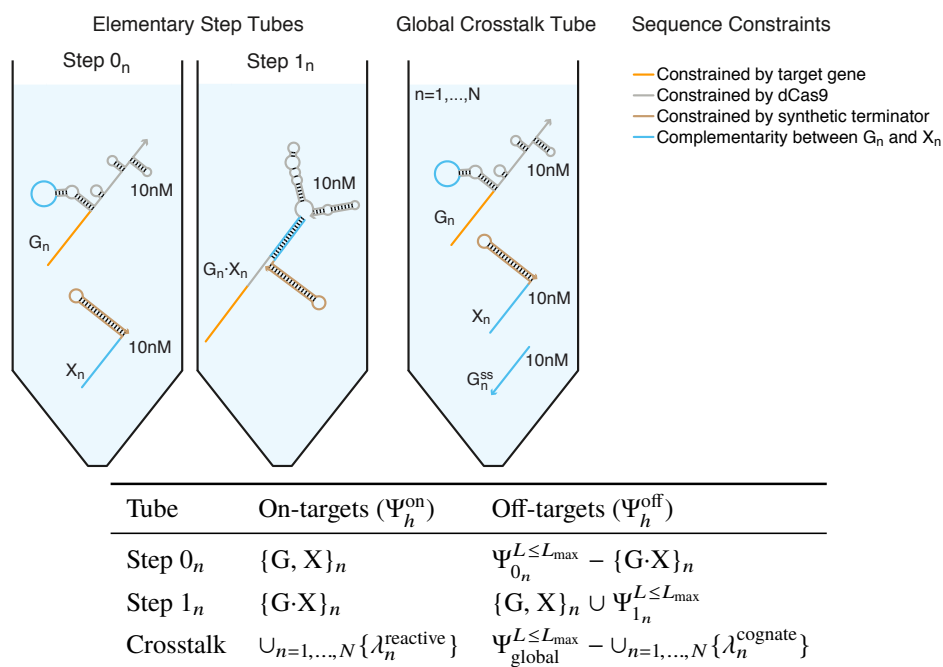


Figure 3.2: Target test tubes for sequence design of candidate single and double sequence insert cgRNAs. Top: Example target test tube schematics. Bottom: Target test tube details. Each target test tube contains the depicted on-target complexes (each with unstructured insert sequence in the cgRNA and trigger monomers and fully paired designed sequence in the cgRNA:trigger duplex, as depicted in examples; target concentration of 10 nM for each) and the off-target complexes listed in the table (each with vanishing target concentration). The example on-target structures depicted above correspond to the 15 nt handle loop insert candidate cgRNA. For the single-stranded input species G_n^{ss} of double insert candidate cgRNAs, the intervening standard gRNA sequence and structure were included between insert domains. The set of cognate interactions $\lambda_n^{\text{cognate}}$ includes all cgRNA:trigger complexes with intended complementarity. To simultaneously design N candidate cgRNAs, the total number of target test tubes is $|\Omega| = 2N + 1$. $L_{\max} = 2$ for all tubes. Design conditions: RNA in 1 M Na^+ at 37 °C.³⁸

to the standard gRNA. For each candidate cgRNA, the cognate trigger corresponds to the expressed reverse complement of the inserted designed sequence plus a synthetic terminator. Expression of the cognate RNA trigger is intended to toggle the cgRNA from ON→OFF leading to an increase in fluorescence. A quantity of interest for assessing candidate cgRNA performance is the fractional dynamic range, the ratio of candidate cgRNA dynamic range (OFF – ON) to the ideal dynamic range defined by the standard gRNA and no-target gRNA controls ($FDR = [OFF - ON]/[ideal\ OFF - ideal\ ON]$). Tables C.1–C.3 report values for ON, OFF, fold change (OFF/ON), dynamic range (OFF – ON), and fractional dynamic range for each dCas9 induction condition. The candidate cgRNA with the highest fractional dynamic range at the moderate (2 nM aTc) dCas9 induction condition was a double modification with 35 nt inserts in the dCas9 handle loop and the terminator loop 1 (an improved “splinted switch” cgRNA mechanism, discussed at length in Chapter 4, with insert lengths and locations different from the in vitro splinted switch mechanism described in Chapter 2). The candidate cgRNAs with two 25 nt or two 35 nt inserts in the 5' extension and dCas9 handle, corresponding to the 5' extension/handle insert splinted switch cgRNA of Chapter 2 with longer inserts, also exhibit a large dynamic range; this suggests that the basic mechanism validated in vitro is functional in *E. coli*, but requires longer trigger binding domains to toggle the cgRNA ON→OFF, highlighting the necessity of domain dimensioning studies specific to the intended setting (i.e., with the particular buffer/lysate/cell and protein effector of interest) for cgRNA mechanism engineering.

Fractional dynamic range for all insert combinations with low, moderate, and high dCas9 induction (0.2, 2, and 20 nM aTc, respectively) is provided in Figure 3.3d. For each candidate cgRNA that produces a distinct conditional response (absolute value fractional dynamic range > 0.01), we observe a decrease in fractional dynamic range with increased dCas9 induction (as well as decreased absolute dynamic range, see Tables C.1–C.3). This trend is unsurprising, as we would expect an increase in dCas9 concentration to favor cgRNA:dCas9 complex formation (i.e., the active complex), in both the absence and presence of trigger. The magnitude of this effect, however, is significant (e.g., a decrease of $FDR \approx 0.5$ to ≈ 0.02 in the most extreme case), and suggests that increasing the strength of cgRNA:trigger hybridization (as compared to the cgRNA:dCas9 interaction) may be important for the engineering of more robust cgRNAs. The potential to improve cgRNA OFF state and conditional response by designing stronger cgRNA:trigger interaction is also supported by the positive correlation between insert length and fractional dynamic range, apparent

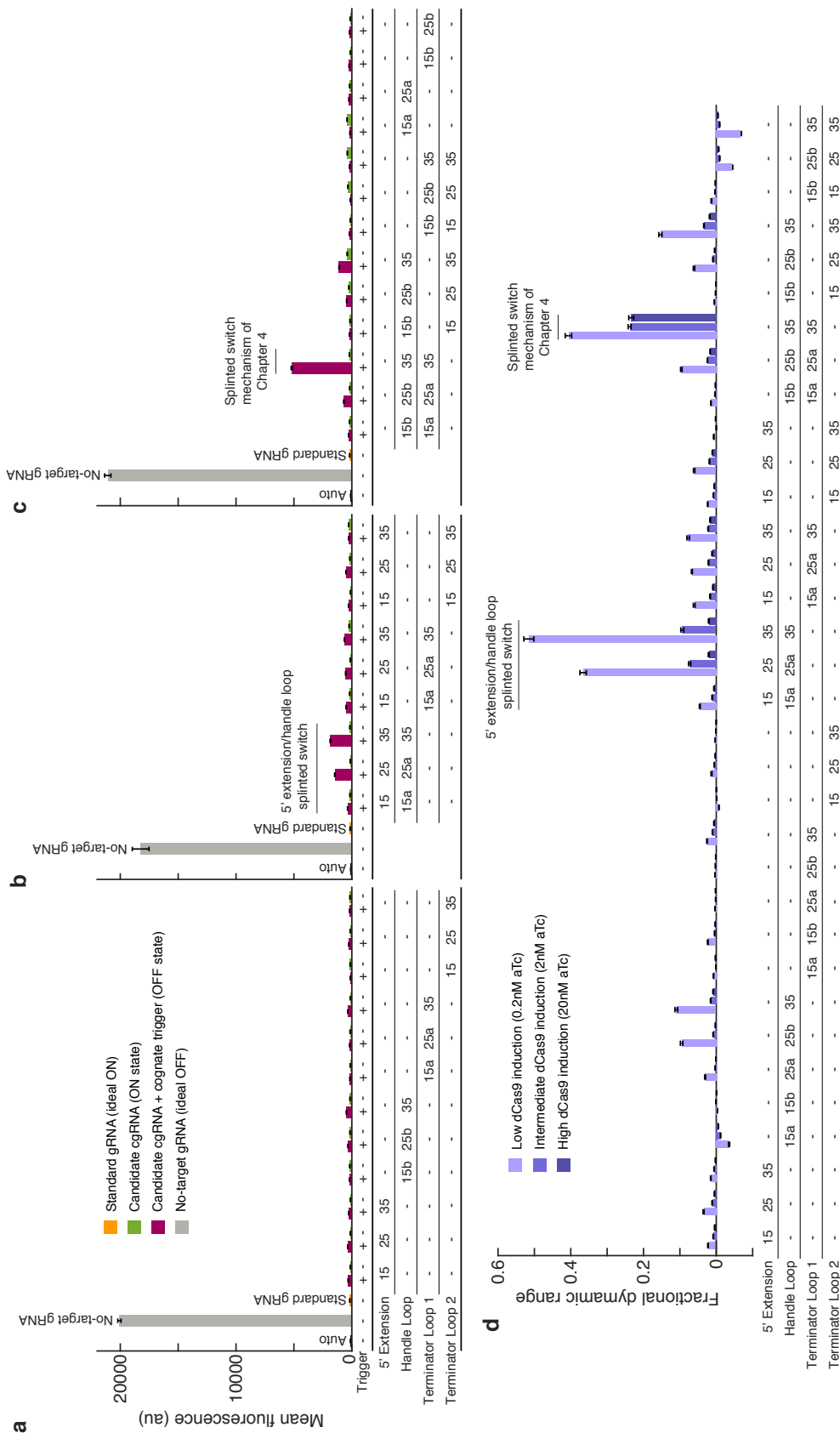


Figure 3.3: Performance of single and double sequence inserts for construction of allosteric cgRNAs in *E. coli*.

Figure 3.3: Performance of single and double sequence inserts for construction of allosteric cgRNAs in *E. coli* (cont'd). (a) Single insert conditional response (15, 25, and 35 nt at each of four insert sites). (b) Double insert conditional response (15, 25, and 35 nt at 5' extension plus same length of insert at each of three other insert sites). (c) Double insert conditional response (15, 25, and 35 nt inserts for remaining combinations of two insert sites) plus alternative single insert sequences for 15 and 25 nt handle loop and terminator loop 1. Panels a-c: Induced expression (2 nM aTc) of silencing dCas9 and constitutive expression of sfGFP target gene Y and either: no-target gRNA, standard gRNA, candidate cgRNA without trigger, or candidate cgRNA + cognate trigger. Autofluorescence: cells with no sfGFP. Raw fluorescence via flow cytometry: mean \pm estimated standard error based on the mean single-cell fluorescence over 20,000 cells for each of $N = 3$ replicate wells. Data for each panel a-c collected on different days. (d) Conditional response for all single- and double-insert candidate cgRNAs with varying induction of dCas9 (0.2, 2, and 20 nM aTc). Fractional dynamic range decreases with increasing dCas9 induction for each candidate cgRNA. Fractional dynamic range = $[\text{OFF} - \text{ON}] / [\text{ideal OFF} - \text{ideal ON}]$, calculated with uncertainty propagation.

for those cgRNAs that produce a distinct conditional response. Another key insight suggested by these data is the importance of the handle loop insert in producing an ON \rightarrow OFF conditional response in this setting. The top 10 highest fractional dynamic ranges observed each correspond to candidate cgRNAs that contain a handle loop insert of 25 nt or more, including the 35 nt single handle loop insert.

Using NUPACK analysis for complex free energy prediction, it is possible to predict the change in free energy for the hybridization reaction of cgRNA and trigger (i.e. $\Delta\Delta G$, where $\Delta\Delta G = \Delta G_{\text{cgRNA:trigger}} - [\Delta G_{\text{cgRNA}} + \Delta G_{\text{trigger}}]$, see Table C.4). Comparison of the observed fractional dynamic range for each candidate cgRNA and the predicted $|\Delta\Delta G|$ of cgRNA:trigger duplex formation (from NUPACK analysis with RNA in 1 M Na⁺ at 37 °C) reveals a positive correlation (Figure C.1), with a significant increase in sensitivity to trigger (i.e., increased slope, with decreased mean squared error of a least squares fitted line¹¹⁸ for each dCas9 induction condition) when limited to those candidate cgRNAs that incorporate a handle loop insert (Figure 3.4). With increasing dCas9 induction, we observe a decrease in the slope of a least squares fitted line (fitted using least squares regression weighted by inverse estimate of variance of the mean¹¹⁸ due to varying estimates of variance over three replicate wells for each candidate cgRNA), suggesting that high expression of dCas9 diminishes our ability to produce a stronger conditional response by increasing the strength of cgRNA:trigger hybridization. With intermediate and high dCas9 induc-

tion (2 and 20 nM aTc, Figure 3.4b-c, respectively), the fractional dynamic range of one candidate cgRNA remained notably high, namely the double modification with 35 nt inserts in the dCas9 handle loop and the terminator loop 1; this alternative “splinted switch” cgRNA mechanism is discussed further in Chapter 4. The relationship between fractional dynamic range, $\Delta\Delta G$, and dCas9 induction points to the potential to improve the automated design of cgRNA sequences by incorporating some proxy for the energetics of cgRNA:dCas9 complex formation. Wright et al. reported an experimentally determined equilibrium dissociation constant (K_d) for the gRNA/catalytically active Cas9 complex,¹¹⁹ but values for the catalytically dead dCas9 have yet to be reported. Quantitation of free cgRNA, cgRNA:trigger duplex, and cgRNA:dCas9 complex with titration of dCas9 may be possible by a combination of electrophoretic mobility shift¹²⁰ and filter binding assay,¹¹⁹ and could enable the inference of the cgRNA/dCas9 binding energy. In the absence of a physical model representing cgRNA/dCas9 interaction, cgRNA performance may be improved by simply constraining the design to produce cgRNA/trigger pairs with increased $|\Delta\Delta G|$, either by specifying minimum G-C content for a particular target structure or by specifying a “soft constraint” target $|\Delta\Delta G|$ for the binding domains or cgRNA:trigger duplex. Of the candidate cgRNAs tested here, the observed high fractional dynamic range and robustness to dCas9 induction of the double 35 nt handle/terminator insert “splinted switch” cgRNA motivates further study of this mechanism; a description of the design and validation of a set of orthogonal splinted switch cgRNAs is provided in the following chapter.

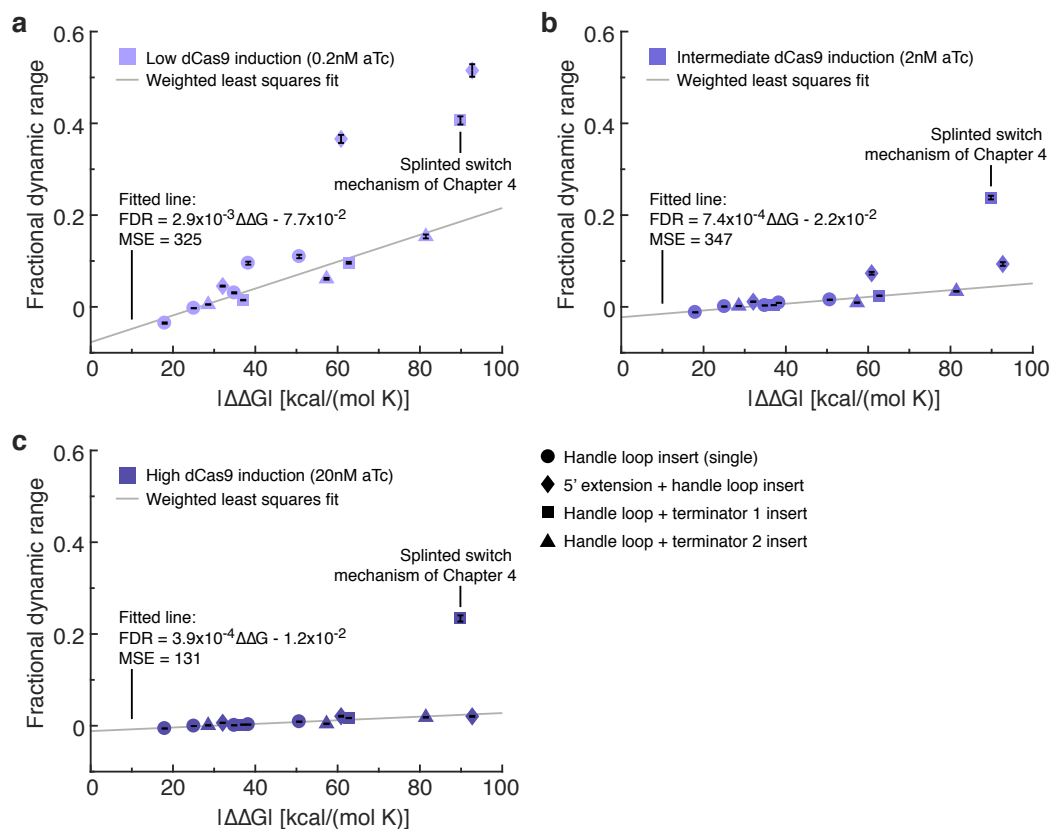


Figure 3.4: Fractional dynamic range vs predicted $\Delta\Delta G$ of trigger binding for candidate cgRNAs with handle loop insert. (a) 0.2 nM aTc induction of dCas9. (b) 2 nM aTc induction of dCas9. (c) 20 nM aTc induction of dCas9. Fractional dynamic range is higher for cgRNA:trigger pairs with high $|\Delta\Delta G|$, but decreases with increased dCas9 induction. $\Delta\Delta G$ values calculated using NUPACK analysis (RNA in 1 M Na^+ at 37 °C,³⁸ $\Delta\Delta G = \Delta G_{\text{cgRNA:trigger}} - [\Delta G_{\text{cgRNA}} + \Delta G_{\text{trigger}}]$, see Table C.4). Fractional dynamic range: mean \pm estimated standard error based on $N = 3$ replicate wells with uncertainty propagation. Fitted lines calculated using least squares regression weighted by inverse estimate of variance of the mean,¹¹⁸ equation for the line of best fit and the estimate of mean squared error (MSE) of the fit are provided as inset.

ENGINEERING ORTHOGONAL CONSTITUTIVELY ACTIVE cgRNAs IN *E. COLI* VIA HYBRIDIZATION OF TARGET SEQUENCE-INDEPENDENT MODIFICATIONS

4.1 Automated sequence design of orthogonal constitutively active splinted switch cgRNAs using NUPACK

The constitutively active “splinted switch” cgRNA mechanism identified through the domain dimensioning studies of Chapter 3 has 35 nt extended loops in both the Cas9 handle (domain “d”, Figure 4.1b) and terminator (domain “e”), intended to minimally interfere with downstream cgRNA-mediated dCas9 function in the ON state (Figure 4.1b reaction arrow “i”). Hybridization of RNA trigger X to both loops is intended to form a splint that is structurally incompatible with cgRNA-mediated dCas9 function (Figure 4.1b reaction arrow “ii”), yielding the conditional logic: “if not X, then not Y” (Figure 4.1a). This splinted switch mechanism exhibited the highest fractional dynamic range of all single and double insert candidate cgRNAs with both moderate (2 nM aTc) and high (20 nM aTc) dCas9 induction (Figure 3.3d), and the observed performance compared to other candidate cgRNAs with similar $\Delta\Delta G$ for cgRNA:trigger hybridization (Figure 3.4b-c) suggests that this cgRNA mechanism is particularly robust.

Following validation of the conditional response of a single splinted switch cgRNA sequence in *E. coli*, we sought to more rigorously test the programmability of the splinted switch mechanism. To do so, a set of four orthogonal cgRNA/trigger sequences was designed using the reaction pathway designer within NUPACK.^{35,37} Target structures were defined using a combination of subsequence minimum free energy (MFE) structures predicted by NUPACK, and the requirements for the intended mechanism function (Figure 4.2a). Although the target-binding region sequence (domain “u” in Figure 4.1b) was fully constrained for this design, the target-binding region target structure was defined to be unstructured to penalize the inadvertent contribution of interactions with designed sequence domains to an increased probability of target-binding region base pairing, as a highly structured target-binding region can reduce gRNA activity.^{95,98,121} To minimize perturbation of the effector-specific standard gRNA structure in the cgRNA ON state (single-stranded cgRNA),

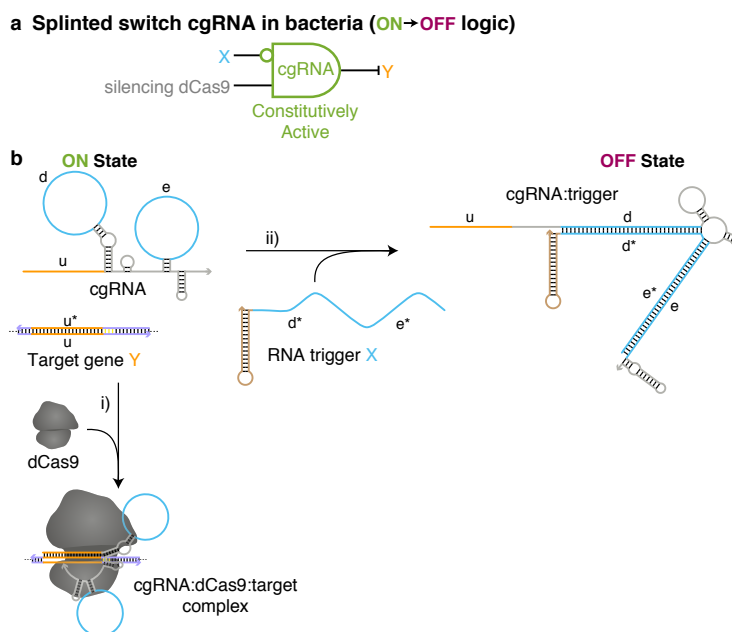


Figure 4.1: Constitutively active splinted switch cgRNAs (ON→OFF logic) with silencing dCas9 in *E. coli*. (a) Conditional logic: if not X, then not Y. (b) Schematic of cgRNA mechanism. ON state: the splinted switch cgRNA is constitutively active, directing the function of protein effector dCas9 (reaction arrow “i”) to a target gene Y in the absence of trigger; the extended loops in the Cas9 handle and terminator region (blue) are intended to not interfere with the activity of the cgRNA:dCas9 complex. OFF state: in the presence of RNA trigger X, hybridization of the trigger is intended to form a splint (reaction arrow “ii”) that is structurally incompatible with cgRNA mediation of dCas9 function, thereby inactivating the cgRNA. Rational sequence design of the 35 nt Cas9 handle loop (domain “d”) and an extended 35 nt terminator hairpin loop (domain “e”).

the target base-pairing state of the remaining constrained sequence was designed to be that of the MFE structure, with the exception of the exterior handle region wobble pair (G-U), which has been shown to form experimentally via X-ray crystallography.¹⁰⁸ It should be noted that although this G-U wobble pair forms in the gRNA:effector complex, the current implementation of the RNA secondary structure physical model³⁷ associates a maximal penalty with an exterior G-U wobble pair, and as such it may be advisable to define the G-U wobble pair as unstructured in future implementations for which this is consequential (e.g., for the design of potentially unstructured target-binding regions). Similarly, target structures for domains constrained by the synthetic terminator (BBa_B1006 trigger terminator) and standard gRNA subsequences (inter-handle/terminator loop standard gRNA sequence for single-stranded input and cgRNA:trigger duplex, pre-handle loop and

post-terminator loop standard gRNA sequence for cgRNA:trigger duplex, Figure 4.2a) were defined to be their respective MFE structures. Designed sequence was defined to be unstructured in the ON state (single-stranded reactant state) to maximize accessibility for cgRNA/trigger hybridization. Designed sequence was defined to be fully paired between trigger and complementary cgRNA insert sequence in the OFF state target structure (cgRNA:trigger duplex product state) to maximize cgRNA/trigger affinity for a given sequence, consistent with the intended mechanism.

Within the ensemble defect, defect weights (see Section S1.6 in the Supplementary Information of Wolfe et al.³⁷) were applied to prioritize design effort for each sequence domain within each on-target complex as depicted in Figure 4.2b. Designed sequence domains were assigned the highest weight across target complexes ($w = 3$) to minimize interaction with constrained sequence domains, maximize accessibility in the reactant state, and prioritize a well formed OFF state (with cgRNA:trigger complex formation dominated by the interaction of designed complementary sequence domains). Constrained sequence domains within the single-stranded reactant cgRNA and trigger complexes were assigned a weight of $w = 1$, with the exception of the Cas9 handle region, which was given a higher priority weight ($w = 1.5$) due to its structural importance for interaction with Cas9.^{89,90} Constrained sequence domains were given the lowest priority ($w = 0$) in the cgRNA:trigger duplex (OFF state), as the base pairing states of these domains are both inflexible (i.e., sequence is fully constrained) and inconsequential to the mechanism function. The fully constrained inter-handle/terminator loop sequence of the single-stranded input target structure was also assigned a weight of $w = 0$, as the internal structure of this domain is inconsequential for designing against pseudoknotted crosstalk interactions. The particular weight values assigned for the final design were determined through iterative design trials and assessment of design quality. Future study of the structure/function relationship of the guide RNA may enable improvements in automated sequence design by providing a basis for a finer resolution (or otherwise better informed) defect weighting scheme.

Sequence design was formulated as a multistate optimization problem using target test tubes to represent reactant and product states of cgRNA/trigger hybridization, as well as to model crosstalk between orthogonal cgRNAs (Figure 4.3). Target test tubes were specified using the general formulation of Section S2.2.1 in the Supplementary Information of Wolfe et al.³⁷ Each reactants tube (Step 0) and products

tube (Step 1) contains a set of desired “on-target” complexes (each with a target secondary structure and target concentration) corresponding to the on-pathway hybridization products for a given step, and a set of undesired “off-target” complexes (each with a target concentration of 0 nM) corresponding to on-pathway reactants and off-pathway hybridization crosstalk for a given step. Hence, these elementary step tubes are designed for full conversion of cognate reactants into cognate products and against local hybridization crosstalk between these same reactants. To simultaneously design N orthogonal systems, elementary step tubes are specified for each system (Figure 4.3; left). Furthermore, to design against off-pathway interactions between systems, a single global crosstalk tube is specified (Figure 4.3; right). In the global crosstalk tube, the on-target complexes correspond to all reactive species generated during all elementary steps ($m = 0, 1$) for all systems ($n = 1, \dots, N$), including single-stranded input complexes (G_n^{ss} , to enable negative design against pseudoknotted crosstalk interactions without explicitly incorporating pseudoknotted structures); the off-target complexes correspond to noncognate interactions between these reactive species. Crucially, the global crosstalk tube ensemble omits the cognate products that the reactive species are intended to form (i.e., they appear as neither on-targets nor off-targets). Hence, all reactive species in the global crosstalk tube are forced to either perform no reaction (remaining as desired on-targets) or undergo a crosstalk reaction (forming undesired off-targets), providing the basis for minimization of global crosstalk during sequence optimization. Note that for the design of a library of N orthogonal cgRNA/trigger pairs, all N cgRNAs have the same on-target structure, and all N triggers have the same on-target structure; within a library, the only difference between cgRNA/trigger pairs designed sequence.

Sequence designs were performed for a library of four orthogonal cgRNA/trigger pairs for several independent design trials. For a given design trial, the sequences were optimized by mutating the sequence set to reduce the multi-tube ensemble defect³⁷ subject to the diverse sequence constraints depicted in Figure 4.3 (top). An additional constraint preventing four consecutive repeats of a single base (viz. [AAAA], [CCCC], [GGGG], [UUUU]) was applied to the designed sequence domains for each cgRNA/trigger pair. A final sequence set was selected from the independent design trials for experimental testing based on inspection of the predicted structural defects (fraction of nucleotides in the incorrect base-pairing state within the ensemble of an on-target complex, see Figure 4.4 example) and concentration defects (fraction of nucleotides in the incorrect base-pairing state because there is a deficiency in the concentration of an on-target complex) for species in the con-

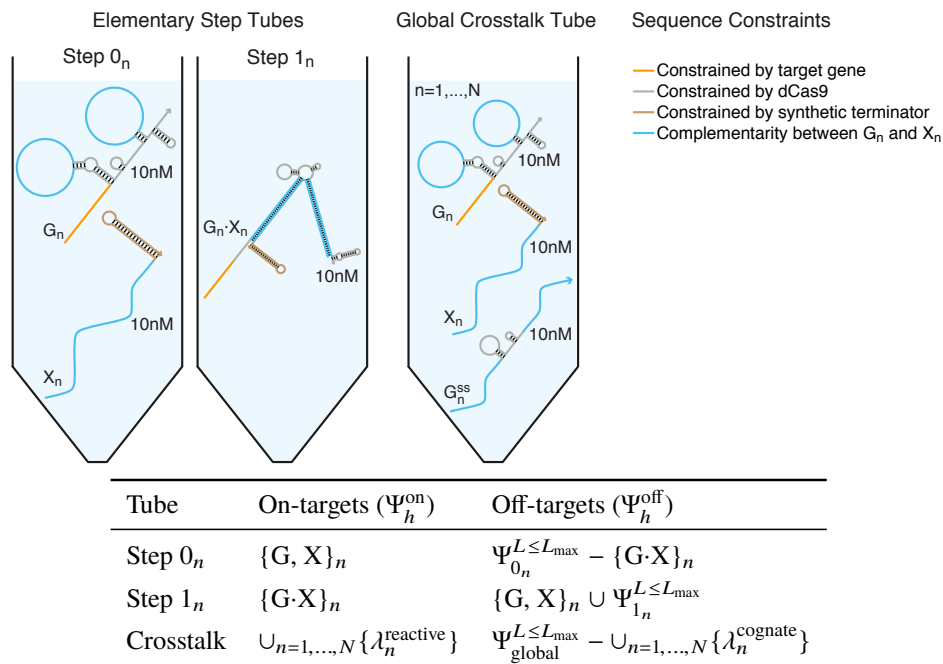


Figure 4.3: Target test tubes for sequence design of orthogonal splinted switch cgRNAs. Top: Target test tube schematics. Bottom: Target test tube details. Each target test tube contains the depicted on-target complexes (each with the depicted target structure and a target concentration of 10 nM) and the off-target complexes listed in the table (each with vanishing target concentration). To simultaneously design N orthogonal systems, the total number of target test tubes is $|\Omega| = 2N + 1$. $L_{\text{max}} = 2$ for all tubes. Design conditions: RNA in 1 M Na^+ at 37 °C.³⁸

text of the target test tubes,^{36,37} and the predicted computational orthogonality of the set of cgRNA/trigger sequences via NUPACK analysis of each cgRNA in the presence of each noncognate trigger (Figure 4.5). For the design trial selected, the predicted structural defects depicted in Figure 4.4 (cgRNA A, trigger X_A) are typical—on-target complexes are predicted to form with quantitative yield at the target concentrations, but with some unintended base-pairing (nucleotides not shaded dark red). These structural defects within the ensemble of on-target complexes reflect the real-world challenges of designing a cgRNA that satisfies biological sequence constraints, changes conformation in response to a cognate RNA trigger, and operates orthogonally to a library of other cgRNAs. In particular, generating a library of four orthogonal trigger sequences with 70 contiguous unstructured nucleotides presents an obvious design challenge. In spite of these structural defects, each cgRNA (A, B, C, and D) is predicted to interact appreciably only with its cognate RNA trigger (and with quantitative yield; Figure 4.5).

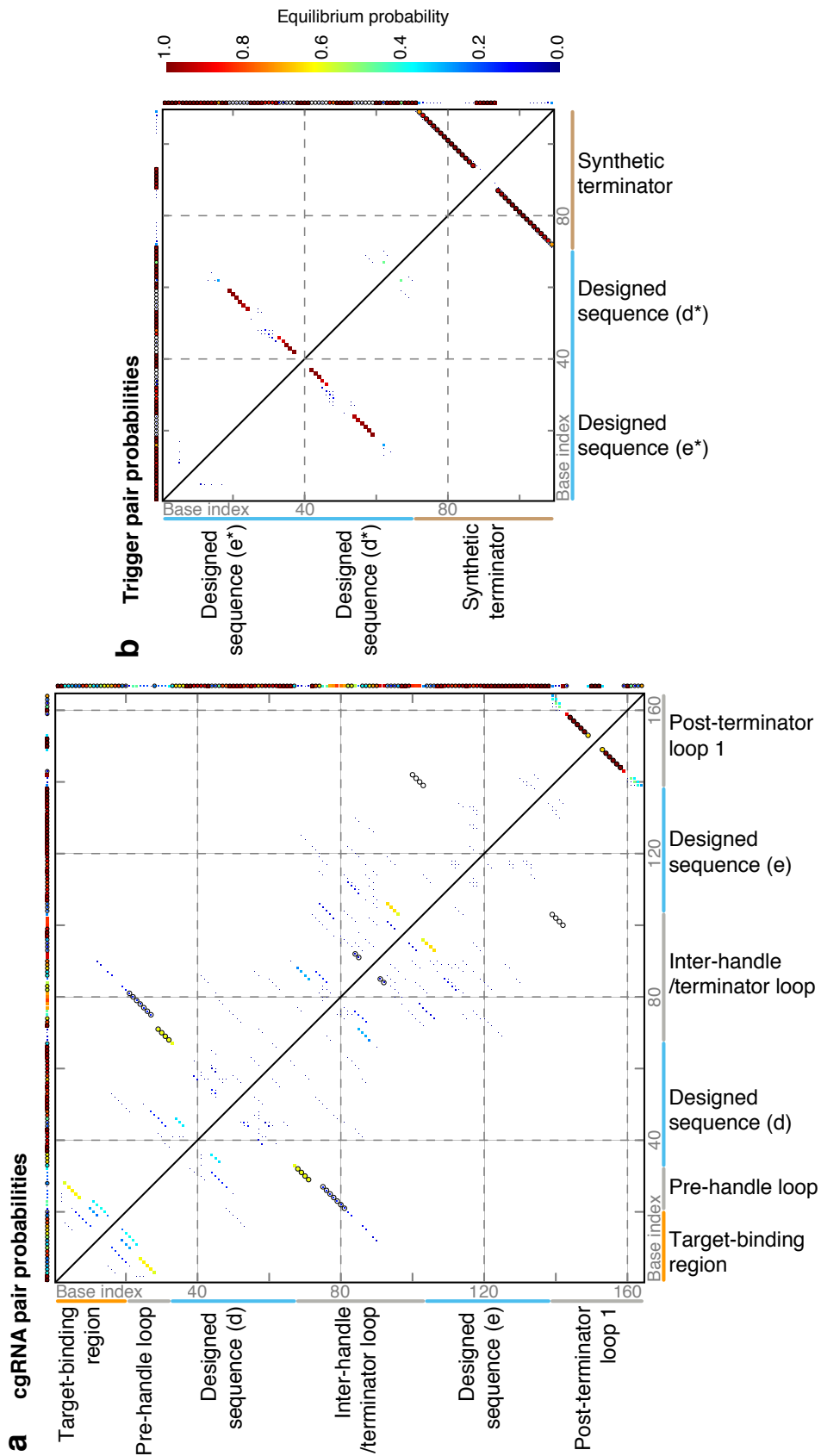


Figure 4.4: Analysis of design quality by equilibrium pair probability.^{34,35}

Figure 4.4: Analysis of design quality by equilibrium pair probability (cont'd).^{34,35} (a) Equilibrium pair probabilities for splinted switch cgRNA A. (b) Equilibrium pair probabilities for splinted switch trigger X_A . Nucleotides shaded and scaled to indicate the probability of adopting the depicted base-pairing state at equilibrium. Pairing states in the target structure are indicated with black circles. For this design, all on-target complexes are predicted to form with quantitative yield at the 10 nM target concentration, but some nucleotides have unwanted base-pairing interactions (circled nucleotides not shaded dark red, uncircled nucleotides with significant pair probability), notably the low probability of cgRNA handle stem formation (panel a) and the high probability of undesired base pairing between domains “e*” and “d*” of the trigger (panel b). Equilibrium pair probabilities for splinted switch cgRNA:trigger complex A are provided in Figure D.1.

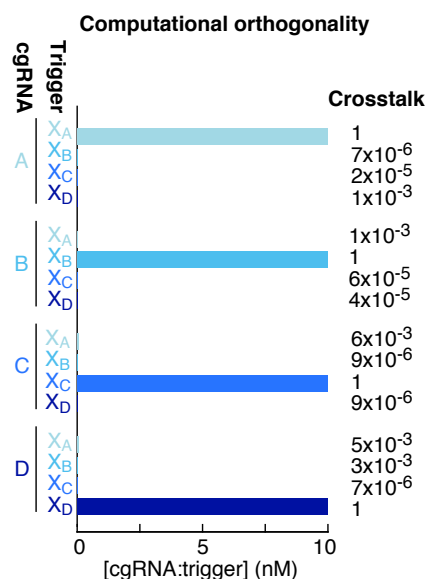


Figure 4.5: Computational orthogonality study for splinted switch design. Predicted equilibrium concentration of each cgRNA:trigger complex for each pairwise combination of cgRNA and trigger from the library of four systems (one cgRNA species and one RNA trigger species per tube). RNA in 1 M Na^+ at 37°C.³⁸

4.2 Performance of orthogonal constitutively active splinted switch cgRNAs in *E. coli*

To screen for performance of the cgRNA ON state, *E. coli* expressing silencing dCas9, a fluorescent protein reporter (sfGFP) as the target gene Y, and constitutively expressed cgRNA were characterized using time course microplate fluorescence (Figure 4.6). In comparison to the ideal ON state of the standard gRNA, we observe a near-ideal ON state for three of the four cgRNAs characterized (A, B, and

C), with distinctly poorer performance for cgRNA D. The nature of this distinctly reduced activity was not identified, but several possible explanations exist, including sequence-dependent expression issues and significant tertiary structure (not captured by computational analysis) interfering with the function of the cgRNA. On this basis, the three cgRNA/trigger pairs A, B, and C were selected for full experimental characterization.

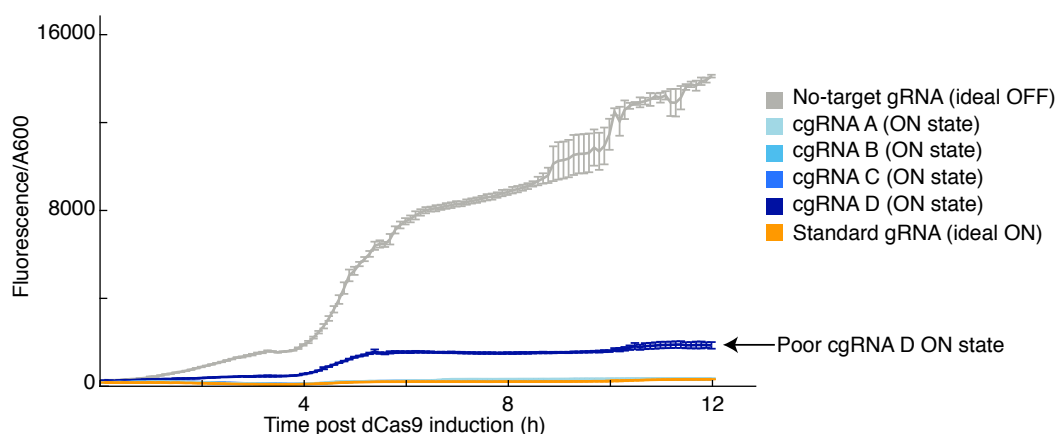


Figure 4.6: Characterization of ON state of four orthogonal splinted switch cgRNAs in *E. coli*. Fluorescence of cgRNAs A–C with no trigger (ON state) overlap with the standard gRNA (ideal ON state), while cgRNA D yields significantly higher fluorescence. Time course microplate fluorescence data normalized by A600. Mean \pm estimated standard error over $N = 3$ replicate wells.

cgRNA-only (ON) and cgRNA+trigger (OFF) strains were characterized by flow cytometry in *E. coli* expressing silencing dCas9 and a fluorescent protein reporter (sfGFP) as the target gene Y. The splinted switch exhibits a conditional ON \rightarrow OFF response to expression of RNA trigger X (Figure 4.7a), with a strong ON state comparable to the ideal ON state of a standard gRNA, and an OFF state with significant potential for improvement relative to the ideal OFF state of a no-target gRNA lacking the target binding region (consistent with results from the domain dimensioning studies, Figure 3.3c). Examining the library of three orthogonal splinted switch cgRNA/trigger pairs (Figure 4.7b; left), we observe a median ≈ 15 -fold ON \rightarrow OFF conditional response with the expression of cognate trigger. With a pairwise expression of each cgRNA (A, B, and C) with each trigger (X_A , X_B , and X_C) (Figure 4.7b; right), we observe high selectivity for cognate trigger for the conditional response of each cgRNA, with median crosstalk of $\approx 2\%$ between noncognate cgRNA/trigger combinations. The strong conditional response and demonstrated programmability of this mechanism suggest that the splinted switch

mechanism, and the cgRNA paradigm more broadly, offers a promising platform for conditional programmable regulation in living cells.

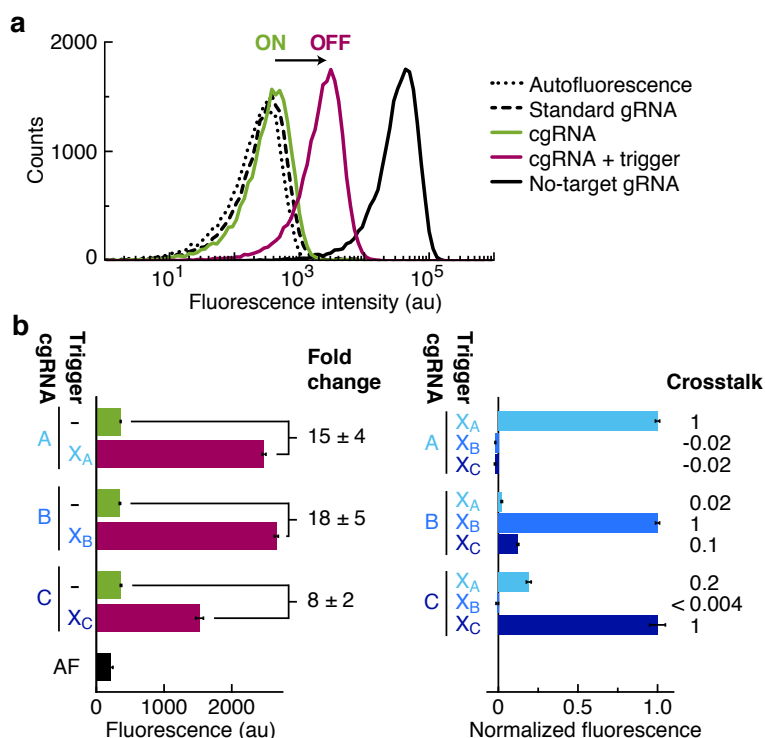


Figure 4.7: Programmable conditional function of three orthogonal splinted switch cgRNAs (ON→OFF logic) with silencing dCas9 in *E. coli*. (a) Expression of RNA trigger X toggles the cgRNA from ON→OFF, leading to an increase in fluorescence. Single-cell fluorescence intensities via flow cytometry. Induced expression (aTc) of silencing dCas9 and constitutive expression of sfGFP target gene Y and either: standard gRNA (ideal ON state), cgRNA (ON state), cgRNA + RNA trigger X (OFF state), or no-target gRNA that lacks target-binding region (ideal OFF state). Autofluorescence (AF): cells with no sfGFP. (b) Programmable conditional regulation using three orthogonal cgRNAs (A, B, and C). Left: Raw fluorescence depicting ON→OFF conditional response to cognate trigger (fold change = OFF/ON = [(cognate trigger)–AF]/[(no trigger)–AF]). Right: normalized fluorescence depicting orthogonality between noncognate cgRNA/trigger pairs (crosstalk = [(noncognate trigger) – (no trigger)]/[(cognate trigger) – (no trigger)]). Bar graphs depict mean ± estimated standard error calculated based on the mean single-cell fluorescence over 20,000 cells for each of $N = 3$ replicate wells (fold change and crosstalk calculated with uncertainty propagation).

4.3 Increasing fractional dynamic range of splinted switch cgRNAs

The conditional and orthogonal performance of the library of splinted switch cgRNAs in living cells highlights their promise and potential usefulness for some regu-

latory applications. Comparison of the cgRNA OFF state with the ideal OFF state of the no-target gRNA control (Figure 4.7a), however, points to an obvious potential for improvement, namely improving the performance of the cgRNA OFF state and hence the fractional dynamic range of the splinted switch mechanism. One potential means to improve the OFF state of this mechanism, discussed in Chapter 3, is to specify target structures and/or to design sequences with an increased $|\Delta\Delta G|$ of cgRNA:trigger hybridization, by extending the designed sequence domains and/or constraining the designed sequence to have a higher G-C content. A potential means to improve the performance of the cgRNA OFF state and the corresponding fractional dynamic range with no change to the cgRNA itself (i.e., using the same cgRNA/trigger sequences) is dCas9 loading competition. gRNA loading competition has been reported elsewhere as a means to characterize the affinity of various gRNAs for Cas9,^{121,122} with lower affinity gRNAs identified by their reduced activity in the presence of a competitor gRNA; by the same token, if the modifications made to the standard gRNA structure to produce the splinted switch cgRNA reduce its affinity for dCas9, expression of a no-target gRNA competitor will displace some fraction of the cgRNA that would otherwise be bound by dCas9 (with adequately low dCas9 expression), thereby potentially improving its OFF state. dCas9 loading competition was examined for splinted switch cgRNA C with triggers X_A (stringent ON state), X_B (stringent ON state), and X_C (cognate trigger, OFF state) with lacI-regulated expression of a no-target gRNA competitor (Figure 4.8). With increasing competitor induction (i.e., increasing [IPTG]), we observed an increase in fluorescence for both cognate trigger OFF state and noncognate trigger ON state strains (Figure 4.8a-c). Crucially, the competition had a differential effect on OFF and stringent ON state fluorescence, resulting in an increase in the fractional dynamic range with increased competitor expression (Figure 4.8d), although at the expense of the ON state performance. Examining the standard gRNA (ideal ON) and no-target gRNA (ideal OFF) controls reveals that the observed increase in fractional dynamic range is in part due to a reduction of the ideal dynamic range; however, the majority of the increase is in fact due to an increase in the absolute dynamic range with increased expression of the no-target gRNA competitor. This approach may be applicable to other cgRNA mechanisms as well (likely in a mechanism-specific manner; provided the cgRNA modifications influence effector affinity, a higher affinity standard gRNA may serve as a competitor for dCas9 loading), and suggests a means for improving the dynamic range of cgRNA response for applications in which the benefit of an increase in absolute dynamic range outweighs the potential worsening

of the ON state.

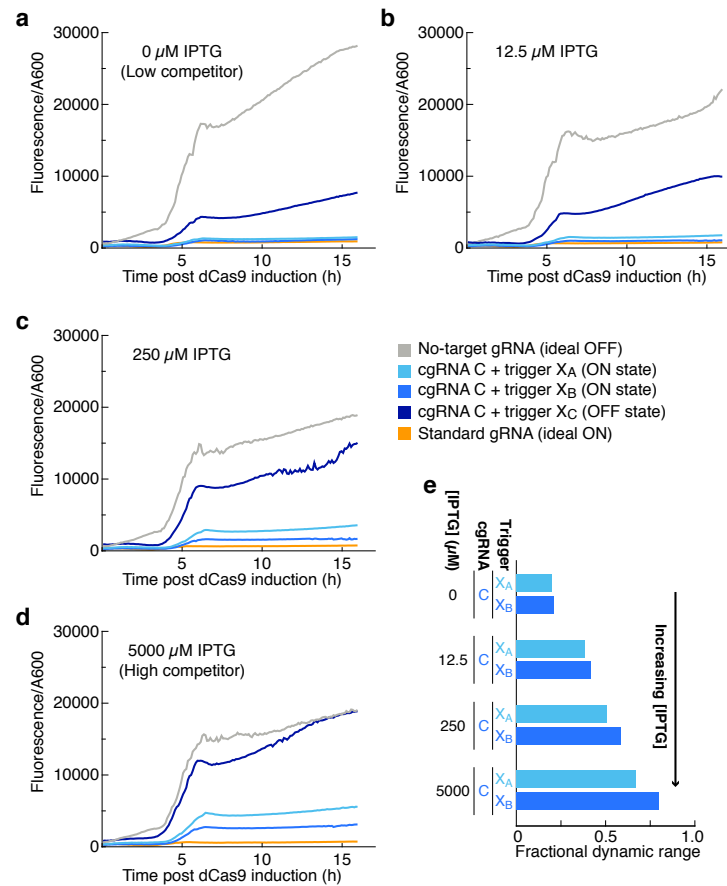


Figure 4.8: Characterization of splinted switch performance with lacI-regulated expression of no-target gRNA competitor. Panels (a-d): Time course microplate fluorescence data normalized by A600. Simultaneous induction of dCas9 (0.2 nM aTc) and no-target gRNA competitor with (a) 0 μM (b) 12.5 μM (c) 250 μM or (d) 5000 μM IPTG at $t = 0$, with constitutive expression of other gRNA/cgRNA and trigger species. Increasing IPTG induction of no-target gRNA competitor leads to an increase in fluorescence for both cgRNA ON state (noncognate trigger) and OFF state (cognate trigger). (e) Fractional dynamic range of cgRNA C + noncognate trigger (X_A , X_B) at $t = 12$ h for different no-target competitor gRNA induction conditions (0-5000 μM IPTG). Increasing induction of no-target gRNA competitor leads to an increase in fractional dynamic range. Fractional dynamic range = [OFF – ON]/[ideal OFF – ideal ON].

4.4 Characterization of cgRNA temporal response with induction of cognate trigger

The study of candidate cgRNA function described for the splinted switch mechanism above and the domain dimensioning studies of Chapter 3 have focused primarily on end point assays to characterize the conditional response of candidate cgRNAs

in the presence or absence of a cognate trigger in separate *E. coli* strains. To gain insight into the temporal response of cgRNAs to trigger expression, and to validate the trigger dependence of the observed conditional ON→OFF response in a single *E. coli* strain, we characterized the splinted switch cgRNA sequence identified in Chapter 3 with constitutive cgRNA expression (BBa_J23114 promoter, Table A.8) and induced expression of the cognate RNA trigger (BBa_R0011 lacI-regulated promoter, Table A.8). In *E. coli* expressing lacI, silencing dCas9, and a fluorescent protein reporter (sfGFP) as the target gene Y, the splinted switch exhibits a conditional ON→OFF response with fully induced expression of RNA trigger X (5 mM IPTG, Figure 4.9a). At low trigger induction ([IPTG] = 0), we observe comparable fluorescence for a strain bearing a constitutive cgRNA + lacI-regulated trigger expression plasmid and for a strain with constitutive cgRNA expression only (Figure 4.9b). With increasing trigger induction, we observe no significant change in fluorescence for the cgRNA-only strain (ON state), but monotonically increasing fluorescence for the cgRNA + lacI-regulated trigger strain, confirming that the magnitude of conditional response is dependent upon trigger expression, and the cgRNA behaves as designed. Time course microplate fluorescence studies (Figure 4.9c) of the same *E. coli* strains with trigger expression induced several hours (4-7 h) post dCas9 induction yields the expected increase in observed normalized fluorescence, with normalized fluorescence of the uninduced cgRNA + pLac-trigger remaining comparable to that of the cgRNA-only strain for the duration of the experiment. Subtraction of the mean normalized fluorescence of uninduced cgRNA + pLac-trigger from each induction time course (Figure 4.9d) reveals time-resolved dependence of the conditional response on induction of cognate trigger, with a substantial increase in $\Delta(\text{Fluorescence}/A600)$ observed 1–2 h after trigger induction.

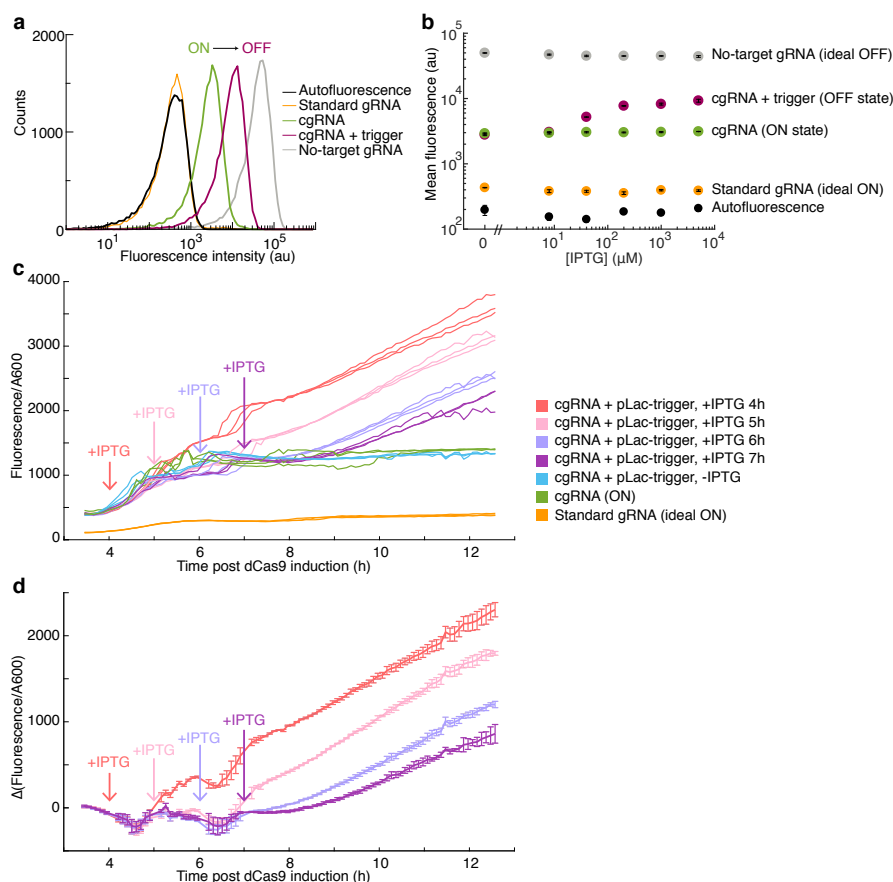


Figure 4.9: Characterization of splinted switch response to *lacI*-regulated trigger expression in *E. coli*. (a) Expression of RNA trigger X induced by IPTG toggles the cgRNA from ON→OFF, leading to an increase in fluorescence. Induced expression (aTc) of silencing dCas9 and constitutive expression of sfGFP target gene Y and either: standard gRNA (ideal ON state), cgRNA (ON state), cgRNA + RNA trigger X (OFF state; trigger expression is IPTG-induced), or no-target gRNA that lacks target-binding region (ideal OFF state). Autofluorescence (AF): cells with no sfGFP. Trigger expression was induced simultaneously with dCas9 expression (5 mM IPTG in each well). (b) ON→OFF conditional response increases with trigger expression level (induced by IPTG). (c) Time course microplate fluorescence data normalized by A600. Identical color traces represent $N = 3$ replicate wells. Induction of trigger (5 mM IPTG, time of induction indicated by arrows) at 4, 5, 6, and 7 h post dCas9 induction (2 nM aTc at $t = 0$). (d) Difference in normalized fluorescence between: 1) cgRNA + trigger induced by IPTG (5 mM IPTG, time of induction indicated by arrows) and 2) uninduced cgRNA + trigger (-IPTG). Induction of trigger expression leads to an increase in fluorescence 1–2 h after addition of IPTG. Flow cytometry (a-b): mean \pm estimated standard error calculated based on the mean single-cell fluorescence over 20,000 cells for each of $N = 3$ replicate wells. Time course data (c-d): mean \pm estimated standard error (with uncertainty propagation) over $N = 3$ replicate wells.

*Chapter 5***ENGINEERING ORTHOGONAL CONSTITUTIVELY INACTIVE
cgRNAs IN *E. COLI* VIA SEQUESTRATION OF THE TARGET
BINDING REGION**

To enable both gene induction and gene silencing in the same setting (i.e., with the same Cas9 variant in the same organism) and to provide cgRNAs for the spatiotemporal control of gene knockdown which minimally perturb the natural system (i.e., with low global activity), it is desirable to engineer a constitutively inactive cgRNA that is conditionally activated in the presence of a trigger X (OFF→ON logic, Figure 5.1a). To implement the OFF→ON conditional logic, we designed a constitutively inactive “toehold switch” cgRNA mechanism (Figure 5.1b). The target-binding region of the cgRNA (domain “u”) is initially sequestered by a 5’ extension to inhibit recognition of target gene Y, providing the OFF state in the absence of a cognate trigger. Hybridization of trigger X to this extension through toehold-mediated branch migration is intended to de-sequester the target-binding region (reaction arrow “i”), yielding a cgRNA:trigger duplex (ON state) capable of directing dCas9 function to target gene Y (reaction arrow “ii”).

A set of four orthogonal cgRNA/trigger sequences was designed using the reaction pathway designer within NUPACK.^{35,37} Analogous to the design specification used for the in vitro splinted switch cgRNA mechanism (Chapter 2), sequence design was formulated as a multistate optimization problem using target test tubes to represent reactant and product states of cgRNA/trigger hybridization, as well as to model crosstalk between orthogonal cgRNAs (Figure 5.2a). As with the design of in vitro splinted switch cgRNA, this design used a previous version of NUPACK that did not yet support exclusion of a set of complexes from a target test tube, and hence a set of crosstalk tubes was specified (Figure 2.3; right) with each noncognate pair defined explicitly as its own tube to design against off-pathway interactions between systems. Within the ensemble defect, defect weights were applied to prioritize design effort (Figure 5.2b).

To screen for performance of the cgRNA ON state of this constitutively inactive cgRNA, *E. coli* expressing silencing dCas9, a fluorescent protein reporter (mRFP) as the target gene Y, and constitutively expressed cgRNA + cognate trigger (ON

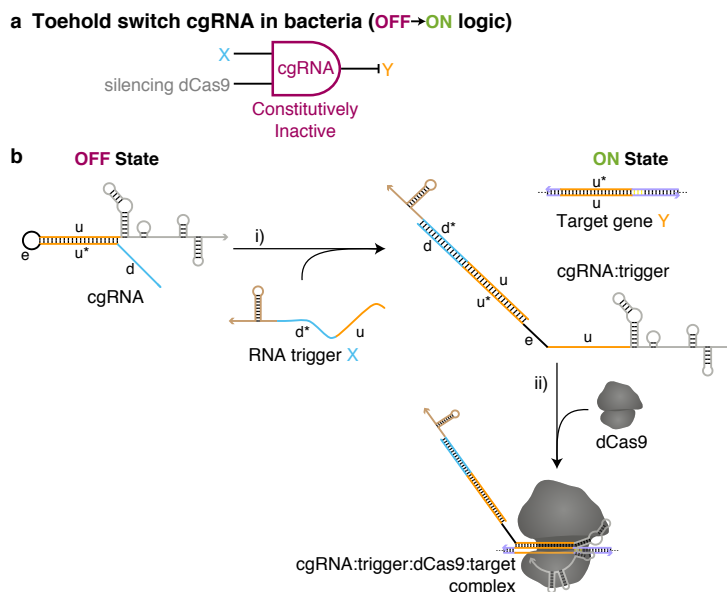


Figure 5.1: Constitutively inactive toehold switch cgRNAs (ON→OFF logic) with silencing dCas9 in *E. coli*. (a) Conditional logic: if X, then not Y. (b) Schematic of cgRNA mechanism. OFF state: the toehold switch cgRNA is constitutively inactive; the target-binding region (domain “u”; orange) is initially sequestered by a 5′ extension to inhibit recognition of target gene Y. ON state: in the presence of RNA trigger X, hybridization of the trigger to this 5′ extension (reaction arrow “i”) via the toehold region (blue) is intended to desquester the target-binding region and enable cgRNA direction of dCas9 function to target gene Y (reaction arrow “ii”).

state) were characterized using time course microplate fluorescence (Figure 5.3). In comparison to the ideal ON state of the standard gRNA, we see room for improvement for each of the four cgRNA/trigger pairs characterized, with distinctly poorer performance of cgRNA D + trigger X_D . On this basis, the three cgRNA/trigger pairs A, B, and C were selected for full experimental characterization.

Conditional response of the toehold switch mechanism was characterized by flow cytometry in *E. coli* expressing silencing dCas9 and a fluorescent protein reporter (mRFP) as the target gene Y (Figure 5.4a). The toehold switch cgRNA exhibits a conditional OFF→ON response to the expression of RNA trigger X, with OFF state imperfect relative to the ideal OFF state (no-target gRNA control) and the ON state imperfect relative to the ideal ON state (standard gRNA control). For a library of three orthogonal toehold switch cgRNA/trigger pairs, we observe a median ≈ 3 -fold OFF→ON conditional response to the expression of the cognate trigger and median crosstalk of $\approx 20\%$ between noncognate cgRNA/trigger combinations. Recently, Siu and Chen demonstrated a median ≈ 6.6 -fold OFF→ON conditional response using

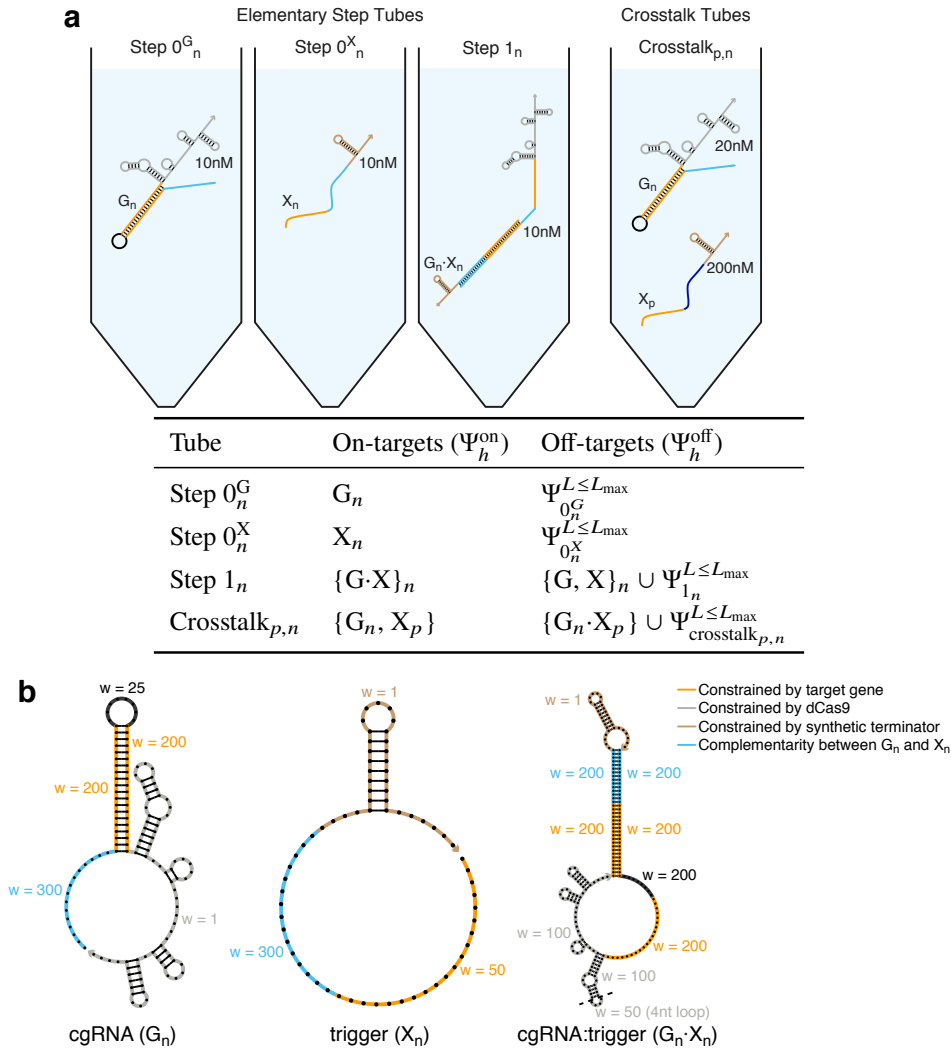


Figure 5.2: Target test tubes for sequence design of orthogonal toehold switch cgRNAs. (a) Top: Target test tube schematics. Bottom: Target test tube details. Each target test tube contains the depicted on-target complexes (each with the depicted target structure and target concentration) and the off-target complexes listed in the table (each with vanishing target concentration). The on-target structures depicted above are used in the mechanism schematic of Figure 5.1. To simultaneously design N orthogonal systems, the total number of target test tubes is $|\Omega| = N^2 + 2N$. $L_{\text{max}} = 2$ for all tubes. Design conditions: RNA in 1 M Na^+ at 37 °C.³⁸ (b) Nucleotide defect weights for sequence design of toehold switch cgRNAs. Nucleotides in a given sequence domain within a given complex are assigned a defect weight w as depicted.

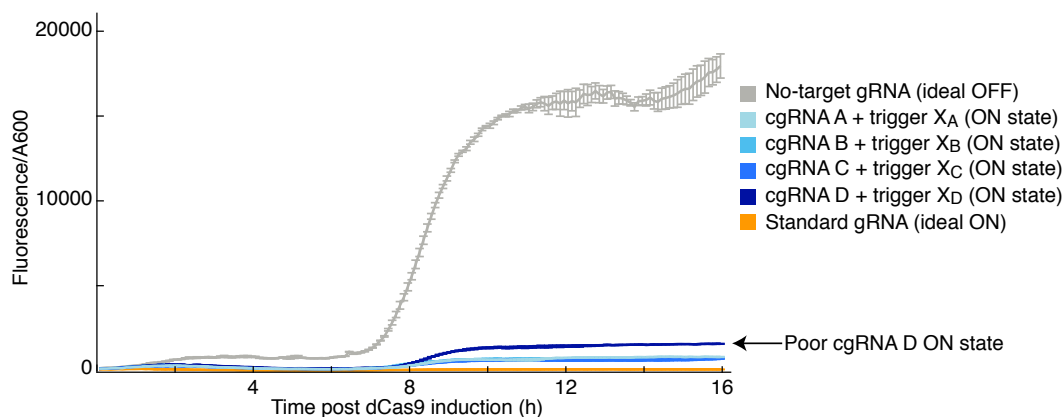


Figure 5.3: Characterization of ON state of four orthogonal toehold switch cgRNAs in *E. coli*. Fluorescence traces of cgRNAs A–C with cognate trigger are overlapping, while cgRNA D with cognate trigger produces significantly higher fluorescence (further from ideal ON standard gRNA). Time course microplate fluorescence data normalized by A600. Mean \pm estimated standard error over $N = 3$ replicate wells.

toehold switch cgRNAs with subtly different structural details in the sequestration of the target-binding region.⁹⁸

In an effort to improve performance of the toehold switch mechanism, we investigated the effect of the cognate trigger domain length on the activity of the cgRNA ON state. The effect of trigger domain length on ON state activity was characterized by time course microplate fluorescence for strains constitutively expressing toehold switch cgRNA A, and cognate trigger X_A with truncations of the strand displacement domain “u” (0-20 nt stem trigger, Figure 5.5a) and truncations or extension of the toehold domain “d*” (0-20 nt toehold trigger, Figure 5.5b; 20 nt extended toehold domain strain also included a 5 nt complementary extension for cgRNA toehold domain “d”; see Figure 5.1b for domain labeled mechanism schematic). As expected, we observed a significant increase in fluorescence with expression of the cognate trigger lacking the strand displacement domain (i.e., hybridization toehold domain only is insufficient to produce the observed OFF \rightarrow ON conditional response; cgRNA A + 0 nt stem trigger, Figure 5.5a). Somewhat surprisingly, a strand displacement domain of only 5 nt (cgRNA A + 5 nt stem trigger) resulted in a significant decrease in fluorescence, and an OFF \rightarrow ON conditional response comparable to that of the full-length strand displacement domain (cgRNA A + 20 nt stem trigger). This suggests that the sequestration of the target-binding region by the 20 nt reverse complementary sequence of the 5' extension is marginal, and hence that the cgRNA OFF state could be improved through extension of the target-

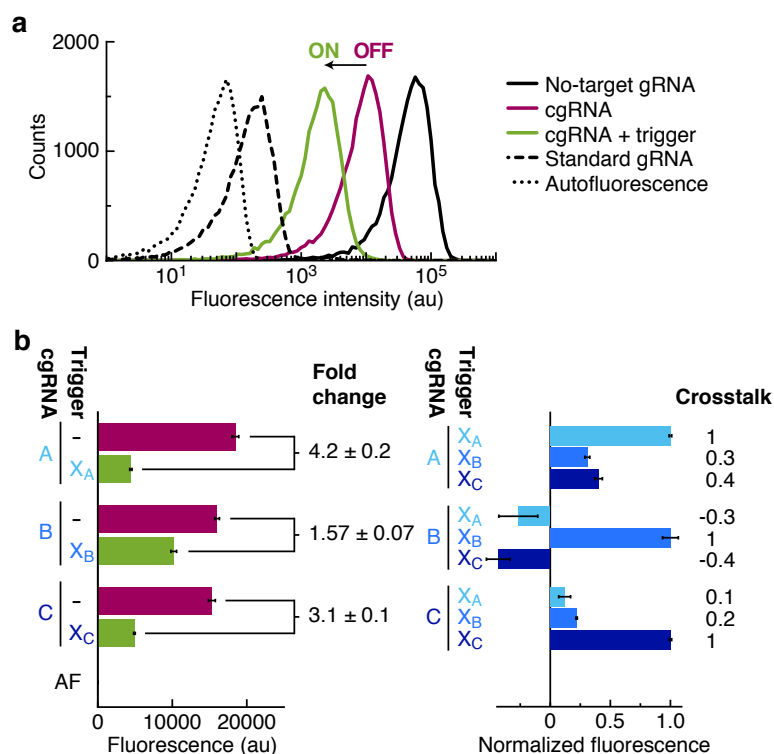


Figure 5.4: Programmable conditional function of three orthogonal toehold switch cgRNAs (OFF→ON logic) with silencing dCas9 in *E. coli*. (a) Expression of RNA trigger X toggles the cgRNA from OFF→ON, leading to a decrease in fluorescence. Single-cell fluorescence intensities via flow cytometry. Induced expression (aTc) of silencing dCas9 and constitutive expression of mRFP target gene Y and either: no-target gRNA that lacks target-binding region (ideal OFF state), cgRNA (OFF state), cgRNA + RNA trigger X (ON state), or standard gRNA (ideal ON state). Autofluorescence (AF): cells with no mRFP. (b) Programmable conditional regulation using three orthogonal cgRNAs (A, B, and C). Left: Raw fluorescence depicting OFF→ON conditional response to cognate trigger (fold change = OFF/ON = [(no trigger)–AF]/[(cognate trigger)–AF]). Right: Normalized fluorescence depicting orthogonality between noncognate cgRNA/trigger pairs (crosstalk = [(noncognate trigger) – (no trigger)]/[(cognate trigger) – (no trigger)]). Bar graphs depict mean ± estimated standard error calculated based on the mean single-cell fluorescence over 20,000 cells for each of $N = 3$ replicate wells (fold change and crosstalk calculated with uncertainty propagation).

binding region (orange domain “u” in Figure 5.1b). Truncation of trigger strand displacement domains to 5 nt could potentially yield a significant improvement to the orthogonality of the library of cgRNAs, as the strand displacement domain “u” is shared between all triggers and may be a major contributor to crosstalk. Truncation of the toehold domain by only three nucleotides (cgRNA A + 12 nt toehold trigger, Figure 5.5b) results in a significant loss of cgRNA function, while a 5 nt extension of both trigger and cgRNA toehold (cgRNA A-20 + 20 nt toehold trigger) performs no better than the 15 nt toehold.

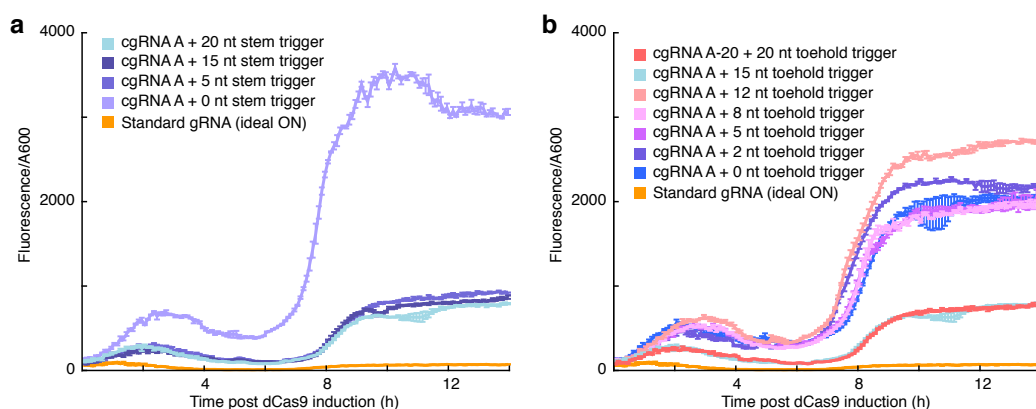


Figure 5.5: Characterization of toehold switch cgRNA with varied trigger domain dimensions. (a) Performance of cgRNA ON state with 0-20 nt strand displacement domain (truncation of domain “u”). Triggers with 0-20 nt strand displacement domain were expressed constitutively with the the previously characterized cognate cgRNA (with 15 nt toehold domain “d”, 20 nt sequestration domain “u*”). A 5 nt strand displacement domain was sufficient for achieving the observed ON state. (b) Performance of cgRNA ON state with 0-20 nt trigger toehold region (truncation of trigger domain “d*”, or extension of trigger domain “d*” and cgRNA domain “d”). Triggers with 0-15 nt toehold domains were expressed constitutively with the previously characterized cognate cgRNA A (with 15 nt cgRNA domain “d”). Trigger with an extended 20 nt toehold domain was expressed constitutively with an extended-toehold cognate cgRNA (20 nt cgRNA domain “d”). Trigger toeholds of length 0-12 nt did not toggle the cgRNA from OFF→ON. The OFF→ON conditional response with a 20 nt cgRNA/trigger toehold is comparable to the previously characterized 15 nt toehold. Time course microplate fluorescence data normalized by A600. Mean \pm estimated standard error over $N = 3$ replicate wells.

Unlike the splinted switch mechanism for ON→OFF logic, toehold switch cgRNAs for OFF→ON logic are not allosteric, as the cgRNA initially down-regulates cgRNA:dCas9 function by sequestering the target-binding region (orange domain “u*” in Figure 5.1b), resulting in only partial sequence-independence between trigger X and target gene Y (as “u” is a

subsequence of both X and Y). This partial sequence dependence is not necessarily limiting for synthetic biology applications where the trigger can be rationally designed and expressed exogenously, but does pose a limitation in situations where X and Y are both endogenous sequences. Another potential limitation for the detection of endogenous sequences is the likely continued association of trigger with cgRNA in complex with dCas9 (i.e., the cgRNA is bound by trigger in its active conformation), as the presence of a long (e.g., hundreds or thousands of nucleotides for mRNA) trigger may inhibit the downstream function of the Cas protein effector. This is of particular concern in eukaryotes, in which the active transport of mRNAs out of the nucleus will potentially sequester active cgRNA:trigger:effector complex from nuclear dsDNA targets. The relatively poor conditional response as compared to existing ON→OFF mechanisms (including the splinted switch mechanism of Chapter 4), the partial sequence dependence of trigger X and target Y, and potential issues for use of the toehold switch cgRNA with mRNA triggers motivate the development of an improved constitutively inactive cgRNA with a fundamentally different mechanism. However, the library of toehold cgRNAs developed exhibited the intended OFF→ON conditional function with selectivity for cognate trigger, and, with potential improvements to orthogonality, may prove useful as regulators for synthetic biology.

CONCLUSIONS AND FUTURE DIRECTIONS

The present work represents only a first step toward our long-term goal of engineering programmable conditional regulators that function robustly in living organisms. Here, I describe progress on multiple fronts: 1) In vitro, we demonstrate a candidate molecular mechanism for conditional regulation with conditional guide RNAs (cgRNAs) in a reconstituted setting, with direct evidence of the interactions of the species involved (cgRNA, trigger, target, and Cas9 effector protein), and the programmability of this cgRNA mechanism based on nucleic acid hybridization; 2) In *E. coli* expressing candidate cgRNAs with an array of sequence inserts in the presence and absence of an insert-complementary trigger, we demonstrate that gRNA activity tolerates significant modification to its structure, and provide a basis for engineering allosteric (i.e., sequence-independent) cgRNAs for conditional regulation in living organisms; 3) In *E. coli* expressing cgRNA regulators and RNA triggers, we demonstrate mechanisms for both logical directions of conditional regulation: ON→OFF logic with constitutively active cgRNAs that are conditionally inactivated by a cognate RNA trigger, and OFF→ON logic with constitutively inactive cgRNAs that are conditionally activated by a cognate RNA trigger; 4) To leverage the programmability of these dynamic regulators, we establish a computational framework for automated sequence design of libraries of orthogonal cgRNA/trigger pairs using the reaction pathway engineering tools within NUPACK; 5) These contributions, in sum, demonstrate the applicability of dynamic RNA nanotechnology for programmable conditional regulation in living cells. In order to develop cgRNAs into a versatile platform for biological research, a number of major improvements are needed. The work presented here points to several prospective paths forward, discussed in the following sections, followed by a discussion of the near- and longer-term applications that programmable conditional regulation with cgRNAs might enable.

6.1 Developing cgRNA mechanisms with improved dynamic range

The single and double insert studies of candidate cgRNAs detailed in Chapter 3 yielded a maximum observed conditional response of ≈ 41 -fold and a maximum fractional dynamic range of ≈ 0.2 at moderate induction of dCas9, compared to the

>200-fold conditional response and unity fractional dynamic range of the standard gRNA (ideal ON) and no-target gRNA (ideal OFF) controls (Table C.2), with performance seemingly limited by an OFF state with significantly higher (undesirable) activity than that of the control. For a library of orthogonal splinted switch cgRNAs (Chapter 4), we observed a further reduction in both conditional response and dynamic range, as could be expected for sequence design subject to more significant constraint. Although the mechanisms described here are of potential use as conditional regulators for synthetic biology, for the more highly constrained design of conditional regulators as a tool for biological study with endogenous trigger it is desirable to exploit the full regulatory dynamic range of standard gRNAs and achieve >100-fold conditional responses. One potential means to improve the dynamic range of conditional regulation with cgRNAs is to improve the observed OFF state via competition of a no-target gRNA with higher putative affinity for dCas9, as was described in Section 4.2. An improved OFF state could also be achieved by incorporating modifications that destabilize the gRNA structure but do not significantly effect ON state activity,⁸⁹ plausibly “lowering the bar” for conditional response via hybridization of trigger. For ON→OFF mechanisms in which OFF state is limited by the undesirable activity of a cgRNA:trigger:effector:dsDNA quadruplex (the extent of which has yet to be characterized), the use of Cas9 engineered to have reduced affinity for dsDNA binding¹²³ may also improve the dynamic range.

The development of novel cgRNA mechanisms and/or refinement of the sequence design process is also merited in the pursuit of cgRNA mechanisms with improved performance. The increased fractional dynamic range observed for both a) an increase in trigger binding domain length, and b) a decrease in dCas9 expression (Chapter 3) suggests that engineering cgRNAs with increased $|\Delta\Delta G|$ of trigger hybridization may improve performance. With the present design approach, we are limited by our ability to design long, unstructured sequence for orthogonal cgRNA/trigger pairs (e.g., a target structure of 70 consecutive unpaired nucleotides for the splinted switch trigger). The current design implementation uses “long” domains (i.e., designed domains of adequate length) and “unstructured” domains of designed sequence in combination as a proxy to guarantee adequate $|\Delta\Delta G|$ of trigger hybridization. Defining sequence similarity constraints to increase G-C content of the designed sequence is possible with the current version of NUPACK, and is an easily implementable approach to increasing $|\Delta\Delta G|$ of trigger hybridization without a computationally expensive increase in domain length. Intentional introduction of structure into the designed sequence domains (i.e., specified complementarity within

the target structure of the currently unstructured inserts) with a concurrent increase in domain length could further increase trigger affinity while preserving our ability to design orthogonal regulators; this approach would also be potentially compatible with G-C content similarity constraints to ensure adequate $|\Delta\Delta G|$ for a given target structure. The extent to which such structured inserts are tolerated by the cgRNA ON state, however, has yet to be characterized. Recent developments in the NUPACK design algorithm enable another possible path to increasing cgRNA/trigger affinity, namely the use of “soft constraints”—secondary design objectives that are not strictly satisfied throughout the design iteration—which allow for the explicit specification of a target duplex free energy, and, combined with a decreased weight for insert domain target structure, could be used for the automated design of sequences with (potentially) structured inserts and high $|\Delta\Delta G|$ of trigger hybridization. Novel mechanism designs in which the cgRNA is composed of two or more strands, with nicks in the solvent-exposed loops (as is the case for the wild-type CRISPR/Cas9 guide RNA^{56,60}), would allow for sequestration of part of the cgRNA OFF state, yielding a bimolecular leakage reaction (i.e., association of the two halves of the cgRNA) and hence reduced dCas9 affinity for the cgRNA in its OFF state. These “split cgRNAs” would have the added benefit of mitigating topological limitations to trigger hybridization,¹²⁴ which would be particularly relevant for long (e.g., mRNA) trigger species.

In pursuing improved cgRNA performance, further understanding of the structure/function relationships between cgRNAs, triggers, and Cas effectors is needed to ascertain how to robustly achieve both a strong ON state and a clean OFF state depending on the presence/absence of the cognate trigger, and to identify the underlying causes of current performance limitations. Studying the effect of sequence and structural modifications at a higher resolution (i.e., beyond the four insert sites detailed here) may inform the design of novel cgRNA mechanisms. For our current cgRNAs, we have yet to fully characterize the mechanism by which the cgRNA OFF state is achieved; the observed conditional response could potentially result from inhibition of cgRNA:dCas9 complex formation, inhibition of dsDNA target binding by the cgRNA:dCas9 complex, decreased silencing efficacy with a fully formed cgRNA:dCas9:target complex, or a combination of the above. As such, the key determinants of the non-ideal OFF-state performance are unknown. In vitro study of the interactions of cgRNAs, triggers, Cas effectors, and dsDNA targets (similar to those described in Chapter 2, but using dCas9 as the protein effector) may shed light on the mechanism of action and hence direct efforts to address non-

ideal performance. Lastly, toward the use of cgRNAs for conditional regulation in eukaryotes, a systematic study of candidate cgRNA modifications analogous to that of Chapter 3 is merited. We have successfully demonstrated the conditional response of a library of constitutively active cgRNAs in cultured mammalian cells,¹²⁵ but mammalian-specific optimization of cgRNA mechanisms will be needed for improved performance.

6.2 Detection of endogenous mRNA inputs with cgRNAs

To enable tissue-selective regulation in living organisms, it is critical that cgRNAs are able to efficiently detect a trigger that is a subsequence of a longer endogenous RNA (e.g., a subsequence of an mRNA). Detection of a subsequence of a full-length mRNA poses significant additional challenges relative to detection of a short RNA trigger,^{45,98} increasing the degree of difficulty in achieving a conditional response that exploits the full dynamic range. The strategies for improving cgRNA performance described above will be of key importance for achieving this goal, but challenges specific to endogenous mRNA targets exist as well. Significant constraint of the sequence of trigger-binding domains (constrained to be complementary to a window of the endogenous trigger sequence) poses a challenge to the design of cgRNA sequence; relaxing overall constraint on design by allowing the target-binding region to be selected from a library of PAM-adjacent sequences within the target gene may be beneficial. Mechanisms with partial sequence dependence (such as the toehold switch mechanism) will not be compatible with the use of an endogenous trigger, and as such the development of sequence-independent (i.e., allosteric) mechanisms is essential. cgRNA mechanisms with secondary structure intentionally incorporated into insert domains (discussed in Section 6.1) also pose a challenge to the selection of an endogenous trigger, as windows of endogenous sequence need to be compatible with the target structure; as such, for structured inserts, it may be necessary to engineer mechanisms with insert domains that are only partially complementary to the constrained trigger. The accessibility of the cgRNA-hybridizing subsequence of an endogenous trigger may also prove to be an issue due to secondary or tertiary structure of the longer RNA sequence, and/or competition with endogenous binding proteins; screening of candidate trigger subsequences for high accessibility by *in vitro*⁴⁵ or *in vivo*^{126,127} methods may be required to enable the design of functional cgRNAs with endogenous trigger.

6.3 Mechanism engineering for versatile constitutively inactive (OFF→ON) cgRNAs

As discussed in Chapter 5, the toehold switch mechanisms studied here and elsewhere⁹⁸ have partial sequence dependence between target and trigger. For future applications, it is important that cgRNA regulators be allosteric, so that the sequence of target gene Y places no restriction on the sequence of RNA trigger X, enabling independent control over the regulatory scope (using X) and the regulatory target (using Y). The use of mRNA or other endogenous species as trigger may also be incompatible with the toehold switch cgRNA mechanism and other mechanisms in which the active state of the cgRNA is the cgRNA:trigger complex, particularly in eukaryotic cells, in which mRNA and other endogenous targets are actively exported from the nucleus and hence actively sequestered from nuclear downstream targets. A constitutively inactive mechanism (OFF→ON) is, however, particularly valuable for spatiotemporal control of gene knockdown with minimal perturbation to the natural system, as downstream function is only mediated by cgRNA in cells with the tissue marker of interest. The incompatibility with future applications of interest and the relatively poor performance of the toehold switch mechanism motivates the development of a fundamentally different constitutively inactive mechanism. The goals of sequence-independence and mobility (i.e., dissociation from trigger) of the ON state of an OFF→ON cgRNA could be achieved by the logical inversion of an ON→OFF cgRNA. Expression of a duplex as a single transcript linked by a self-cleaving ribozyme¹²⁸ would insure a 1:1 stoichiometric ratio of strands for multi-stranded cgRNAs (note that this self-cleaving approach to generating multi-stranded cgRNAs may present a issue if an uncleaved transcript is active, resulting in a poor OFF state). Finally, development of RNA-targeting Cas13 cgRNAs could circumvent issues of cgRNA:mRNA association, as endogenous trigger X and RNA target Y could both be localized to the cytoplasm; however, the tolerance of the Cas13 gRNA to modification has yet to be adequately established.

6.4 Future applications for cgRNAs

The ability to rationally design cgRNAs suggests a conceptual framework for enabling biologists to exert spatiotemporal control over regulatory perturbations in living organisms using CRISPR/Cas technology. The target of regulation, target Y, is programmed via the cgRNA target-binding sequence, which can be reprogrammed as desired. A trigger X can be selected to restrict downstream regulatory functions to only those cells that express trigger X, thereby targeting a specific cell type,

tissue, organ, or temporal expression profile. For allosteric (sequence-independent) cgRNA mechanisms, trigger X and target Y can be selected independently, providing a versatile tool for probing genetic circuitry and studying the role of genes that lead to unwanted developmental perturbations (including lethality) when regulated globally with existing programmable regulators. If engineered to be appropriately robust, this same cgRNA logic would have attractive therapeutic potential. Restricting gene editing to a tissue or cell type of interest could provide a basis for gene therapy limited to cells in which a disease is manifest. Similarly, with trigger X as a programmable disease marker and target Y as an essential target, regulation with cgRNAs could enable targeted treatment via conditional cell death.

The potential to design large libraries of interoperable cgRNA/trigger components makes cgRNA regulation an ideal platform for scalable synthetic biology. With mechanisms for both ON→OFF and OFF→ON logical directions, and the ability to select other cgRNA or trigger species as the target of transcriptional regulation, cgRNA regulation may be implemented to construct large, integrated, and complex circuits.

BIBLIOGRAPHY

1. Kallenbach, N. R., Ma, R.-I. & Seeman, N. C. An immobile nucleic acid junction constructed from oligonucleotides. *Nature* **305**, 829–831 (1983).
2. Chen, J. & Seeman, N. C. Synthesis from DNA of a molecule with the connectivity of a cube. *Nature* **350**, 631–633 (1991).
3. Winfree, E., Liu, F., Wenzler, L. A. & Seeman, N. C. Design and self-assembly of two-dimensional DNA crystals. *Nature* **394**, 539–544 (1998).
4. Seeman, N. C. & Sleiman, H. F. DNA nanotechnology. *Nat. Rev. Mater.* **3**, 17068 (2017).
5. Ke, Y., Castro, C. & Choi, J. H. Structural DNA Nanotechnology: Artificial Nanostructures for Biomedical Research. *Annu. Rev. Biomed. Eng.* **20**, 375–401 (2018).
6. Rothmund, P. W. Folding DNA to create nanoscale shapes and patterns. *Nature* **440**, 297–302 (2006).
7. Douglas, S. M. *et al.* Self-assembly of DNA into nanoscale three-dimensional shapes. *Nature* **459**, 414–418 (2009).
8. Funke, J. J. & Dietz, H. Placing molecules with Bohr radius resolution using DNA origami. *Nat. Nanotechnol.* **11**, 47–52 (2016).
9. Strauss, M. T., Schueder, F., Haas, D., Nickels, P. C. & Jungmann, R. Quantifying absolute addressability in DNA origami with molecular resolution. *Nat. Commun.* **9**, 1600 (2018).
10. Jaeger, L. TectoRNA: modular assembly units for the construction of RNA nano-objects. *Nucleic Acids Res.* **29**, 455–463 (2001).
11. Afonin, K. A. *et al.* In vitro assembly of cubic RNA-based scaffolds designed in silico. *Nat. Nanotechnol.* **5**, 676–682 (2010).
12. Guo, P. The emerging field of RNA nanotechnology. *Nat. Nanotechnol.* **5**, 833 (2010).
13. Grabow, W. W. & Jaeger, L. RNA self-assembly and RNA nanotechnology. *Acc. Chem. Res.* **47**, 1871–1880 (2014).
14. Jasinski, D., Haque, F., Binzel, D. W. & Guo, P. Advancement of the Emerging Field of RNA Nanotechnology. *ACS Nano* **11**, 1142–1164 (2017).
15. Geary, C., Rothmund, P. W. & Andersen, E. S. A single-stranded architecture for cotranscriptional folding of RNA nanostructures. *Science* **345**, 799–804 (2014).

16. Delebecque, C. J., Lindner, A. B., Silver, P. A. & Aldaye, F. A. Organization of intracellular reactions with rationally designed RNA assemblies. *Science* **333**, 470–474 (2011).
17. Li, M. *et al.* In vivo production of RNA nanostructures via programmed folding of single-stranded RNAs. *Nat. Commun.* **9**, 2196 (2018).
18. Zhang, D. Y. & Winfree, E. Control of DNA Strand Displacement Kinetics Using Toehold Exchange. *J Am Chem Soc* **131**, 17303–17314 (2009).
19. Zhang, D. Y. & Seelig, G. Dynamic DNA nanotechnology using strand-displacement reactions. *Nat. Chem.* **3**, 103–113 (2011).
20. Guo, Y. *et al.* Recent advances in molecular machines based on toehold-mediated strand displacement reaction. *Quant. Biol.* **5**, 25–41 (2017).
21. Shin, J. S. & Pierce, N. A. A synthetic DNA walker for molecular transport. *J. Am. Chem. Soc.* **126**, 10834–10835 (2004).
22. Jung, C., Allen, P. B. & Ellington, A. D. A stochastic DNA walker that traverses a microparticle surface. *Nat. Nanotechnol.* **11**, 157–163 (2016).
23. Thubagere, A. J. *et al.* A cargo-sorting DNA robot. *Science* **357**, eaan6558 (2017).
24. Seelig, G., Soloveichik, D., Zhang, D. Y. & Winfree, E. Enzyme-Free Nucleic Acid Logic Circuits. *Science* **314**, 1585–1588 (2006).
25. Qian, L. & Winfree, E. Scaling Up Digital Circuit Computation with DNA Strand Displacement Cascades. *Science* **332**, 1196–1201 (2011).
26. Cherry, K. M. & Qian, L. Scaling up molecular pattern recognition with DNA-based winner-take-all neural networks. *Nature* **559**, 370–388 (2018).
27. Dirks, R. M. & Pierce, N. A. Triggered amplification by hybridization chain reaction. *Proc. Natl. Acad. Sci.* **101**, 15275–15278 (2004).
28. Yin, P., Choi, H. M., Calvert, C. R. & Pierce, N. A. Programming biomolecular self-assembly pathways. *Nature* **451**, 318–322 (2008).
29. Choi, H. M. *et al.* Programmable in situ amplification for multiplexed imaging of mRNA expression. *Nat. Biotechnol.* **28**, 1208–1212 (2010).
30. Bath, J. & Turberfield, A. J. DNA nanomachines. *Nat. Nanotechnol.* **2**, 275–284 (2007).
31. Bi, S., Yue, S. & Zhang, S. Hybridization chain reaction: A versatile molecular tool for biosensing, bioimaging, and biomedicine. *Chem. Soc. Rev.* **46**, 4281–4298 (2017).
32. McCaskill, J. S. The equilibrium partition function and base pair binding probabilities for RNA secondary structure. *Biopolymers* **29**, 1105–1119 (1990).

33. Dirks, R. M. & Pierce, N. A. A partition function algorithm for nucleic acid secondary structure including pseudoknots. *J. Comput. Chem.* **24**, 1664–1677 (2003).
34. Dirks, R. M., Bois, J. S., Schaeffer, J. M., Winfree, E. & Pierce, N. A. Thermodynamic Analysis of Interacting Nucleic Acid Strands. *SIAM Rev.* **49**, 65–88 (2007).
35. Zadeh, J. N., Wolfe, B. R. & Pierce, N. A. Nucleic Acid Sequence Design via Efficient Ensemble Defect Optimization. *J. Comput. Chem.* **32**, 439–452 (2011).
36. Wolfe, B. R. & Pierce, N. A. Sequence Design for a Test Tube of Interacting Nucleic Acid Strands. *ACS Synth. Biol.* **4**, 1086–1100 (2015).
37. Wolfe, B. R., Porubsky, N. J., Zadeh, J. N., Dirks, R. M. & Pierce, N. A. Constrained Multistate Sequence Design for Nucleic Acid Reaction Pathway Engineering. *J. Am. Chem. Soc.* **139**, 3134–3144 (2017).
38. Serra, M. J. & Turner, D. H. Predicting thermodynamic properties of RNA. *Methods Enzymol.* **259**, 242–261 (1995).
39. SantaLucia, J. A unified view of polymer, dumbbell, and oligonucleotide DNA nearest-neighbor thermodynamics. *Proc. Natl. Acad. Sci.* **95**, 1460–1465 (1998).
40. Mathews, D. H., Sabina, J., Zuker, M. & Turner, D. H. Expanded Sequence Dependence of Thermodynamic Parameters Improves Prediction of RNA Secondary Structure. *J. Mol. Biol.* **288**, 911–940 (1999).
41. Wachsmuth, M., Findeiß, S., Weissheimer, N., Stadler, P. F. & Mörl, M. De novo design of a synthetic riboswitch that regulates transcription termination. *Nucleic Acids Res.* **41**, 2541–2551 (2013).
42. Chappell, J., Watters, K. E., Takahashi, M. K. & Lucks, J. B. A renaissance in RNA synthetic biology: New mechanisms, applications and tools for the future. *Curr. Opin. Chem. Biol.* **28**, 47–56 (2015).
43. Green, A. A., Silver, P. A., Collins, J. J. & Yin, P. Toehold switches: De-novo-designed regulators of gene expression. *Cell* **159**, 925–939 (2014).
44. Hochrein, L. M., Schwarzkopf, M., Shahgholi, M., Yin, P. & Pierce, N. A. Conditional dicer substrate formation via shape and sequence transduction with small conditional RNAs. *J. Am. Chem. Soc.* **135**, 17322–17330 (2013).
45. Hochrein, L. M., Ge, T. J., Schwarzkopf, M. & Pierce, N. A. Signal Transduction in Human Cell Lysate via Dynamic RNA Nanotechnology. *ACS Synth. Biol.* **7**, 2796–2802 (2018).
46. Li, J., Green, A. A., Yan, H. & Fan, C. Engineering nucleic acid structures for programmable molecular circuitry and intracellular biocomputation. *Nat. Chem.* **9**, 1056–1067 (2017).

47. Xie, M. & Fussenegger, M. Designing cell function: assembly of synthetic gene circuits for cell biology applications. *Nat. Rev. Mol. Cell Biol.* **19**, 507–525 (2018).
48. Jani, M. S., Veetil, A. T. & Krishnan, Y. Precision immunomodulation with synthetic nucleic acid technologies. *Nat. Rev. Mater.* **1** (2019).
49. Xie, Z., Liu, S. J., Bleris, L. & Benenson, Y. Logic integration of mRNA signals by an RNAi-based molecular computer. *Nucleic Acids Res.* **38**, 2692–2701 (2010).
50. Masu, H. *et al.* An activatable siRNA probe: Trigger-RNA-dependent activation of RNAi function. *Angew. Chemie - Int. Ed.* **48**, 9481–9483 (2009).
51. Kumar, D., Kim, S. H. & Yokobayashi, Y. Combinatorially inducible RNA interference triggered by chemically modified oligonucleotides. *J. Am. Chem. Soc.* **133**, 2783–2788 (2011).
52. Bindewald, E. *et al.* Multistrand Structure Prediction of Nucleic Acid Assemblies and Design of RNA Switches. *Nano Lett.* **16**, 1726–1735 (2016).
53. Knott, G. J. & Doudna, J. A. CRISPR-Cas guides the future of genetic engineering. *Science* **361**, 866–869 (2018).
54. Cameron, D. E., Bashor, C. J. & Collins, J. J. A brief history of synthetic biology. *Nat. Rev. Microbiol.* **12**, 381 (Apr. 1, 2014).
55. Brophy, J. A. N. & Voigt, C. A. Principles of genetic circuit design. *Nat. Methods* **11**, 508 (2014).
56. Barrangou, R. *et al.* CRISPR Provides Acquired Resistance Against Viruses in Prokaryotes. *Science* **315**, 1709 (Mar. 23, 2007).
57. Horvath, P. & Barrangou, R. CRISPR/Cas, the immune system of bacteria and archaea. *Science* **327**, 167–70 (2010).
58. Hille, F. *et al.* The Biology of CRISPR-Cas: Backward and Forward. *Cell* **172**, 1239–1259 (2018).
59. Sapranaukas, R. *et al.* The *Streptococcus thermophilus* CRISPR/Cas system provides immunity in *Escherichia coli*. *Nucleic Acids Res.* **39**, 9275–9282 (2011).
60. Jinek, M. *et al.* A programmable dual-RNA-guided DNA endonuclease in adaptive bacterial immunity. *Science* **337**, 816–822 (2012).
61. Abudayyeh, O. O. *et al.* C2c2 is a single-component programmable RNA-guided RNA-targeting CRISPR effector. *Science* **353**, aaf5573 (2016).
62. Sander, J. D. & Joung, J. K. CRISPR-Cas systems for editing, regulating and targeting genomes. *Nat. Biotechnol.* **32**, 347–55 (2014).

63. Ishino, Y., Krupovic, M. & Forterre, P. History of CRISPR-Cas from Encounter with a Mysterious Repeated Sequence to Genome Editing Technology. *J. Bacteriol.* **200**, e00580–17 (2018).
64. Eid, A. & Mahfouz, M. M. Genome editing: The road of CRISPR/Cas9 from bench to clinic. *Exp. Mol. Med.* **48**, e265–11 (2016).
65. Cong, L. *et al.* Multiplex Genome Engineering Using CRISPR/Cas Systems. *Science* **339**, 819–823 (2013).
66. Mali, P. *et al.* CAS9 transcriptional activators for target specificity screening and paired nickases for cooperative genome engineering. *Nat. Biotechnol.* **31**, 833–838 (2013).
67. Zetsche, B. *et al.* Multiplex gene editing by CRISPR-Cpf1 using a single crRNA array. *Nat. Biotechnol.* **35**, 31–34 (2017).
68. Qi, L. S. *et al.* Repurposing CRISPR as an RNA-guided platform for sequence-specific control of gene expression. *Cell* **152**, 1173–1183 (2013).
69. Larson, M. H. *et al.* CRISPR interference (CRISPRi) for sequence-specific control of gene expression. *Nat. Protoc.* **8**, 2180–96 (2013).
70. Gilbert, L. A. *et al.* CRISPR-mediated modular RNA-guided regulation of transcription in eukaryotes. *Cell* **154**, 442–451 (2013).
71. Konermann, S. *et al.* Transcriptome Engineering with RNA-Targeting Type VI-D CRISPR Effectors. *Cell* **173**, 665–676.e14 (2018).
72. Abudayyeh, O. O. *et al.* RNA targeting with CRISPR-Cas13. *Nature* **550**, 280–284 (2017).
73. Cox, D. B. *et al.* RNA editing with CRISPR-Cas13. *Science* **358**, 1019–1027 (2017).
74. Aman, R. *et al.* RNA virus interference via CRISPR/Cas13a system in plants. *Genome Biol.* **19**, 1 (2018).
75. O’Connell, M. R. Molecular Mechanisms of RNA Targeting by Cas13-containing Type VI CRISPR–Cas Systems. *J. Mol. Biol.* **431**, 66–87 (2019).
76. Terns, M. P. CRISPR-Based Technologies: Impact of RNA-Targeting Systems. *Mol. Cell* **72**, 404–412 (2018).
77. Chen, B. *et al.* Dynamic imaging of genomic loci in living human cells by an optimized CRISPR/Cas system. *Cell* **155**, 1479–1491 (2013).
78. Knight, S. C., Tjian, R. & Doudna, J. A. Genomes in Focus: Development and Applications of CRISPR-Cas9 Imaging Technologies. *Angew. Chemie - Int. Ed.* **57**, 4329–4337 (2018).
79. Hilton, I. B. *et al.* Epigenome editing by a CRISPR-Cas9-based acetyltransferase activates genes from promoters and enhancers. *Nat. Biotechnol.* **33**, 510–7 (2015).

80. Gaudelli, N. M. *et al.* Programmable base editing of A•T to G•C in genomic DNA without DNA cleavage. *Nature* **551**, 464–471 (2017).
81. Zhou, W. & Deiters, A. Conditional Control of CRISPR/Cas9 Function. *Angew. Chemie - Int. Ed.* **55**, 5394–5399 (2016).
82. Aubrey, B. J. *et al.* An Inducible Lentiviral Guide RNA Platform Enables the Identification of Tumor-Essential Genes and Tumor-Promoting Mutations In Vivo. *Cell Rep.* **10**, 1422–1432 (2015).
83. Bertero, A. *et al.* Optimized inducible shRNA and CRISPR/Cas9 platforms for in vitro studies of human development using hPSCs. *Development* **143**, 4405–4418 (2016).
84. Chen, T. *et al.* Chemically Controlled Epigenome Editing through an Inducible dCas9 System. *J. Am. Chem. Soc.* **139**, 11337–11340 (2017).
85. Nihongaki, Y., Otabe, T. & Sato, M. Emerging Approaches for Spatiotemporal Control of Targeted Genome with Inducible CRISPR-Cas9. *Anal. Chem.* **90**, 429–439 (2018).
86. Shen, Z. *et al.* Conditional knockouts generated by engineered CRISPR-Cas9 endonuclease reveal the roles of coronin in *C. elegans* neural development. *Dev. Cell* **30**, 625–636 (2014).
87. Ablain, J., Durand, E. M., Yang, S., Zhou, Y. & Zon, L. I. A CRISPR/Cas9 vector system for tissue-specific gene disruption in zebrafish. *Dev. Cell* **32**, 756–764 (2015).
88. Hirosawa, M. *et al.* Cell-type-specific genome editing with a microRNA-responsive CRISPR-Cas9 switch. *Nucleic Acids Res.* **45**, e118–e118 (2017).
89. Briner, A. E. *et al.* Guide RNA functional modules direct Cas9 activity and orthogonality. *Mol. Cell* **56**, 333–339 (2014).
90. Nowak, C. M., Lawson, S., Zerez, M. & Bleris, L. Guide RNA engineering for versatile Cas9 functionality. *Nucleic Acids Res.* **44**, 9555–9564 (2016).
91. Liu, Y. *et al.* Directing cellular information flow via CRISPR signal conductors. *Nat. Methods* **13**, 938–944 (2016).
92. Tang, W., Hu, J. H. & Liu, D. R. Aptazyme-embedded guide RNAs enable ligand-responsive genome editing and transcriptional activation. *Nat. Commun.* **8**, 15939 (2017).
93. Kundert, K. *et al.* Controlling CRISPR-Cas9 with ligand-activated and ligand-deactivated sgRNAs. *Nat. Commun.* **10**, 2127 (2019).
94. Lee, Y. J., Hoynes-O'Connor, A., Leong, M. C. & Moon, T. S. Programmable control of bacterial gene expression with the combined CRISPR and antisense RNA system. *Nucleic Acids Res.* **44**, 2462–2473 (2016).

95. Ferry, Q. R., Lyutova, R. & Fulga, T. A. Rational design of inducible CRISPR guide RNAs for de novo assembly of transcriptional programs. *Nat. Commun.* **8**, 14633 (2017).
96. Mückl, A., Schwarz-Schilling, M., Fischer, K. & Simmel, F. C. Filamentation and restoration of normal growth in *Escherichia coli* using a combined CRISPRi sgRNA/antisense RNA approach. *PLoS One* **13**, e0198058 (2018).
97. Jain, P. K. *et al.* Development of Light-Activated CRISPR Using Guide RNAs with Photocleavable Protectors. *Angew. Chemie - Int. Ed.* **55**, 12440–12444 (2016).
98. Siu, K. H. & Chen, W. Riboregulated toehold-gated gRNA for programmable CRISPR–Cas9 function. *Nat. Chem. Biol.* **15**, 217–220 (2019).
99. Oesinghaus, L. & Simmel, F. C. Switching the activity of Cas12a using guide RNA strand displacement circuits. *Nat. Commun.* **10**, 2092 (2019).
100. Konermann, S. *et al.* Genome-scale transcriptional activation by an engineered CRISPR-Cas9 complex. *Nature* **517**, 583–8 (2015).
101. Zalatan, J. G. *et al.* Engineering complex synthetic transcriptional programs with CRISPR RNA scaffolds. *Cell* **160**, 339–350 (2015).
102. Ma, H. *et al.* Multiplexed labeling of genomic loci with dCas9 and engineered sgRNAs using CRISPRainbow. *Nat. Biotechnol.* **34**, 528–530 (2016).
103. Wang, S., Su, J. H., Zhang, F. & Zhuang, X. An RNA-aptamer-based two-color CRISPR labeling system. *Sci. Rep.* **6**, 26857 (2016).
104. Liao, H. K. *et al.* In Vivo Target Gene Activation via CRISPR/Cas9-Mediated Trans-epigenetic Modulation. *Cell* **171**, 1495–1507 (2017).
105. Chavez, A. *et al.* Comparison of Cas9 activators in multiple species. *Nat. Methods* **13**, 563–567 (2016).
106. Shao, S. *et al.* Long-term dual-color tracking of genomic loci by modified sgRNAs of the CRISPR/Cas9 system. *Nucleic Acids Res.* **44**, e86–e86 (2016).
107. Jinek, M. *et al.* Structures of Cas9 endonucleases reveal RNA-mediated conformational activation. *Science* **343**, 1247997 (2014).
108. Anders, C., Niewoehner, O., Duerst, A. & Jinek, M. Structural basis of PAM-dependent target DNA recognition by the Cas9 endonuclease. *Nature* **513**, 569–573 (2014).
109. Nishimasu, H. *et al.* Crystal structure of Cas9 in complex with guide RNA and target DNA. *Cell* **156**, 935–949 (2014).
110. Jiang, F., Zhou, K., Ma, L., Gressel, S. & Doudna, J. A. A Cas9-guide RNA complex preorganized for target DNA recognition. *Science* **348**, 1477–1481 (2015).

111. Fu, Y., Sander, J. D., Reyon, D., Cascio, V. M. & Joung, J. K. Improving CRISPR-Cas nuclease specificity using truncated guide RNAs. *Nat. Biotechnol.* **32**, 279–284 (2014).
112. Dang, Y. *et al.* Optimizing sgRNA structure to improve CRISPR-Cas9 knock-out efficiency. *Genome Biol.* **16**, 280 (2015).
113. Xu, X., Duan, D. & Chen, S. J. CRISPR-Cas9 cleavage efficiency correlates strongly with target sgRNA folding stability: from physical mechanism to off-target assessment. *Sci. Rep.* **7**, 143 (2017).
114. Zhou, H.-X., Rivas, G. & Minton, A. P. Macromolecular Crowding and Confinement: Biochemical, Biophysical, and Potential Physiological Consequences. *Annu. Rev. Biophys.* **37**, 375–397 (2008).
115. Lipfert, J., Doniach, S., Das, R. & Herschlag, D. Understanding Nucleic Acid–Ion Interactions. *Annu. Rev. Biochem.* **83**, 813–841 (2014).
116. Cencic, R. *et al.* Protospacer Adjacent Motif (PAM)-Distal Sequences Engage CRISPR Cas9 DNA Target Cleavage. *PLOS ONE* **9**, e109213 (2014).
117. Jiang, F. & Doudna, J. A. CRISPR–Cas9 Structures and Mechanisms. *Annu. Rev. Biophys.* **46**, 505–529 (2017).
118. Taylor, J. R. *An Introduction to Error Analysis: The Study of Uncertainties in Physical Measurements* (University Science Books, Sausalito, CA, 1997).
119. Wright, A. V. *et al.* Rational design of a split-Cas9 enzyme complex. *Proc. Natl. Acad. Sci.* **112**, 2984 (2015).
120. Anders, C., Niewoehner, O., Jinek, M., Woodson, S. A. & Allain, F. H. T. in, 515–537 (Academic Press, 2015).
121. Thyme, S. B., Akhmetova, L., Montague, T. G., Valen, E. & Schier, A. F. Internal guide RNA interactions interfere with Cas9-mediated cleavage. *Nat. Commun.* **7**, 11750 (2016).
122. Graf, R., Li, X., Chu, V. T. & Rajewsky, K. sgRNA Sequence Motifs Blocking Efficient CRISPR/Cas9-Mediated Gene Editing. *Cell Rep.* **26**, 1098–1103 (2019).
123. Kleinstiver, B. P. *et al.* High-fidelity CRISPR–Cas9 nucleases with no detectable genome-wide off-target effects. *Nature* **529**, 490 (2016).
124. Bois, J. S. *et al.* Topological constraints in nucleic acid hybridization kinetics. *Nucleic Acids Res.* **33**, 4090–4095 (2005).
125. Hanewich-Hollatz, M. H., Chen, Z., Hochrein, L. M., Huang, J. & Pierce, N. A. Conditional Guide RNAs: Programmable Conditional Regulation of CRISPR/Cas Function in Bacterial and Mammalian Cells via Dynamic RNA Nanotechnology. *ACS Cent. Sci.* doi:10.1021/acscentsci.9b00340 (2019).

126. Mihailovic, M. K. *et al.* High-throughput in vivo mapping of RNA accessible interfaces to identify functional sRNA binding sites. *Nat. Commun.* **9**, 4084 (2018).
127. Watters, K. E., Yu, A. M., Strobel, E. J., Settle, A. H. & Lucks, J. B. Characterizing RNA structures in vitro and in vivo with selective 2'-hydroxyl acylation analyzed by primer extension sequencing (SHAPE-Seq). *Methods* **103**, 34–48 (2016).
128. He, Y. *et al.* Self-cleaving ribozymes enable the production of guide RNAs from unlimited choices of promoters for CRISPR/Cas9 mediated genome editing. *J. Genet. Genomics* **44**, 469–472 (2017).
129. Shetty, R. P., Endy, D. & Knight, T. F. Engineering BioBrick vectors from BioBrick parts. *J. Biol. Eng.* **2**, 5 (2008).
130. Elowitz, M. B. & Leibler, S. A synthetic oscillatory network of transcriptional regulators. *Nature* **403**, 335–338 (2000).

MATERIALS AND METHODS

A.1 Rational design of libraries of orthogonal cgRNAs using NUPACK

For each mechanism, orthogonal cgRNA/trigger pairs were designed using the reaction pathway engineering tools within NUPACK (nupack.org; see the NUPACK 3.2 User Guide).^{35,37} Target test tubes were specified using the general formulation of Section S2.2.1 in the Supplementary Information of Wolfe et al.³⁷ using the definitions provided below for the splinted switch mechanism of Chapter 4. Sequence designs were performed for libraries of four orthogonal cgRNA/trigger pairs. For a given design trial, the sequences were optimized by mutating the sequence set to reduce the multi-tube ensemble defect³⁷ subject to the diverse sequence constraints for each mechanism. Within the ensemble defect, defect weights (see Section S1.6 in the Supplementary Information of Wolfe et al.³⁷) were applied to prioritize design effort. Designs were performed using RNA parameters for 1 M Na⁺ at 37 °C.³⁸ After performing several independent design trials for a given mechanism, a final sequence set was selected for experimental testing based on inspection of the predicted structural defects (fraction of nucleotides in the incorrect base-pairing state within the ensemble of an on-target complex) and concentration defects (fraction of nucleotides in the incorrect base-pairing state because there is a deficiency in the concentration of an on-target complex) for species in the context of the target test tubes,^{36,37} as well as for each cgRNA in the presence of each non-cognate trigger. After preliminary experimental studies, cgRNA/trigger pairs were selected for full experimental characterization.

Example design specification: splinted switch cgRNA in *E. coli*.

To design N orthogonal systems, the total number of target test tubes is $|\Omega| = \sum_{n=1,\dots,N} \{\text{Step 0, Step 1}\}_n + \text{Crosstalk} = 2N + 1$; the target test tubes in the multi-tube ensemble, Ω , are indexed by $h = 1, \dots, |\Omega|$. $L_{\max} = 2$ for all tubes (i.e., each target test tube contains all off-target complexes of up to two strands). Final sequence designs for orthogonal cgRNAs/trigger pairs A, B, C, and D are shown in Table A.5.

Reactants for system n

- cgRNAs: G_n
- Triggers: X_n

Elementary step tubes for system n

- Step 0_n tube: $\Psi_{0_n}^{\text{products}} \equiv \{G, X\}_n$; $\Psi_{0_n}^{\text{reactants}} \equiv \emptyset$; $\Psi_{0_n}^{\text{exclude}} \equiv \{G \cdot X\}_n$
- Step 1_n tube: $\Psi_{1_n}^{\text{products}} \equiv \{G \cdot X\}_n$; $\Psi_{1_n}^{\text{reactants}} \equiv \{G, X\}_n$; $\Psi_{1_n}^{\text{exclude}} \equiv \emptyset$

Global crosstalk tube

- Crosstalk tube: $\Psi_{\text{global}}^{\text{reactive}} \equiv \cup_{n=1, \dots, N} \{\lambda_n^{\text{reactive}}\}$; $\Psi_{\text{global}}^{\text{crosstalk}} \equiv \Psi_{\text{global}}^{L \leq L_{\text{max}}} - \cup_{n=1, \dots, N} \{\lambda_n^{\text{cognate}}\}$

The reactive species and cognate products for system n are:

- $\lambda_n^{\text{simple}} \equiv \{G, X\}_n$
- $\lambda_n^{\text{ss-out}} \equiv X_n$
- $\lambda_n^{\text{ss-in}} \equiv G_n^{\text{ss}}$, the 35nt single stranded handle and terminator loop insert domains, with intervening gRNA sequence
- $\lambda_n^{\text{reactive}} \equiv \{G, X, G^{\text{ss}}\}_n$
- $\lambda_n^{\text{cognate}} \equiv \{G \cdot X, G^{\text{ss}} \cdot X\}_n$

Sequence constraints

- Assignment constraints: portions of the cgRNA are constrained to match standard gRNA sequences for use with dCas9 (shaded gray in Figure 4.2, Figure 4.3, and Table A.5), and the synthetic terminator for the trigger is fully constrained (shaded tan in Figure 4.2, Figure 4.3, and Table A.5).
- Watson–Crick constraints: cgRNA sequence domains “d” and “e” are constrained to be complementary to the trigger sequence domains “d*” and “e*” (shaded blue in Figure 4.2, Figure 4.3, and Table A.5).
- Assignment constraint: cgRNA domain “u” is constrained to be complementary to a subsequence of the target gene sfGFP (full template sequence in Section A.6, constrained sequence shaded orange in Figure 4.2, Figure 4.3, and Table A.5).
- Pattern prevention constraints: the following patterns are prevented for cgRNA sequence domains “d” and “e”: AAAA, CCCC, GGGG, UUUU.

A.2 In vitro assay of gRNA/cgRNA activity with catalytically active Cas9

Sequences for parts used in in vitro studies are provided in Section A.4.

A double stranded DNA standard gRNA template lacking the target-binding region (NT_g) was ordered as a gene fragment from IDT. Extended T7 promoter sequence (T7_E), target-binding region, and modifications to the standard gRNA sequence were added via PCR to generate dsDNA template for in vitro transcription. Following PCR product clean up (with QIAquick PCR Purification Kit, QIAGEN #28104), gRNAs and cgRNAs were in vitro transcribed using the T7-Scribe kit (Cellsript #C-AS3107) as per manufacturer instructions, and IVT products were purified via denaturing gel electrophoresis (10% polyacrylamide w/urea; eluted overnight at 4 °C in 1x TAE + Mg²⁺). Trigger strands were ordered as RNA from IDT and purified via denaturing gel electrophoresis. dsDNA target templates were ordered as gene fragments from IDT, and amplified via PCR with subsequent PCR product clean up (QIAquick PCR Purification Kit). For the cleavage assay, the RNA species for each reaction (2 μL gRNA or cgRNA at 150 nM, and 2 μL trigger at 0.3 or 1.5 μM if applicable) were added to 0.8 μL 10x NEBuffer 3.1 (NEB #B7203S) and total volume normalized to 6 μL with water, then snap cooled by heating to 65 °C for 3 min and transferring to ice for 5 min (unless otherwise noted; see Figure 2.6). 2 μL purified recombinant *S. pyogenes* Cas9 (NEB #M0386S) diluted 6.67-fold in 1x NEBuffer 3.1 was added to each reaction tube and incubated at room temperature for 10 min. The reaction was started at $t = 0$ by adding 2 μL dsDNA target at 15 nM (10 μL final reaction volume), and incubated at 37 °C for 1 h. The reaction was halted by denaturing Cas9 with a 10 min incubation at 70 °C. Reaction products were characterized by nondenaturing gel electrophoresis (4–20% Mini-PROTEAN TBE Gel, Bio-Rad #4565016) with nucleic acid gel stain as per manufacturer instructions (SYBR gold stain, Thermo Fisher #S11494).

A.3 Methods for bacterial studies in *E. coli*

Plasmid construction and molecular cloning for bacterial cgRNA studies

Sequences for parts used in bacterial studies are provided in Section A.4.

Control gRNA and cgRNA constructs were generated by inverse PCR, inserting sequence modifications into the previously described pgRNA-bacteria vector⁶⁸ (Addgene plasmid #44251; gift from S. Qi). All PCR steps for the generation of experimental constructs were performed using Q5 Hot Start High-Fidelity polymerase (NEB #M0494) according to manufacturer instructions using primers designed

using standard molecular cloning techniques and synthesized by Integrated DNA Technologies. Introduced sequences were verified by Sanger sequencing for single colony picks via colony PCR using GoTaq Green polymerase (Promega #M7122).

For the single and double insert studies (Chapter 3) and splinted switch cgRNAs (Chapter 4), trigger-expressing constructs were generated by first cloning synthetic promoter, trigger template, and synthetic terminator (BBa_B1006) into a trigger-only cassette via inverse PCR, followed by insertion of trigger cassette into the cgRNA vector using BioBrick assembly to yield cgRNA+trigger expressing constructs.^{69,129} For the 5' extension/handle loop splinted switch cgRNAs (Chapter 2) and toehold switch cgRNAs (Chapter 5), trigger-expressing constructs were generated by first cloning synthetic promoter, trigger template, and synthetic terminator (BBa_B0050) into a trigger-only cassette via inverse PCR, followed by insertion of trigger cassette into the cgRNA vector using DNA assembly according to manufacturer instructions (NEBuilder HiFi DNA Assembly, NEB #E2621) to yield cgRNA+trigger expressing constructs.

A lacI+dCas9 expression construct was generated by inserting a lacI template sequence with J23108 constitutive promoter¹³⁰ into the previously described pdCas9-bacteria vector⁶⁸ (Addgene plasmid #44249; gift from S. Qi) between the dCas9 gene and the p15A origin with a synthetic terminator (BBa_B0010) added upstream of lacI as a transcriptional terminator for dCas9, using DNA assembly according to manufacturer instructions (NEBuilder HiFi DNA Assembly, NEB #E2621).

Bacterial culture and time course microplate fluorescence silencing assay for cgRNA studies

A previously described *E. coli* MG1655 strain with constitutively expressed mRFP and sfGFP inserted into the *nfsA* locus⁶⁸ (Ec001; gift from S. Qi) was used for all fluorescence assays. For experiments with constitutive expression of trigger, the previously described pdCas9-bacteria vector⁶⁸ (Addgene plasmid #44251) was used for tetR-regulated dCas9 expression. For experiments with lacI-regulated expression of trigger, the lacI+dCas9 vector was used for tetR-regulated dCas9 expression and constitutive expression of lacI. Chemically competent chloramphenicol-resistant cells carrying either the dCas9 or lacI+dCas9 construct were transformed with gRNA, cgRNA, or cgRNA+trigger expression vectors and cultivated in EZ-RDM (Teknova #M2105) containing 100 $\mu\text{g}/\text{mL}$ carbenicillin and 34 $\mu\text{g}/\text{mL}$ chloramphenicol (EZ-RDM+Carb+Cam).

Sequence-verified strains were grown overnight in EZ-RDM+Carb+Cam, then seeded at 100× dilution in 100 μL fresh medium and grown at 37 °C with shaking in the Neo2 microplate reader (Biotek) to monitor absorbance at 600 nm. When cells had reached mid-log phase (≈ 4 h), cells were again diluted ≈ 100 -fold in fresh medium with cell density normalized by A600 and, if applicable, dCas9 expression and trigger expression were induced with aTc and IPTG, respectively, in $N = 3$ replicate wells at 400 μL final volume in a 96-well high-volume glass bottom plate (Matriplate, Brooks #MGB096-1-2-LG-L). A final working concentration of 2 nM aTc was used for 35 nt insert splinted switch cgRNA experiments (Chapter 4) unless otherwise noted, with IPTG concentration as indicated for induction experiments. A final working concentration of 200 nM aTc was used for the 5' extension/handle loop splinted switch (Chapter 2) and toehold switch (Chapter 5) cgRNA experiments. Induced cells were grown at 37 °C with continuous linear shaking for the duration of the experiment, with A600 and fluorescence monitoring (sfGFP: 479 \pm 20 nm excitation, 520 \pm 20 nm emission; mRFP: 579 \pm 10 nm excitation, 616 \pm 20 nm emission).

Flow cytometry for bacterial cgRNA studies

Cell strains were cultured and induced as described above, and induced cells were grown at 37 °C with continuous shaking for 12 h. Protein fluorescence was measured using the MACSQuant VYB flow cytometer (Miltenyi Biotec) using FSC/SSC to gate for 20,000 live cells per well at a flow rate of 25 $\mu\text{L}/\text{min}$. sfGFP fluorescence was measured using the B1 channel (488 nm laser, 525/50 nm filter) and mRFP fluorescence was measured using the Y2 channel (561 nm laser, 615/20 nm filter).

Quantitative fluorescence analysis for *E. coli*

Measuring signal in *E. coli*

For a bacterial strain containing a fluorescent reporter protein, the total fluorescence (SIG+AF) in the relevant fluorescent channel (sfGFP for the 35 nt splinted switch cgRNA and insert studies, mRFP for the toehold switch and 15 nt splinted switch cgRNA) is a combination of signal (SIG) from the reporter and autofluorescence (AF) inherent to the cells. Autofluorescence is characterized for a given fluorescent channel in strain MG1655 containing no fluorescent reporters. For cell j of replicate well i of a given bacterial strain, we denote the autofluorescence:

$$X_{i,j}^{\text{AF}},$$

the signal:

$$X_{i,j}^{\text{SIG}},$$

and the total fluorescence (SIG + AF):

$$X_{i,j}^{\text{SIG+AF}}.$$

For replicate well i of a given strain, we measure the mean fluorescence ($\bar{X}_i^{\text{SIG+AF}}$ for a strain containing the reporter, \bar{X}_i^{AF} for strain MG1655 lacking reporters) over $N = 20,000$ cells. Performance across $N = 3$ replicate wells is characterized by the sample means ($\bar{X}^{\text{SIG+AF}}$ and \bar{X}^{AF}) and estimated standard errors ($s_{\bar{X}^{\text{SIG+AF}}}$ and $s_{\bar{X}^{\text{AF}}}$). Let (n, p) denote a strain containing cgRNA n and trigger p . The mean signal is estimated as

$$\bar{X}(n, p)^{\text{SIG}} = \bar{X}(n, p)^{\text{SIG+AF}} - \bar{X}^{\text{AF}}$$

with the standard error estimated via uncertainty propagation as

$$s_{\bar{X}(n,p)^{\text{SIG}}} \leq \sqrt{(s_{\bar{X}(n,p)^{\text{SIG+AF}}})^2 + (s_{\bar{X}^{\text{AF}}})^2}.$$

The upper bound on estimated standard error holds under the assumption that the correlation between SIG and AF is non-negative.

Fold change for constitutively active cgRNAs (ON→OFF logic) with silencing dCas9 in *E. coli*

For a constitutively active cgRNA with silencing dCas9, the ON state for cgRNA n corresponds to low fluorescence using no trigger ($p = 0$) and the OFF state corresponds to high fluorescence using cognate trigger ($p = n$). The fold change is estimated as

$$\bar{X}(n)^{\text{OFF:ON}} = \bar{X}(n, n)^{\text{SIG}} / \bar{X}(n, 0)^{\text{SIG}}$$

with standard error estimated via uncertainty propagation as

$$s_{\bar{X}(n)^{\text{OFF:ON}}} \leq \bar{X}(n)^{\text{OFF:ON}} \sqrt{\left(\frac{s_{\bar{X}(n,n)^{\text{SIG}}}}{\bar{X}(n,n)^{\text{SIG}}}\right)^2 + \left(\frac{s_{\bar{X}(n,0)^{\text{SIG}}}}{\bar{X}(n,0)^{\text{SIG}}}\right)^2}.$$

The upper bound on estimated standard error holds under the assumption that the correlation between SIG in the two strains is non-negative.

Dynamic range for constitutively active cgRNAs (ON→OFF logic) with silencing dCas9 in *E. coli*

For a constitutively active cgRNA with silencing dCas9, the ON state for cgRNA n corresponds to low fluorescence using no trigger ($p = 0$) and the OFF state corresponds to high fluorescence using cognate trigger ($p = n$). The dynamic range is estimated as

$$\bar{X}(n)^{\text{DR}} = \bar{X}(n, n)^{\text{SIG+AF}} - \bar{X}(n, 0)^{\text{SIG+AF}}$$

with standard error estimated via uncertainty propagation as

$$s_{\bar{X}(n)^{\text{DR}}} \leq \sqrt{(s_{\bar{X}(n, n)^{\text{SIG+AF}}})^2 + (s_{\bar{X}(n, 0)^{\text{SIG+AF}}})^2}.$$

The upper bound on estimated standard error holds under the assumption that the correlation between SIG+AF in the two strains is non-negative.

Fold change for constitutively inactive cgRNAs (OFF→ON logic) with silencing dCas9 in *E. coli*

For a constitutively inactive cgRNA with silencing dCas9, the OFF state for cgRNA n corresponds to high fluorescence using no trigger ($p = 0$) and the ON state corresponds to low fluorescence using cognate trigger ($p = n$). The fold change is estimated as

$$\bar{X}(n)^{\text{OFF:ON}} = \bar{X}(n, 0)^{\text{SIG}} / \bar{X}(n, n)^{\text{SIG}}$$

with standard error estimated via uncertainty propagation as

$$s_{\bar{X}(n)^{\text{OFF:ON}}} \leq \bar{X}(n)^{\text{OFF:ON}} \sqrt{\left(\frac{s_{\bar{X}(n, 0)^{\text{SIG}}}}{\bar{X}(n, 0)^{\text{SIG}}}\right)^2 + \left(\frac{s_{\bar{X}(n, n)^{\text{SIG}}}}{\bar{X}(n, n)^{\text{SIG}}}\right)^2}.$$

The upper bound on estimated standard error holds under the assumption that the correlation between SIG in the two strains is non-negative.

Dynamic range for constitutively inactive cgRNAs (OFF→ON logic) with silencing dCas9 in *E. coli*

For a constitutively inactive cgRNA with silencing dCas9, the OFF state for cgRNA n corresponds to high fluorescence using no trigger ($p = 0$) and the ON state corresponds to low fluorescence using cognate trigger ($p = n$). The dynamic range is estimated as

$$\bar{X}(n)^{\text{DR}} = \bar{X}(n, 0)^{\text{SIG+AF}} - \bar{X}(n, n)^{\text{SIG+AF}}$$

with standard error estimated via uncertainty propagation as

$$s_{\bar{X}(n)^{\text{DR}}} \leq \sqrt{(s_{\bar{X}(n,0)^{\text{SIG+AF}}})^2 + (s_{\bar{X}(n,n)^{\text{SIG+AF}}})^2}.$$

The upper bound on estimated standard error holds under the assumption that the correlation between SIG+AF in the two strains is non-negative.

Fractional dynamic range for cgRNAs with silencing dCas9 in *E. coli*

For a cgRNA with silencing dCas9, the ideal OFF state corresponds to high fluorescence with a no-target gRNA lacking the target-binding region and the ideal ON state corresponds to low fluorescence with a standard gRNA with a target-binding region for the target Y. The ideal dynamic range is estimated as

$$\bar{X}_{\text{ideal}}^{\text{DR}} = \bar{X}_{\text{no-target}}^{\text{SIG+AF}} - \bar{X}_{\text{standard}}^{\text{SIG+AF}}$$

with standard error estimated via uncertainty propagation as

$$s_{\bar{X}_{\text{ideal}}^{\text{DR}}} \leq \sqrt{(s_{\bar{X}_{\text{no-target}}^{\text{SIG+AF}}})^2 + (s_{\bar{X}_{\text{standard}}^{\text{SIG+AF}}})^2}.$$

The upper bound on estimated standard error holds under the assumption that the correlation between SIG+AF in the two strains is non-negative. The fractional dynamic range is estimated as

$$\bar{X}(n)^{\text{FDR}} = \bar{X}(n)^{\text{DR}} / \bar{X}_{\text{ideal}}^{\text{DR}}$$

with standard error estimated via uncertainty propagation as

$$s_{\bar{X}(n)^{\text{FDR}}} \leq \bar{X}(n)^{\text{FDR}} \sqrt{\left(\frac{s_{\bar{X}(n)^{\text{DR}}}}{\bar{X}(n)^{\text{DR}}}\right)^2 + \left(\frac{s_{\bar{X}_{\text{ideal}}^{\text{DR}}}}{\bar{X}_{\text{ideal}}^{\text{DR}}}\right)^2}.$$

The upper bound on estimated standard error holds under the assumption that the correlation between the ideal dynamic range and the cgRNA dynamic range is non-negative.

Crosstalk for orthogonal cgRNAs in *E. coli*

Crosstalk (CT) is estimated for cgRNA n with trigger p as

$$\bar{X}(n, p)^{\text{CT}} = [\bar{X}(n, p)^{\text{SIG+AF}} - \bar{X}(n, 0)^{\text{SIG+AF}}] / [\bar{X}(n, n)^{\text{SIG+AF}} - \bar{X}(n, 0)^{\text{SIG+AF}}]$$

with the standard error estimated via uncertainty propagation as

$$s_{\bar{X}(n,p)^{\text{CT}}} \leq \bar{X}(n,p)^{\text{CT}} \left(\left(\frac{\sqrt{(s_{\bar{X}(n,p)^{\text{SIG+AF}}})^2 + (s_{\bar{X}(n,0)^{\text{SIG+AF}}})^2}}{\bar{X}(n,p)^{\text{SIG+AF}} - \bar{X}(n,0)^{\text{SIG+AF}}} \right)^2 + \left(\frac{\sqrt{(s_{\bar{X}(n,n)^{\text{SIG+AF}}})^2 + (s_{\bar{X}(n,0)^{\text{SIG+AF}}})^2}}{\bar{X}(n,n)^{\text{SIG+AF}} - \bar{X}(n,0)^{\text{SIG+AF}}} \right)^2 \right)^{\frac{1}{2}}.$$

The upper bound on estimated standard error holds under the assumption that the correlation between strains is non-negative. Note that crosstalk values can be positive or negative. The bar graphs for orthogonality studies are annotated with $\bar{X}(n,p)^{\text{CT}}$ except that in instances where $|\bar{X}(n,p)^{\text{CT}}| < s_{\bar{X}(n,p)^{\text{CT}}}$, we instead report $\bar{X}(n,p)^{\text{CT}} + s_{\bar{X}(n,p)^{\text{CT}}}$ as an estimated upper bound.

The bar graphs for the bacterial studies for orthogonality studies plot normalized fluorescence. For replicate well i of cgRNA n and trigger p , the normalized mean fluorescence over 20,000 cells is

$$\bar{X}(n,p)_i^{\text{Norm}} = [\bar{X}(n,p)_i^{\text{SIG+AF}} - \bar{X}(n,0)^{\text{SIG+AF}}] / [\bar{X}(n,n)^{\text{SIG+AF}} - \bar{X}(n,0)^{\text{SIG+AF}}].$$

The bar graphs display the mean normalized fluorescence over $N = 3$ replicate wells ($\bar{X}(n,p)^{\text{Norm}} \pm$ the standard error of the mean ($s_{\bar{X}(n,p)^{\text{Norm}}}$) calculated treating the normalizing values $\bar{X}(n,0)^{\text{SIG+AF}}$ and $\bar{X}(n,n)^{\text{SIG+AF}}$ as exact (i.e., $s_{\bar{X}(n,p)^{\text{Norm}}}$ is calculated without error propagation) so as to display the uncertainty corresponding to the particular trigger p with cgRNA n . By contrast, $s_{\bar{X}(n,p)^{\text{CT}}}$ is calculated with error propagation so as to characterize the uncertainty arising from cognate trigger ($p = n$), noncognate trigger ($p \neq n$), and no trigger ($p = 0$) with cgRNA n .

A.4 Part sequences for cgRNA, trigger, and control gRNA

Splinted switch mechanism in vitro		
Name	Sequence	Legend
IVSS_5pA	5'-GGGATAATAAAAGAA AACTTTCAGTTTAGCGGTCT GTTTTAGA GCTAGAAATAGCAAGTTAAAATAAGGCTAGTCCGTATCAACTTGA AAAAGTGGCACCGAGTCGGTGCTTTTTTT-3'	5' A
IVSS_5pB	5'-GGGCATAAGTGTAGAA AACTTTCAGTTTAGCGGTCT GTTTTAGA GCTAGAAATAGCAAGTTAAAATAAGGCTAGTCCGTATCAACTTGA AAAAGTGGCACCGAGTCGGTGCTTTTTTT-3'	5' B
IVSS_5pC	5'-GGGAAACAGCAACAT AACTTTCAGTTTAGCGGTCT GTTTTAGA GCTAGAAATAGCAAGTTAAAATAAGGCTAGTCCGTATCAACTTGA AAAAGTGGCACCGAGTCGGTGCTTTTTTT-3'	5' C
IVSS_5pD	5'-GGGAGAAATTATGAT AACTTTCAGTTTAGCGGTCT GTTTTAGA GCTAGAAATAGCAAGTTAAAATAAGGCTAGTCCGTATCAACTTGA AAAAGTGGCACCGAGTCGGTGCTTTTTTT-3'	5' D
IVSS_hIA	5'- AACTTTCAGTTTAGCGGTCT GTTTTAGAGCTA CGAACGAAATA AAAG TAGCAAGTTAAAATAAGGCTAGTCCGTATCAACTTGAAAAA GTGGCACCGAGTCGGTGCTTTTTTT-3'	Handle A
IVSS_hIB	5'- AACTTTCAGTTTAGCGGTCT GTTTTAGAGCTA ATAAGAATAAT AAAG TAGCAAGTTAAAATAAGGCTAGTCCGTATCAACTTGAAAAA GTGGCACCGAGTCGGTGCTTTTTTT-3'	Handle B
IVSS_hIC	5'- AACTTTCAGTTTAGCGGTCT GTTTTAGAGCTA TAAAGAGTGAA TAGG TAGCAAGTTAAAATAAGGCTAGTCCGTATCAACTTGAAAAA GTGGCACCGAGTCGGTGCTTTTTTT-3'	Handle C
IVSS_hID	5'- AACTTTCAGTTTAGCGGTCT GTTTTAGAGCTA TGGAGAAGTAA GAAG TAGCAAGTTAAAATAAGGCTAGTCCGTATCAACTTGAAAAA GTGGCACCGAGTCGGTGCTTTTTTT-3'	Handle D
IVSS_cgA	5'-GGGATAATAAAAGAA AACTTTCAGTTTAGCGGTCT GTTTTAGA GCTA CGAACGAAATAAAAG TAGCAAGTTAAAATAAGGCTAGTCCGT TATCAACTTGAAAAAGTGGCACCGAGTCGGTGCTTTTTTT-3'	A/A cgRNA A cgRNA
IVSS_cgB	5'-GGGCATAAGTGTAGAA AACTTTCAGTTTAGCGGTCT GTTTTAGA GCTA ATAAGAATAATAAAG TAGCAAGTTAAAATAAGGCTAGTCCGT TATCAACTTGAAAAAGTGGCACCGAGTCGGTGCTTTTTTT-3'	B/B cgRNA B
IVSS_cgC	5'-GGGAAACAGCAACAT AACTTTCAGTTTAGCGGTCT GTTTTAGA GCTA TAAAGAGTGAATAGG TAGCAAGTTAAAATAAGGCTAGTCCGT TATCAACTTGAAAAAGTGGCACCGAGTCGGTGCTTTTTTT-3'	C/C cgRNA C
IVSS_cgD	5'-GGGAGAAATTATGAT AACTTTCAGTTTAGCGGTCT GTTTTAGA GCTA TGGAGAAGTAAAG TAGCAAGTTAAAATAAGGCTAGTCCGT TATCAACTTGAAAAAGTGGCACCGAGTCGGTGCTTTTTTT-3'	D/D cgRNA D
IVSS_tA	5'- CTTTTATTTTCGTTCTTTTATTATCCC -3'	trigger X _A
IVSS_tB	5'- CTTTATTATTCTTATTCTACTTATGCC -3'	trigger
IVSS_tC	5'- CCTATTCACTCTTAATGTTGCTGTTCCC -3'	trigger X _B trigger X _C

Splinted switch mechanism in vitro		
Name	Sequence	Legend
IVSS_tD	5'-CTTCTACTTCTCCAATCATAATTTCTCCC-3'	trigger X_D

Table A.2: Splinted switch sequences for in vitro studies (Chapter 2). Nucleotides shaded orange are constrained by the target gene. Nucleotides shaded gray are constrained by Cas9. Nucleotides shaded blue are designed as described in Chapter 2.

Insert studies in <i>E. coli</i>		
Part name	Candidate cgRNA/trigger sequence	Legend
i-15_cg	5'-TATCATCCATCAACC CATCTAATTC CAACAAGAAT TGTTTTAGAGCTAGAAATAGCAAGTTAAAATAAGGCT AGTCCGTTATCAACTTGAAAAAGTGGCACCAGTCGG TGCTTTTTTT-3'	5' extension: 15
i-25_cg	5'-ACTATAGACTTATCATCCATCAACC CATCTAATTC CAACAAGAATT TGTTTTAGAGCTAGAAATAGCAAGTTAA AATAAGGCTAGTCCGTTATCAACTTGAAAAAGTGGCA CCGAGTCGGTGCTTTTTTT-3'	5' extension: 25
i-35_cg	5'-GCTACTCATTACTATAGACTTATCATCCATCAAC CCATCTAATTC CAACAAGAATTGTTTTAGAGCTAGAAA TAGCAAGTTAAAATAAGGCTAGTCCGTTATCAACTG AAAAAGTGGCACCAGTCGGTGCTTTTTTT-3'	5' extension: 35
ii-15a_cg	5'- CATCTAATTC CAACAAGAATTGTTTTAGAGCTAGCT ATTCGAGAAAAGT TAGCAAGTTAAAATAAGGCTAGTCC GTTATCAACTTGAAAAAGTGGCACCAGTCGGTGCTT TTTTT-3'	Handle loop: 15a
ii-15b_cg	5'- CATCTAATTC CAACAAGAATTGTTTTAGAGCTAATC CCGTGTTCCGTG TAGCAAGTTAAAATAAGGCTAGTCC GTTATCAACTTGAAAAAGTGGCACCAGTCGGTGCTT TTTTT-3'	Handle loop: 15b
ii-25a_cg	5'- CATCTAATTC CAACAAGAATTGTTTTAGAGCTAGCT ATTCGAGAAAAGTTTCAGATCCC TAGCAAGTTAAAATA AGGCTAGTCCGTTATCAACTTGAAAAAGTGGCACCAG GTCGGTGCTTTTTTT-3'	Handle loop: 25a
ii-25b_cg	5'- CATCTAATTC CAACAAGAATTGTTTTAGAGCTAAAA GTTTCAGATCCC GTGTTCCGTGTTAGCAAGTTAAAATA AGGCTAGTCCGTTATCAACTTGAAAAAGTGGCACCAG GTCGGTGCTTTTTTT-3'	Handle loop: 25b

Insert studies in *E. coli*

Part name	Candidate cgRNA/trigger sequence	Legend
ii-35_cg	5'-CATCTAATTCAACAAGAATTGTTTTAGAGCTAGCT ATTCGAGAAAAGTTTCAGATCCCGTGTCCGTGTAGCA AGTTAAAATAAGGCTAGTCCGTTATCAACTTGAAAAA GTGGCACCGAGTCGGTGCTTTTTTT-3'	Handle loop: 35
iii-15a_cg	5'-CATCTAATTCAACAAGAATTGTTTTAGAGCTAGA AATAGCAAGTTAAAATAAGGCTAGTCCGTTATCAACT TAAACCTTACCACAATAAGTGGCACCGAGTCGGTGCT TTTTTT-3'	Terminator loop 1: 15a
iii-15b_cg	5'-CATCTAATTCAACAAGAATTGTTTTAGAGCTAGA AATAGCAAGTTAAAATAAGGCTAGTCCGTTATCAACT TCATTACATAAGCACAAAGTGGCACCGAGTCGGTGCT TTTTTT-3'	Terminator loop 1: 15b
iii-25a_cg	5'-CATCTAATTCAACAAGAATTGTTTTAGAGCTAGA AATAGCAAGTTAAAATAAGGCTAGTCCGTTATCAACT TAAACCTTACCACAATTCACCATTCAAGTGGCACCG AGTCGGTGCTTTTTTT-3'	Terminator loop 1: 25a
iii-25b_cg	5'-CATCTAATTCAACAAGAATTGTTTTAGAGCTAGA AATAGCAAGTTAAAATAAGGCTAGTCCGTTATCAACT TACAATTCACCATTACATAAGCACAAAGTGGCACCG AGTCGGTGCTTTTTTT-3'	Terminator loop 1: 25b
iii-35_cg	5'-CATCTAATTCAACAAGAATTGTTTTAGAGCTAGA AATAGCAAGTTAAAATAAGGCTAGTCCGTTATCAACT TAAACCTTACCACAATTCACCATTACATAAGCACAA AGTGGCACCGAGTCGGTGCTTTTTTT-3'	Terminator loop 1: 35
iv-15_cg	5'-CATCTAATTCAACAAGAATTGTTTTAGAGCTAGAA ATAGCAAGTTAAAATAAGGCTAGTCCGTTATCAACTT GAAAAAGTGGCACCGCAAGAACGTAACAATCGGTGCT TTTTTT-3'	Terminator loop 2: 15
iv-25_cg	5'-CATCTAATTCAACAAGAATTGTTTTAGAGCTAGAA ATAGCAAGTTAAAATAAGGCTAGTCCGTTATCAACTT GAAAAAGTGGCACCGCAAGAACGTAACAATGAGAACA GAACGGTGCTTTTTTT-3'	Terminator loop 2: 25
iv-35_cg	5'-CATCTAATTCAACAAGAATTGTTTTAGAGCTAGAA ATAGCAAGTTAAAATAAGGCTAGTCCGTTATCAACTT GAAAAAGTGGCACCGCAAGAACGTAACAATGAGAACA GAAGATAGAAATACGGTGCTTTTTTT-3'	Terminator loop 2: 35
i-15_ii-15a_cg	5'-TATCATCCATCAACCATCTAATTCAACAAGAAT TGTTTTAGAGCTAGCTATTCGAGAAAAGTTAGCAAGTT AAAATAAGGCTAGTCCGTTATCAACTTGAAAAAGTGG CACCGAGTCGGTGCTTTTTTT-3'	5' extension: 15 / Handle loop: 15a

Insert studies in *E. coli*

Part name	Candidate cgRNA/trigger sequence	Legend
i-25_ii-25a_cg	5'-ACTATAGACTTATCATCCATCAACCCATCTAATTC AACAGAATTGTTTTAGAGCTAGCTATTCGAGAAAGT TTCAGATCCCTAGCAAGTAAAATAAGGCTAGTCCGT TATCAACTTGAAAAAGTGGCACCAGTCGGTGCTTTT TTT-3'	5' extension: 25 / Handle loop: 25a
i-35_ii-35_cg	5'-GCTACTCATTACTATAGACTTATCATCCATCAAC CCATCTAATTCACAAGAATTGTTTTAGAGCTAGCTA TTCGAGAAAGTTTCAGATCCCGTGTCCGTGTAGCAA GTTAAAATAAGGCTAGTCCGTTATCAACTTGAAAAAG TGGCACCAGTCGGTGCTTTTTTT-3'	5' extension 35 / Handle loop: 35
i-15_iii-15a_cg	5'-TATCATCCATCAACCCATCTAATTCACAAGAAT TGTTTTAGAGCTAGAAATAGCAAGTAAAATAAGGCT AGTCCGTTATCAACTTAAACCTTACCACAATAAGTGG CACCGAGTCGGTGCTTTTTTT-3'	5' extension: 15 / Term loop 1: 15a
i-25_iii-25a_cg	5'-ACTATAGACTTATCATCCATCAACCCATCTAATTC AACAGAATTGTTTTAGAGCTAGAAATAGCAAGTTAA AATAAGGCTAGTCCGTTATCAACTTAAACCTTACCAC AATTTACCATTCAAGTGGCACCAGTCGGTGCTTTT TTT-3'	5' extension: 25 / Term loop 1: 25a
i-35_iii-35_cg	5'-GCTACTCATTACTATAGACTTATCATCCATCAAC CCATCTAATTCACAAGAATTGTTTTAGAGCTAGAAA TAGCAAGTAAAATAAGGCTAGTCCGTTATCAACTTA AACCTTACCACAATTTACCATTACATAAGCACAAAG TGGCACCAGTCGGTGCTTTTTTT-3'	5' extension: 35 / Term loop 1: 35
i-15_iv-15_cg	5'-TATCATCCATCAACCCATCTAATTCACAAGAAT TGTTTTAGAGCTAGAAATAGCAAGTAAAATAAGGCT AGTCCGTTATCAACTTGAAAAAGTGGCACCAGAA CGTAACAATCGGTGCTTTTTTT-3'	5' extension: 15 / Term loop 2: 15
i-25_iv-25_cg	5'-ACTATAGACTTATCATCCATCAACCCATCTAATTC AACAGAATTGTTTTAGAGCTAGAAATAGCAAGTTAA AATAAGGCTAGTCCGTTATCAACTTGAAAAAGTGGCA CCGCAAGAACGTAACAATGAGAACAGAACGGTGCTTT TTTT-3'	5' extension: 25 / Term loop 2: 25
i-35_iv-35_cg	5'-GCTACTCATTACTATAGACTTATCATCCATCAAC CCATCTAATTCACAAGAATTGTTTTAGAGCTAGAAA TAGCAAGTAAAATAAGGCTAGTCCGTTATCAACTTG AAAAAGTGGCACCAGAACGTAACAATGAGAACAG AAGATAGAAATACGGTGCTTTTTTT-3'	5' extension: 35 / Term loop 2: 35

Insert studies in *E. coli*

Part name	Candidate cgRNA/trigger sequence	Legend
ii-15b_iii-15a_cg	5'-CATCTAATTCAACAAGAATTGTTTTAGAGCTAATC CCGTGTTCCGTGTAGCAAGTTAAAATAAGGCTAGTCC GTTATCAACTTAAACCTTACCACAATAAGTGGCACCG AGTCGGTGCTTTTTTT-3'	Handle loop: 15b / Term loop 1: 15a
ii-25b_iii-25a_cg	5'-CATCTAATTCAACAAGAATTGTTTTAGAGCTAAA AGTTTCAGATCCCGTGTTCGGTGTAGCAAGTTAAA TAAGGCTAGTCCGTTATCAACTTAAACCTTACCACAA TTTACCATTCAAGTGGCACCGAGTCGGTGCTTTTTT T-3'	Handle loop: 25b / Term loop 1: 25a
ii-35_iii-35_cg	5'-CATCTAATTCAACAAGAATTGTTTTAGAGCTAGCT ATTCGAGAAAAGTTTCAGATCCCGTGTTCGGTGTAGCA AGTTAAAATAAGGCTAGTCCGTTATCAACTTAAACCT TACCACAATTTACCATTACATAAGCACAAAGTGGCA CCGAGTCGGTGCTTTTTTT-3'	Handle loop: 35 / Term loop 1: 35
ii-15b_iv-15_cg	5'-CATCTAATTCAACAAGAATTGTTTTAGAGCTAATC CCGTGTTCCGTGTAGCAAGTTAAAATAAGGCTAGTCC GTTATCAACTTGAAAAAGTGGCACCGCAAGAACGTAA CAATCGGTGCTTTTTTT-3'	Handle loop: 15b / Term loop 2: 15
ii-25b_iv-25_cg	5'-CATCTAATTCAACAAGAATTGTTTTAGAGCTAAA GTTTCAGATCCCGTGTTCGGTGTAGCAAGTTAAAATA AGGCTAGTCCGTTATCAACTTGAAAAAGTGGCACCGC AAGAACGTAACAATGAGAACAGAACGGTGCTTTTTT T-3'	Handle loop: 25b / Term loop 2: 25
ii-35_iv-35_cg	5'-CATCTAATTCAACAAGAATTGTTTTAGAGCTAGCT ATTCGAGAAAAGTTTCAGATCCCGTGTTCGGTGTAGCA AGTTAAAATAAGGCTAGTCCGTTATCAACTTGAAAA GTGGCACCGCAAGAACGTAACAATGAGAACAGAAGAT AGAAATACGGTGCTTTTTTT-3'	Handle loop: 35 / Term loop 2: 35
iii-15b_iv-15_cg	5'-CATCTAATTCAACAAGAATTGTTTTAGAGCTAGA AATAGCAAGTTAAAATAAGGCTAGTCCGTTATCAACT TCATTACATAAGCACAAAGTGGCACCGCAAGAACGTA ACAATCGGTGCTTTTTTT-3'	Term loop 1: 15b / Term loop 2: 15
iii-25b_iv-25_cg	5'-CATCTAATTCAACAAGAATTGTTTTAGAGCTAGA AATAGCAAGTTAAAATAAGGCTAGTCCGTTATCAAC TTACAATTTACCATTACATAAGCACAAAGTGGCACCG GCAAGAACGTAACAATGAGAACAGAACGGTGCTTTTT TT-3'	Term loop 1: 25b / Term loop 2: 25

Insert studies in *E. coli*

Part name	Candidate cgRNA/trigger sequence	Legend
iii-35_iv-35_cg	5'-CATCTAATTCAACAAGAATTGTTTTAGAGCTAGA AATAGCAAGTTAAAATAAGGCTAGTCCGTTATCAACT TAAACCTTACCACAATTCACCATTACATAAGCAC AGTGGCACCGCAAGAACGTAACAATGAGAACAGAAGA TAGAAATACGGTGCTTTTTTT-3'	Term loop 1: 35 / Term loop 2: 35
i-15_t	5'-GGTTGATGGATGATA-3'	5' extension: 15 +Trigger
i-25_t	5'-GGTTGATGGATGATAAGTCTATAGT-3'	5' extension: 25 +Trigger
i-35_t	5'-GGTTGATGGATGATAAGTCTATAGTAATGAGTAG C-3'	5' extension: 35 +Trigger
ii-15a_t	5'-ACTTTCTCGAATAGC-3'	Handle loop: 15a +Trigger
ii-15b_t	5'-CACGGAACACGGGAT-3'	Handle loop: 15b +Trigger
ii-25a_t	5'-GGGATCTGAACTTTCTCGAATAGC-3'	Handle loop: 25a +Trigger
ii-25b_t	5'-CACGGAACACGGGATCTGAACTTT-3'	Handle loop: 25b +Trigger
ii-35_t	5'-CACGGAACACGGGATCTGAACTTTCTCGAATAG C-3'	Handle loop: 35 +Trigger
iii-15a_t	5'-ATTGTGGTAAGGTTT-3'	Terminator loop 1: 15a +Trigger
iii-15b_t	5'-GTGCTTATGTGAATG-3'	Terminator loop 1: 15b +Trigger
iii-25a_t	5'-GAATGGTGAATTGTGGTAAGGTTT-3'	Terminator loop 1: 25a +Trigger
iii-25b_t	5'-GTGCTTATGTGAATGGTGAATTGT-3'	Terminator loop 1: 25b +Trigger
iii-35_t	5'-GTGCTTATGTGAATGGTGAATTGTGGTAAGGTT T-3'	Terminator loop 1: 35 +Trigger
iv-15_t	5'-ATTGTTACGTTCTTG-3'	Terminator loop 2: 15 +Trigger
iv-25_t	5'-TTCTGTTCTCATTGTTACGTTCTTG-3'	Terminator loop 2: 25 +Trigger
iv-35_t	5'-TATTTCTATCTTCTGTTCTCATTGTTACGTTCTT G-3'	Terminator loop 2: 35 +Trigger
i-15_ii-15a_t	5'-ACTTTCTCGAATAGCGGTTGATGGATGATA-3'	5' extension: 15 / Handle loop: 15a +Trigger

Insert studies in *E. coli*

Part name	Candidate cgRNA/trigger sequence	Legend
i-25_ii-25a_t	5'-GGGATCTGAACTTTCTCGAATAGCGGTTGATGGA TGATAAGTCTATAGT-3'	5' extension: 25 / Handle loop: 25a +Trigger
i-35_ii-35_t	5'-CACGGAACACGGGATCTGAACTTTCTCGAATAGC GGTTGATGGATGATAAGTCTATAGTAATGAGTAGC-3'	5' extension: 35 / Handle loop: 35 +Trigger
i-15_iii-15a_t	5'-ATTGTGGTAAGGTTTGGTTGATGGATGATA-3'	5' extension: 15 / Term loop 1: 15a +Trigger
i-25_iii-25a_t	5'-GAATGGTGAAATTGTGGTAAGGTTTGGTTGATGGA TGATAAGTCTATAGT-3'	5' extension: 25 / Term loop 1: 25a +Trigger
i-35_iii-35_t	5'-GTGCTTATGTGAATGGTAAAATTGTGGTAAGGTTT GGTTGATGGATGATAAGTCTATAGTAATGAGTAGC-3'	5' extension: 35 / Term loop 1: 35 +Trigger
i-15_iv-15_t	5'-ATTGTTACGTTCTTGGGTTGATGGATGATA-3'	5' extension: 15 / Term loop 2: 15 +Trigger
i-25_iv-25_t	5'-TTCTGTTCTCATTGTTACGTTCTTGGGTTGATGGA TGATAAGTCTATAGT-3'	5' extension: 25 / Term loop 2: 25 +Trigger
i-35_iv-35_t	5'-TATTTCTATCTTCTGTTCTCATTGTTACGTTCTTG GGTTGATGGATGATAAGTCTATAGTAATGAGTAGC-3'	5' extension: 35 / Term loop 2: 35 +Trigger
ii-15b_iii-15a_t	5'-ATTGTGGTAAGGTTTACGGAACACGGGAT-3'	Handle loop: 15b / Term loop 1: 15a +Trigger
ii-25b_iii-25a_t	5'-GAATGGTGAAATTGTGGTAAGGTTTACGGAACAC GGGATCTGAACTTT-3'	Handle loop: 25b / Term loop 1: 25a +Trigger
ii-35_iii-35_t	5'-GTGCTTATGTGAATGGTAAAATTGTGGTAAGGTTT CACGGAACACGGGATCTGAACTTTCTCGAATAGC-3'	Handle loop: 35 / Term loop 1: 35 +Trigger
ii-15b_iv-15_t	5'-ATTGTTACGTTCTTGCACGGAACACGGGAT-3'	Handle loop: 15b / Term loop 2: 15 +Trigger
ii-25b_iv-25_t	5'-TTCTGTTCTCATTGTTACGTTCTTGCACGGAACAC GGGATCTGAACTTT-3'	Handle loop: 25b / Term loop 2: 25 +Trigger

Insert studies in *E. coli*

Part name	Candidate cgRNA/trigger sequence	Legend
ii-35_iv-35_t	5'-TATTTCTATCTTCTGTTCTCATTGTTACGTTCTTG CACGGAACACGGGATCTGAACTTTCTCGAATAGC-3'	Handle loop: 35 / Term loop 2: 35 +Trigger
iii-15b_iv-15_t	5'-ATTGTTACGTTCTTGGTGCTTATGTGAATG-3'	Term loop 1: 15b / Term loop 2: 15 +Trigger
iii-25b_iv-25_t	5'-TTCTGTTCTCATTGTTACGTTCTTGGTGCTTATGT GAATGGTGAAATTGT-3'	Term loop 1: 25b / Term loop 2: 25 +Trigger
iii-35_iv-35_t	5'-TATTTCTATCTTCTGTTCTCATTGTTACGTTCTTG GTGCTTATGTGAATGGTGAATTGTGGTAAGGTTT-3'	Term loop 1: 35 / Term loop 2: 35 +Trigger

Table A.4: Candidate cgRNA/trigger sequences for insert studies in *E. coli* (Chapter 3). Nucleotides shaded orange are constrained by the target gene. Nucleotides shaded gray are constrained by dCas9. Nucleotides shaded blue are designed as described in Chapter 3.

Splinted switch mechanism in *E. coli*

Name	Sequence	Legend
SplS_cgA	5'-CATCTAATTCAACAAGAATTGTTTTAGAGCTACACCTTACGCC	cgRNA
	GGTTCAATTCCAAGTCCCTTCCAGTAGCAAGTTAAAATAAGGCTAG	cgRNA A
	TCCGTTATCAACTTAAACACCCTTACAAACCTTCTCTTCCTTTAC	
	CCTAAGTGGCACCGAGTCGGTGCTTTTTTT-3'	
SplS_cgB	5'-CATCTAATTCAACAAGAATTGTTTTAGAGCTAGTAATCGAATC	cgRNA B
	ATAGTAAATTTCCCATCGTCATAATAGCAAGTTAAAATAAGGCTAG	
	TCCGTTATCAACTTCATACGGGTCTGAAGTAGTTCATTCTTATACA	
	GTCAAGTGGCACCGAGTCGGTGCTTTTTTT-3'	
SplS_cgC	5'-CATCTAATTCAACAAGAATTGTTTTAGAGCTAGTCGTTACCTT	cgRNA C
	ATCAATATCAACCTCCGCATACACTAGCAAGTTAAAATAAGGCTAG	
	TCCGTTATCAACTTGCACATAGGACCCAACATGCCAACAGAGAAGA	
	GTTAAGTGGCACCGAGTCGGTGCTTTTTTT-3'	
SplS_cgD	5'-CATCTAATTCAACAAGAATTGTTTTAGAGCTAAACATACAAAC	cgRNA D
	CACTACCGACAACCTAAACACTTTTAGCAAGTTAAAATAAGGCTAG	
	TCCGTTATCAACTTCACTACATCATATCATACGCGGAATTAACA	
	ATCAAGTGGCACCGAGTCGGTGCTTTTTTT-3'	
SplS_tA	5'-AGGGTAAAGGAAGAGGAAGGTTTGTAAGGGTGTCTGGAAGG	Trigger
	GACTTGGAATTGAACCGCGTAAGGTG-3'	Trigger X _A
SplS_tB	5'-GACTGTATAAGAATGAACTACTTCAGACCCGTATGTTATGACG	Trigger X _B
	ATGGGAAATTTACTATGATTCGATTAC-3'	
SplS_tC	5'-AACTCTTCTCTGTTGGCATGTTGGTCCTATGTGCGTGTATGC	Trigger X _C
	GGAGGTTGATATTGATAAGGTAACGAC-3'	
SplS_tD	5'-GATTGTTTAAATTCGCGTATGATATGATGTAGTAAAAAGTGT	Trigger X _D
	TAAGTTGTCGGTAGTGTTTGTATGTT-3'	

Table A.5: Splinted switch sequences for studies in *E. coli* (Chapter 4). Nucleotides shaded orange are constrained by the target gene. Nucleotides shaded gray are constrained by dCas9. Nucleotides shaded blue are designed as described in Chapter 4.

Toehold switch mechanism in *E. coli*

Name	Sequence	Legend
ToeS_cgA	5'-ATGTTTCGTTGTATTAAGACCGCTAAACTGAAAGTTACACGCC CAACTTTCAGTTTAGCGGTCTGTTTTAGAGCTAGAAATAGCAAGTT AAAATAAGGCTAGTCCGTTATCAACTTGAAAAAGTGGCACCGAGTC GGTGCTTTTTTTT-3'	cgRNA cgRNA A
ToeS_cgB	5'-GTATATGAAATTGAAAGACCGCTAAACTGAAAGTTACACGCC CAACTTTCAGTTTAGCGGTCTGTTTTAGAGCTAGAAATAGCAAGTT AAAATAAGGCTAGTCCGTTATCAACTTGAAAAAGTGGCACCGAGTC GGTGCTTTTTTTT-3'	cgRNA B
ToeS_cgC	5'-AAGGTGATAGTAAAGAGACCGCTAAACTGAAAGTTACACGCC CAACTTTCAGTTTAGCGGTCTGTTTTAGAGCTAGAAATAGCAAGTT AAAATAAGGCTAGTCCGTTATCAACTTGAAAAAGTGGCACCGAGTC GGTGCTTTTTTTT-3'	cgRNA C
ToeS_cgD	5'-TATACTTATACTTGGAGACCGCTAAACTGAAAGTTACACGCC CAACTTTCAGTTTAGCGGTCTGTTTTAGAGCTAGAAATAGCAAGTT AAAATAAGGCTAGTCCGTTATCAACTTGAAAAAGTGGCACCGAGTC GGTGCTTTTTTTT-3'	cgRNA D
ToeS_tA	5'-AACTTTCAGTTTAGCGGTCTTAATACAACGAACAT-3'	Trigger Trigger X _A
ToeS_tB	5'-AACTTTCAGTTTAGCGGTCTTTCAATTTTACATATAC-3'	Trigger X _B
ToeS_tC	5'-AACTTTCAGTTTAGCGGTCTCTTACTATCACCTT-3'	Trigger X _C
ToeS_tD	5'-AACTTTCAGTTTAGCGGTCTCCAAGTATAAGTATA-3'	Trigger X _D

Table A.6: Toehold switch sequences for studies in *E. coli* (Chapter 5). Nucleotides shaded orange are constrained by the target gene. Nucleotides shaded gray are constrained by dCas9. Nucleotides shaded blue are designed as described in Chapter 5.

Control gRNA sequences

Name	Sequence
CT_g	5'-CACATCCCATCCACCGCCACGTTTTAGAGCTAGAAATAGCAAGTTAAAAT AAGGCTAGTCCGTTATCAACTTGAAAAAGTGGCACCGAGTCGGTGCTTTTTTT T-3'
mRFP_g	5'-AACTTTCAGTTTAGCGGTCTGTTTTAGAGCTAGAAATAGCAAGTTAAAAT AAGGCTAGTCCGTTATCAACTTGAAAAAGTGGCACCGAGTCGGTGCTTTTTTT T-3'
sfGFP_g	5'-CATCTAATTCAACAAGAATTGTTTTAGAGCTAGAAATAGCAAGTTAAAAT AAGGCTAGTCCGTTATCAACTTGAAAAAGTGGCACCGAGTCGGTGCTTTTTTT T-3'
NT_g	5'-GTTTTAGAGCTAGAAATAGCAAGTTAAAATAAGGCTAGTCCGTTATCAAC TTGAAAAAGTGGCACCGAGTCGGTGCTTTTTTTT-3'

Table A.7: Control gRNA sequences. For the standard gRNAs, nucleotides shaded orange are constrained by the target gene (mRFP or sfGFP for bacterial studies) or target dsDNA sequence (CT gRNA binding site or sfGFP binding site for in vitro studies). Nucleotides shaded gray are constrained by Cas protein. The no-target gRNA contains no target-binding region. For bacterial studies, the autofluorescence control strain was transformed with the no-target gRNA control plasmid (sequence NT_g).

Transcriptional promoter and terminator sequences		
Name	Type	Sequence
T7_E	T7 promoter	5'-CCTCTAATACGACTCACTATA-3'
BBa_J23100	Constitutive promoter	5'-TTGACGGCTAGCTCAGTCCTAGGTACAGTGCTAGC-3'
BBa_J23108	Constitutive promoter	5'-CTGACAGCTAGCTCAGTCCTAGGTATAATGCTAGC-3'
BBa_J23114	Constitutive promoter	5'-TTTATGGCTAGCTCAGTCCTAGGTACAATGCTAGC-3'
BBa_R0011	lacI-regulated promoter	5'-AATTGTGAGCGGATAACAATTGACATTGTGAGCGGATAACAAGATACTGAGCACA-3'
BBa_B0015	Terminator	5'-CCAGGCATCAAATAAAACGAAAGGCTCAGTCGAAAGACTGGGCCTTTCGTTTTATCTGTTGTTTGTGCGGTGACGCTCTCTACTAGAGTCACACTGGCTCACCTTCGGGTGGGCCTTCTGCGTTTATA-3'
BBa_B0050	Terminator	5'-AAAAAAAAGGATCTCAAGAAGATCCTTTGATTTT-3'
BBa_B1006	Terminator	5'-AAAAAAAACCCCGCCCCTGACAGGGCGGGGTTTTTTT-3'
BBa_B1010	Terminator	5'-CGCCGCAAACCCCGCCCCTGACAGGGCGGGGTTTCGCCG-3'

Table A.8: Transcriptional promoter and terminator sequences.

A.5 Plasmids Constitutively active splinted switch in *E. coli*

Note that the plasmids used for the insert studies of Chapter 3 (not shown) use the same plasmid layout as the cgRNA-only and cgRNA + cognate trigger plasmids of the splinted switch studies of Chapter 4 (below).

Name	Parts	Legend
pdCas9-bacteria	Addgene plasmid #44249	No-target gRNA; Autofluorescence
pdCas9+lacI	See Figure A.5, Figure A.6	Autofluorescence
pag-NT	ColE1 ori; amp-R; BBa_J23108-NT_g-BBa_B1006	Standard gRNA
pg-sfGFP	ColE1 ori; amp-R; BBa_J23108-sfGFP_g-BBa_B1006	cgRNA
pSpIS-cgA-nT	ColE1 ori; amp-R; BBa_J23108-SplS_cgA-BBa_B1006	cgRNA A
pSpIS-cgA-tA	ColE1 ori; amp-R; BBa_J23100-SplS_tA-BBa_B1006-BBa_B0015; BBa_J23108-SplS_cgA-BBa_B1006	cgRNA + trigger
pSpIS-cgA-tB	See Figure A.1, Figure A.2	cgRNA A, trigger X _A
pSpIS-cgA-tC	ColE1 ori; amp-R; BBa_J23100-SplS_tB-BBa_B1006-BBa_B0015; BBa_J23108-SplS_cgA-BBa_B1006	cgRNA A, trigger X _B
pSpIS-cgB-nT	ColE1 ori; amp-R; BBa_J23108-SplS_tC-BBa_B1006-BBa_B0015; BBa_J23108-SplS_cgA-BBa_B1006	cgRNA A, trigger X _C
pSpIS-cgB-tA	ColE1 ori; amp-R; BBa_J23108-SplS_cgB-BBa_B1006	cgRNA B
pSpIS-cgB-tB	ColE1 ori; amp-R; BBa_J23100-SplS_tA-BBa_B1006-BBa_B0015; BBa_J23108-SplS_cgB-BBa_B1006	cgRNA B, trigger X _A
pSpIS-cgB-tC	ColE1 ori; amp-R; BBa_J23100-SplS_tB-BBa_B1006-BBa_B0015; BBa_J23108-SplS_cgB-BBa_B1006	cgRNA B, trigger X _B
pSpIS-cgC-nT	ColE1 ori; amp-R; BBa_J23100-SplS_tC-BBa_B1006-BBa_B0015; BBa_J23108-SplS_cgB-BBa_B1006	cgRNA B, trigger X _C
pSpIS-cgC-tA	ColE1 ori; amp-R; BBa_J23108-SplS_cgC-BBa_B1006	cgRNA C
pSpIS-cgC-tB	ColE1 ori; amp-R; BBa_J23100-SplS_tA-BBa_B1006-BBa_B0015; BBa_J23108-SplS_cgC-BBa_B1006	cgRNA C, trigger X _A
pSpIS-cgC-tC	ColE1 ori; amp-R; BBa_J23100-SplS_tB-BBa_B1006-BBa_B0015; BBa_J23108-SplS_cgC-BBa_B1006	cgRNA C, trigger X _B
pSpIS-cgD-nT	ColE1 ori; amp-R; BBa_J23108-SplS_cgD-BBa_B1006	cgRNA C, trigger X _C

Table A.9: Plasmids used with splinted switch cgRNAs in *E. coli*.

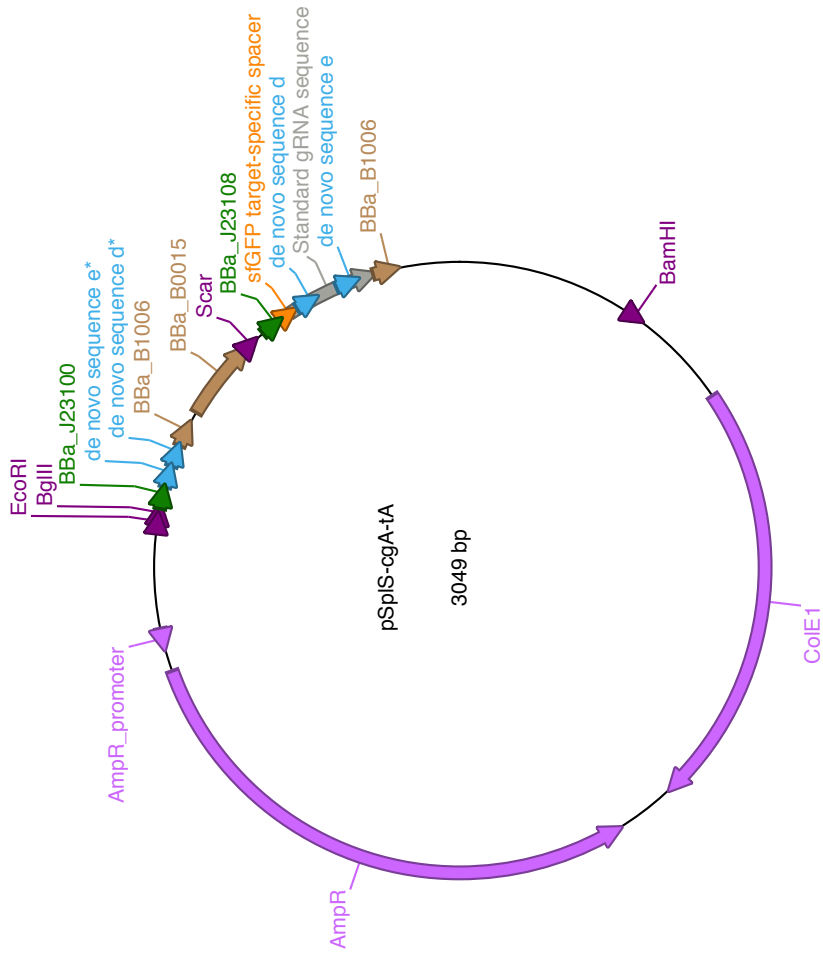


Figure A.1: Example plasmid map for splinted switch in *E. coli*. Plasmid: pSpIS-cgA-tA for cgRNA A + trigger X_A.

Constitutively inactive toehold switch in *E. coli*

Note that the plasmids used for the characterization of the 15 nt insert splinted switch of Chapter 2 in *E. coli* (not shown) use the same plasmid layout as the cgRNA-only and cgRNA + trigger plasmids of the toehold switch studies of Chapter 5 (below).

Name	Parts	Figure	Legend
pdCas9-bacteria	Addgene plasmid #44249		No-target gRNA; Autofluorescence
psg-NT	ColE1 ori; amp-R; BBa_J23108-NT_g		Autofluorescence
psg-mRFP	ColE1 ori; amp-R; BBa_J23108-mRFP_g		Standard gRNA
pToeS-cgA-nT	ColE1 ori; amp-R; BBa_J23100-BBa_B0050; BBa_J23108-ToeS_cgA		cgRNA
pToeS-cgA-tA	ColE1 ori; amp-R; BBa_J23100-ToeS_tA-BBa_B0050; BBa_J23108-ToeS_cgA		cgRNA A
pToeS-cgA-tB	See Figure A.3, Figure A.4		cgRNA A + trigger
pToeS-cgA-tC	ColE1 ori; amp-R; BBa_J23100-ToeS_tB-BBa_B0050; BBa_J23108-ToeS_cgA		cgRNA A, trigger X _A
pToeS-cgB-nT	ColE1 ori; amp-R; BBa_J23100-ToeS_tC-BBa_B0050; BBa_J23108-ToeS_cgA		cgRNA A, trigger X _B
pToeS-cgB-tA	ColE1 ori; amp-R; BBa_J23100-BBa_B0050; BBa_J23108-ToeS_cgB		cgRNA A, trigger X _C
pToeS-cgB-tB	ColE1 ori; amp-R; BBa_J23100-ToeS_tA-BBa_B0050; BBa_J23108-ToeS_cgB		cgRNA B
pToeS-cgB-tC	ColE1 ori; amp-R; BBa_J23100-ToeS_tB-BBa_B0050; BBa_J23108-ToeS_cgB		cgRNA B, trigger X _A
pToeS-cgC-nT	ColE1 ori; amp-R; BBa_J23100-ToeS_tC-BBa_B0050; BBa_J23108-ToeS_cgB		cgRNA B, trigger X _B
pToeS-cgC-tA	ColE1 ori; amp-R; BBa_J23100-BBa_B0050; BBa_J23108-ToeS_cgC		cgRNA B, trigger X _C
pToeS-cgC-tB	ColE1 ori; amp-R; BBa_J23100-ToeS_tA-BBa_B0050; BBa_J23108-ToeS_cgC		cgRNA C
pToeS-cgC-tC	ColE1 ori; amp-R; BBa_J23100-ToeS_tB-BBa_B0050; BBa_J23108-ToeS_cgC		cgRNA C, trigger X _A
pToeS-cgD-tD	ColE1 ori; amp-R; BBa_J23100-ToeS_tD-BBa_B0050; BBa_J23108-ToeS_cgD		cgRNA C, trigger X _B
			cgRNA C, trigger X _C
			cgRNA D, trigger X _D

Table A.10: Plasmids used with toehold switch cgRNAs in *E. coli*.

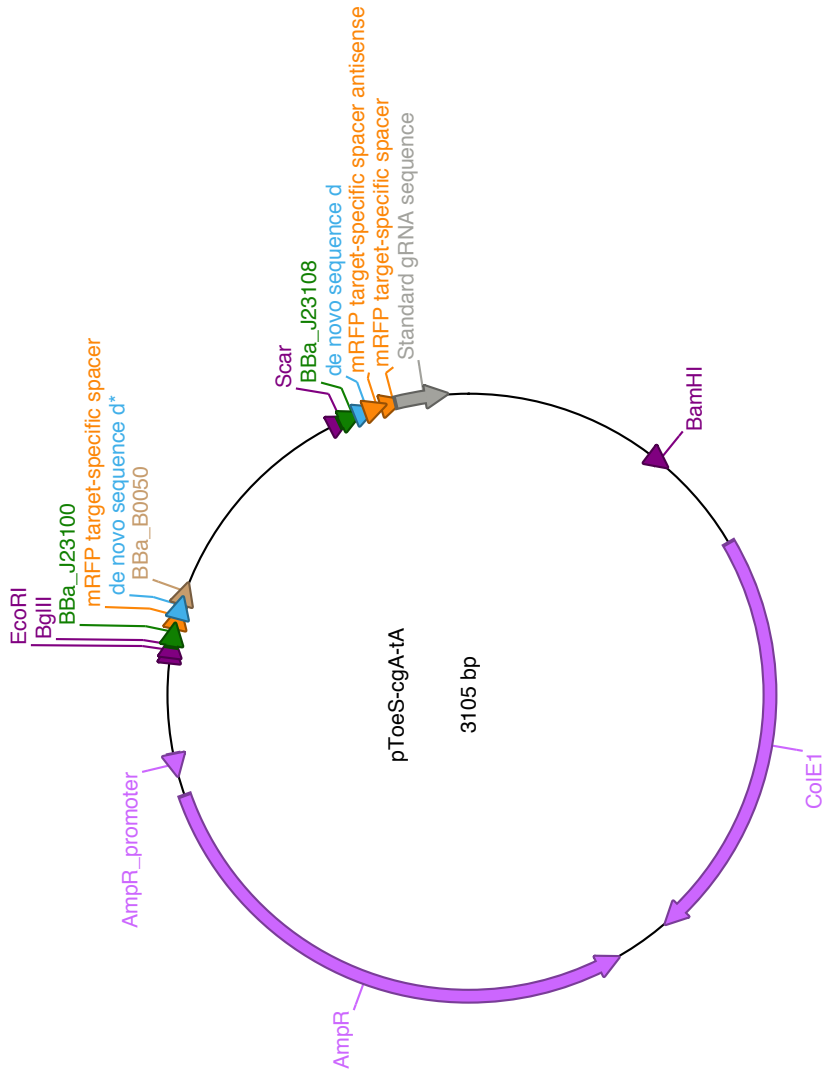


Figure A.3: Example plasmid map for toehold switch in *E. coli*. Plasmid: pToeS-cgA-tA for cgRNA A + trigger X_A.

pdCas9+lacI in *E. coli*

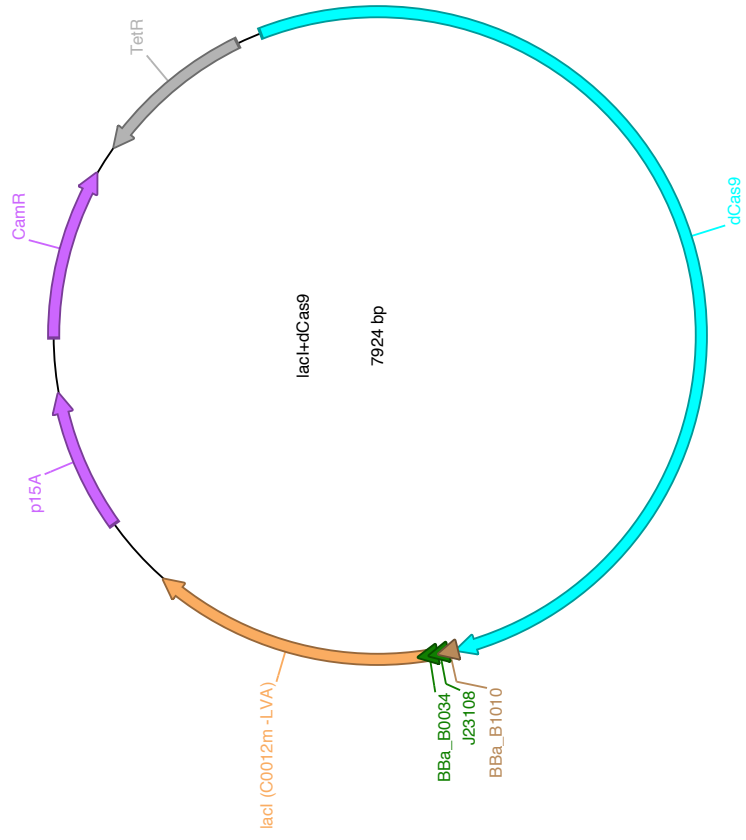


Figure A.5: Plasmid map for pdCas9+lacI in *E. coli*.

A.6 Sequences for dsDNA target

dsDNA target sequence for in vitro cleavage assay

Nucleotides highlighted in orange indicate the control gRNA (CT_g) target sequence (cleavage site for assay of Figure 2.1). Nucleotides highlighted in green indicate the sfGFP target sequence (cleavage site for assay of Figures 2.4, 2.5, and 2.6).

```

1 TATGTA AAC CTGTGACATT TCCCATCTTT GAAACTATTT AGTACTTTGT ATTTCTCACA
61 AGCACTTAGA GGCTGCCTTC TATTATAGTT ATTTACAGAG ATGCCTTTC TCCTTTCATA
121 TTAAGCTGAA TCCCTATTCC TCTCTTACTA ATCTTTCTAT AGCCCGTAAT ATCCACCTAA
181 CTAGTATAGT CACTTACATA GAGGGCATGT TTAATAGAAA CTGATGAAT TGAATGGAGC
241 AAAAAAATC AAATAGGCAA AAACCATATC TACGTTAGAG GTCATGAAG TATCACAAAA
301 GCAAAGGAAA CACATACAAA AAATTGTCTC ATACACACAC ACACACACAA TGGGCAATAA
361 ACACAAAGTT CAAAAACGTT GTCCTCAGCA CGGCGTCGCG TGCGAGGACC TCTTTGATT
421 AGGGCGTGCA GCCGTGGCCT CAGCTGTCTT TTTTCTTGAT CCTCCTACAT TAGATGACTC
481 TGGGATTTTC TTGTTGCCCC TTTGCAGCCC ACCATGAGCT GATTTTGTGA AGACTTTGAC
541 TTTACTTAAA TTGACTGCTT CAGATTCTGT ATTAATAAGG TGATCTGATC TCTTCTGACA
601 CGTCCTTCC TGCAGTGAAT TTGACTTCT ACATCTCTT TTTGACGCT GTGACCTCTC
661 ACTAGAAAGT TCCACAGAAA GCTGACTCTC ATGTAAAGTA CTTGCATCAA ATTCTAAATC
721 ACTTAAAGAT TTTTCTGCTT TCCTCTTGCA CAATCTTGT TGAATTAGAT GAGGACTTGG
781 AACTGGATTT AAGTTTATCC CTTCTAATGC ACTTTCCCCT AGCAATTTCT CTTCTTTCT
841 TTTGGGAGGT AGTCCAAAAT ACACACCTAT ATCCATTTGC TTCATTACCT TGGTAGAAGG
901 ATGTCTTGCA TTATACTTAA GACCAGAAGG CAATATTTTC AAATACTTCG GAGCAGGTGT
961 ACTAGACAAG TTTTCTGTAT TAAAAATTGT AGCTTACCA ACTGGCACAC CCTCTAATGC
1021 CTTTCTGCAG AAACATGCTG AGTTAGTATT ATTCTTAGCA TTCAAGTTCT CACTTGATAA
1081 TCTTCTAATT GTATTTTGGG TTGTTGGGA AGAAAGATAC CCTTCTACCT GACTTTCAAA
1141 AGTTTCAAC

```

Ec001 genomically incorporated mRFP template sequence

Nucleotides highlighted in orange indicate the gRNA/cgRNA target sequence.

```

1 ATGGCGAGTA GCGAAGACGT TATCAAAGAG TTCATGCGTT TCAAAGTTCG TATGGAAGGT
61 TCCGTTAACG GTCACGAGTT CGAAATCGAA GGTGAAGGTG AAGGTCGTCC GTACGAAGGT
121 ACCCAGACCG CTAAACTGAA AGTTACCAAAA GGTGTTCCGC TGCCGTTCCG TTGGGACATC
181 CTGTCCCCGC AGTTCCAGTA CGGTTCCAAA GCTTACGTTA AACACCCGGC TGACATCCCG
241 GACTACCTGA AACTGTCCTT CCCGGAAGGT TTCAAATGGG AACGTGTTAT GAACTTCGAA
301 GACGGTGGTG TTGTTACCGT TACCCAGGAC TCCTCCCTGC AAGACGGTGA GTTCATCTAC
361 AAAGTTAAAC TGCGTGGTAC CAACTTCCCG TCCGACGGTC CGGTTATGCA GAAAAAACC
421 ATGGGTTGGG AAGCTTCCAC CGAACGTATG TACCCGGAAG ACGGTGCTCT GAAAGGTGAA
481 ATCAAAAATGC GTCTGAAACT GAAAGACGGT GGTCACTACG ACGCTGAAGT TAAAACCACC
541 TACATGGCTA AAAAAACGGT TCAGCTGCCG GGTGCTTACA AAACCGACAT CAAACTGGAC
601 ATCACCTCCC ACAACGAAGA CTACACCATC GTTGAACAGT ACGAACGTGC TGAAGGTCGT
661 CACTCCACCG GTGCTTAA

```

Ec001 genomically incorporated sfGFP template sequence

Nucleotides highlighted in orange indicate the gRNA/cgRNA target sequence.

```

1  ATGAGCAAAG GAGAAGAACT TTCACTGGA GTTGTCCCAA TTCTTGTGA ATTAGATGGT
61  GATGTTAATG GGCACAAATT TTCTGTCCGT GGAGAGGGTG AAGGTGATGC TACAAACGGA
121 AAACTCACCC TTAAATTTAT TTGCACTACT GGAAAACACTAC CTGTTCCGTG GCCAACACTT
181 GTCACTACTC TGACCTATGG TGTTCAATGC TTTTCCCGTT ATCCGGATCA CATGAAACGG
241 CATGACTTTT TCAAGAGTGC CATGCCCGAA GGTTATGTAC AGGAACGCAC TATATCTTTC
301 AAAGATGACG GGACCTACAA GACGCGTGCT GAAGTCAAGT TTGAAGGTGA TACCCTTGTT
361 AATCGTATCG AGTTAAAGGG TATTGATTTT AAAGAAGATG GAAACATTCT TGGACACAAA
421 CTCGAGTACA ACTTAACTC ACACAATGTA TACATCACGG CAGACAAACA AAAGAATGGA
481 ATCAAAGCTA ACTTCAAAAT TCGCCACAAC GTTGAAGATG GTTCCGTTCA ACTAGCAGAC
541 CATTATCAAC AAAATACTCC AATTGGCGAT GGCCCTGTCC TTTTACCAGA CAACCATTAC
601 CTGTCGACAC AATCTGTCCT TTCGAAAGAT CCCAACGAAA AGCGTGACCA CATGGTCCTT
661 CTTGAGTTG TAACTGCTGC TGGGATTACA CATGGCATGG ATGAGCTCTA CAAA

```

Appendix B

SUPPLEMENTARY FIGURES AND DATA FOR CHAPTER 2

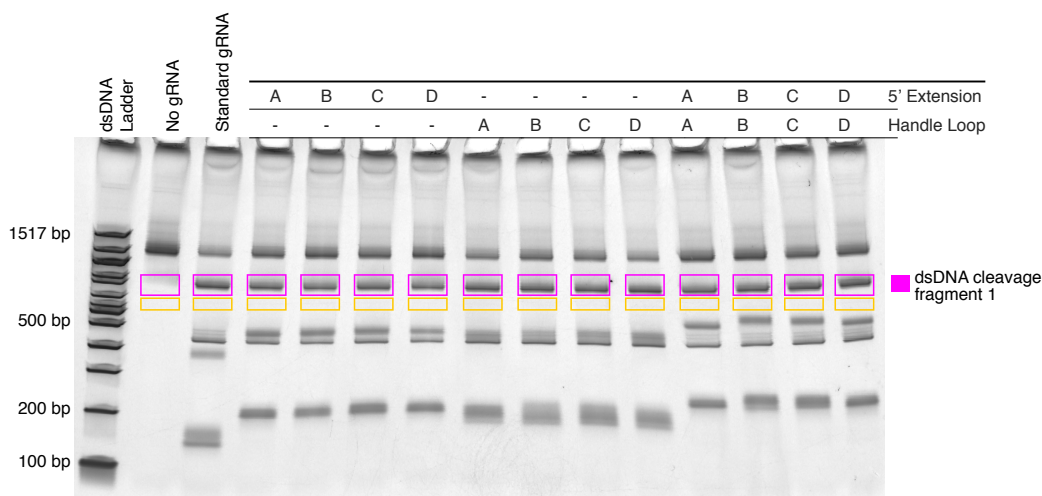


Figure B.1: Quantifying in vitro cgRNA insert study (cf. Figure 2.4). Non-denaturing PAGE (4-20% 1xTBE polyacrilimide gel) of reaction products for single 5' extension inserts, single handle loop inserts, and for each of four 5' extension/handle insert splinted switch cgRNAs (A, B, C, and D). gRNA or candidate cgRNA was pre-incubated with recombinant Cas9 (10 min) prior to addition of dsDNA target (final reaction concentrations: 30 nM (c)gRNA, 3 nM dsDNA cleavage target). All gRNA and cgRNA containing lanes include Cas9 and dsDNA target. Magenta boxes were used for mean pixel intensity quantification of signal + background for Figure 2.4b, orange boxes were used for mean pixel intensity quantification of subtracted background.

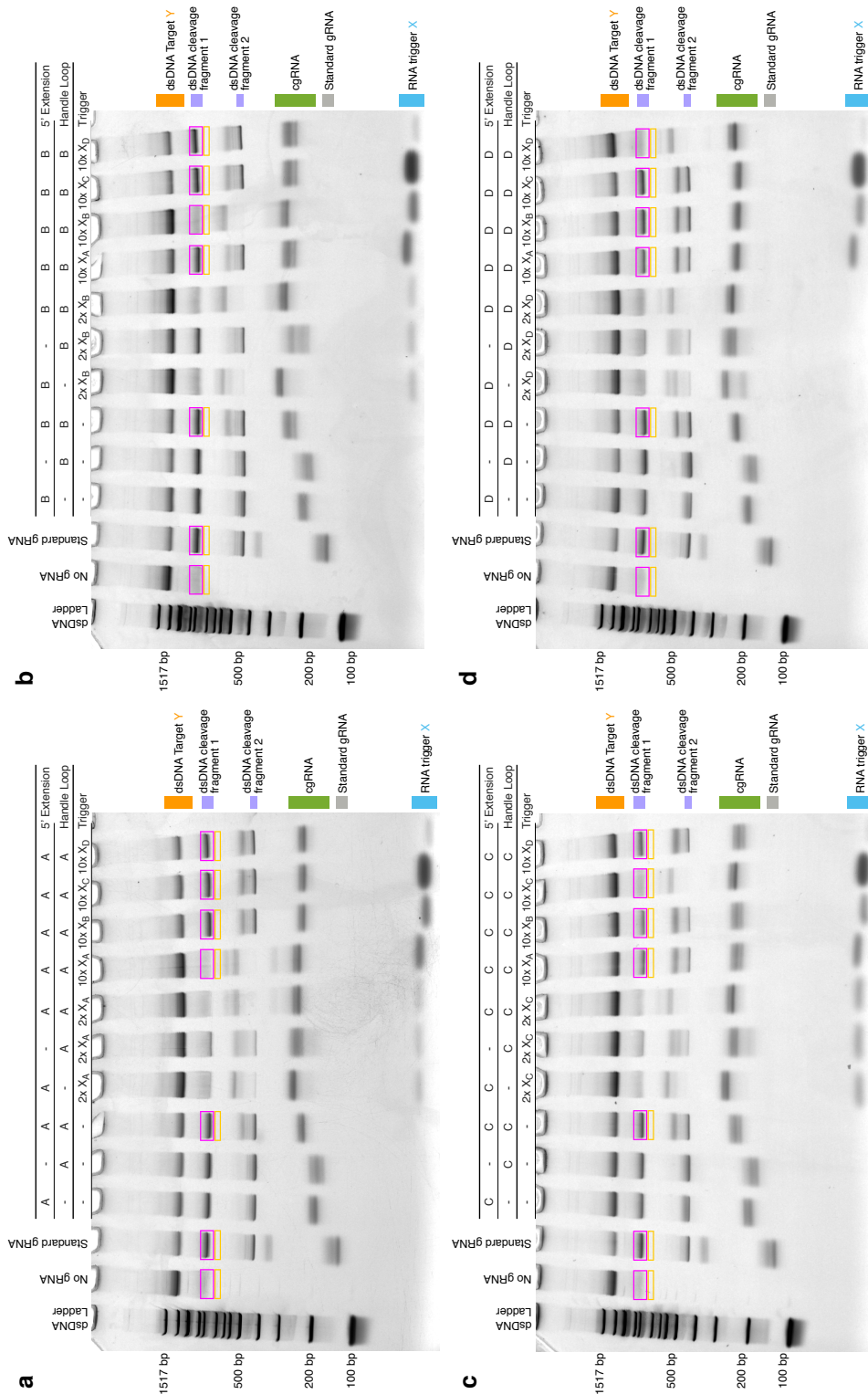


Figure B.2: Additional reaction conditions and quantification of in vitro cgRNAs.

Figure B.2: Additional reaction conditions and quantification of in vitro cgRNAs (cont'd). (a) cgRNA A. (b) cgRNA B. (c) cgRNA C. (d) cgRNA D. Non-denaturing PAGE (4-20% 1xTBE polyacrilimide gel) of reaction products for single 5' extension inserts, single handle loop inserts, and for each of four 5' extension/handle insert splinted switch cgRNAs (A, B, C, and D) with cognate trigger at a 2:1 molar ratio and each of four synthetic RNA triggers (X_A , X_B , X_C , X_D) at a 10:1 molar ratio. cgRNA was snap-cooled with RNA trigger in buffer and pre-incubated with recombinant Cas9 (10 min) prior to addition of dsDNA target (final reaction concentrations: 30 nM cgRNA, 60 nM or 300 nM RNA trigger, 3 nM dsDNA cleavage target). All gRNA and cgRNA containing lanes include Cas9 and dsDNA target. Magenta boxes were used for mean pixel intensity quantification of signal + background for Figure 2.5b, orange boxes were used for mean pixel intensity quantification of subtracted background.

Appendix C

SUPPLEMENTARY FIGURES AND DATA FOR CHAPTER 3

cgRNA	ON	OFF	Fold Change	Dynamic Range	Fractional Dynamic Range
a					
Ideal 1	355 ± 9	20100 ± 700	57 ± 2	19700 ± 700	1
5' extension: 15	362 ± 11	809 ± 9	2.23 ± 0.07	446 ± 8	0.0227 ± 0.0009
5' extension: 25	347 ± 9	1030 ± 20	2.98 ± 0.09	690 ± 20	0.0349 ± 0.0014
5' extension: 35	403 ± 12	702 ± 9	1.74 ± 0.06	299 ± 9	0.0152 ± 0.0007
Handle loop: 15b	421 ± 9	364 ± 9	0.86 ± 0.03	-58 ± 5	-0.0029 ± 0.0003
Handle loop: 25b	339 ± 9	2220 ± 20	6.5 ± 0.2	1880 ± 20	0.095 ± 0.003
Handle loop: 35	342 ± 10	2500 ± 20	7.3 ± 0.2	2160 ± 20	0.110 ± 0.004
Terminator loop 1: 15a	240 ± 10	390 ± 20	1.63 ± 0.09	152 ± 14	0.0077 ± 0.0007
Terminator loop 1: 25a	274 ± 9	340 ± 10	1.24 ± 0.05	66 ± 7	0.0034 ± 0.0004
Terminator loop 1: 35	290 ± 9	792 ± 8	2.73 ± 0.09	502 ± 2	0.0255 ± 0.0009
Terminator loop 2: 15	310 ± 11	163 ± 11	0.52 ± 0.04	-148 ± 10	-0.0075 ± 0.0006
Terminator loop 2: 25	293 ± 11	550 ± 30	1.88 ± 0.11	260 ± 20	0.0131 ± 0.0013
Terminator loop 2: 35	296 ± 9	353 ± 9	1.19 ± 0.05	57 ± 5	0.0029 ± 0.0003
b					
Ideal 2	326 ± 3	19200 ± 300	58.7 ± 1.2	18800 ± 300	1
5' extension: 15 / Handle loop: 15a	474 ± 12	1327 ± 12	2.80 ± 0.08	850 ± 20	0.0453 ± 0.0012
5' extension: 25 / Handle loop: 25a	450 ± 8	1340 ± 110	16.3 ± 0.4	6890 ± 110	0.366 ± 0.009
5' extension: 35 / Handle loop: 35	599 ± 7	10300 ± 200	17.2 ± 0.4	9700 ± 200	0.515 ± 0.014
5' extension: 15 / Term loop 1: 15a	659 ± 7	1800 ± 40	2.73 ± 0.07	1140 ± 40	0.061 ± 0.002
5' extension: 25 / Term loop 1: 25	534 ± 9	1797 ± 5	3.36 ± 0.06	1263 ± 10	0.0671 ± 0.0013
5' extension: 35 / Term loop 1: 35	1042 ± 9	2500 ± 60	2.40 ± 0.06	1460 ± 60	0.077 ± 0.003
5' extension: 15 / Term loop 2: 15	277 ± 6	720 ± 8	2.60 ± 0.07	443 ± 10	0.0235 ± 0.0007
5' extension: 25 / Term loop 2: 25	460 ± 20	1600 ± 30	3.49 ± 0.13	1140 ± 30	0.061 ± 0.002
5' extension: 35 / Term loop 2: 35	924 ± 11	1054 ± 11	1.14 ± 0.02	130 ± 20	0.0069 ± 0.0008
c					
Ideal 3	335 ± 10	19200 ± 400	57 ± 2	18900 ± 400	1
Handle loop: 15b / Term loop 1: 15a	359 ± 10	640 ± 20	1.77 ± 0.06	277 ± 12	0.0147 ± 0.0007
Handle loop: 25b / Term loop 1: 25a	383 ± 14	2200 ± 20	5.7 ± 0.2	1810 ± 20	0.096 ± 0.002
Handle loop: 35 / Term loop 1: 35	561 ± 10	8220 ± 80	14.7 ± 0.3	7660 ± 80	0.406 ± 0.009
Handle loop: 15b / Term loop 2: 15	216 ± 10	314 ± 14	1.46 ± 0.09	99 ± 11	0.0052 ± 0.0006
Handle loop: 25b / Term loop 2: 25	670 ± 30	1820 ± 20	2.73 ± 0.11	1150 ± 30	0.061 ± 0.002
Handle loop: 35 / Term loop 2: 35	1770 ± 30	4660 ± 50	2.64 ± 0.06	2890 ± 60	0.153 ± 0.004
Term loop 1: 15b / Term loop 2: 15	177 ± 11	430 ± 20	2.4 ± 0.2	250 ± 20	0.0135 ± 0.0008
Term loop 1: 25b / Term loop 2: 25	1030 ± 20	200 ± 11	0.193 ± 0.011	-835 ± 14	-0.0443 ± 0.0011
Term loop 1: 35 / Term loop 2: 35	1740 ± 20	473 ± 12	0.272 ± 0.008	-1270 ± 20	-0.067 ± 0.002
Handle loop: 15a	1000 ± 30	334 ± 10	0.334 ± 0.014	-670 ± 20	-0.035 ± 0.002
Handle loop: 25a	354 ± 12	930 ± 20	2.63 ± 0.11	580 ± 20	0.0306 ± 0.0013
Terminator loop 1: 15b	209 ± 12	650 ± 20	3.1 ± 0.2	440 ± 20	0.0233 ± 0.0011
Terminator loop 1: 25b	309 ± 10	371 ± 10	1.20 ± 0.05	62 ± 4	0.0033 ± 0.0002

Table C.1: Quantifying ON state, OFF state, fold change, and dynamic range for gRNA insert studies, 0.2 nM aTc.

Table C.1: Quantifying ON state, OFF state, fold change, and dynamic range for gRNA insert studies, 0.2 nM aTc (cont'd). ON = (cgRNA, no trigger) – AF; OFF = (cgRNA + cognate trigger) – AF; fold change = OFF/ON; dynamic range = OFF–ON; fractional dynamic range = [OFF–ON]/[ideal OFF – ideal ON]. Ideal values correspond to a standard gRNA for ideal ON and a no-target gRNA for ideal OFF. Autofluorescence values (AF) were 120 ± 8 (panel a), 102 ± 2 (panel b), and 113 ± 9 (panel c). Mean \pm estimated standard error (with uncertainty propagation) based on the mean single-cell fluorescence over 20,000 cells for each of $N = 3$ replicate wells.

cgRNA	ON	OFF	Fold Change	Dynamic Range	Fractional Dynamic Range
a					
Ideal	59 ± 12	19 970 ± 140	340 ± 70	19 910 ± 140	1
5' extension: 15	28 ± 11	200 ± 12	7 ± 3	172 ± 6	0.0086 ± 0.0003
5' extension: 25	20 ± 11	246 ± 11	13 ± 7	226 ± 4	0.0114 ± 0.0002
5' extension: 35	24 ± 10	149 ± 11	6 ± 3	125 ± 2	0.00629 ± 0.00013
Handle loop: 15b	66 ± 10	81 ± 13	1.2 ± 0.3	15 ± 9	0.0008 ± 0.0004
Handle loop: 25b	48 ± 11	223 ± 11	4.6 ± 1.0	175 ± 5	0.0088 ± 0.0003
Handle loop: 35	47 ± 10	350 ± 20	8 ± 2	310 ± 12	0.0154 ± 0.0006
Terminator loop 1: 15a	30 ± 11	53 ± 11	1.8 ± 0.7	23 ± 3	0.0012 ± 0.0002
Terminator loop 1: 25a	40 ± 12	71 ± 13	1.8 ± 0.6	30.5 ± 9.9	0.0015 ± 0.0005
Terminator loop 1: 35	21 ± 11	233 ± 11	11 ± 6	213 ± 5	0.0107 ± 0.0002
Terminator loop 2: 15	41 ± 11	24 ± 11	0.6 ± 0.3	-18 ± 5	-0.0009 ± 0.0003
Terminator loop 2: 25	38 ± 10	146 ± 11	3.9 ± 1.1	108 ± 5	0.0054 ± 0.0002
Terminator loop 2: 35	51 ± 11	73 ± 11	1.4 ± 0.4	22 ± 4	0.0011 ± 0.0002
b					
Ideal	65 ± 10	18 200 ± 700	280 ± 50	18 000 ± 700	1
5' extension: 15 / Handle loop: 15a	72 ± 9	276 ± 13	3.9 ± 0.5	200 ± 12	0.0113 ± 0.0008
5' extension: 25 / Handle loop: 25a	59 ± 8	1380 ± 20	23 ± 3	1320 ± 15	0.073 ± 0.003
5' extension: 35 / Handle loop: 35	77 ± 8	1770 ± 30	23 ± 3	1690 ± 28	0.093 ± 0.004
5' extension: 15 / Term loop 1: 15a	95 ± 8	402 ± 13	4.2 ± 0.4	310 ± 11	0.0170 ± 0.0009
5' extension: 25 / Term loop 1: 25a	58.0 ± 9.8	443 ± 9	7.6 ± 1.3	385 ± 8	0.0213 ± 0.0010
5' extension: 35 / Term loop 1: 35	144 ± 8	545 ± 9	3.8 ± 0.2	401 ± 6	0.0222 ± 0.0010
5' extension: 15 / Term loop 2: 15	43 ± 8	186 ± 8	4.3 ± 0.8	143 ± 3	0.0079 ± 0.0003
5' extension: 25 / Term loop 2: 25	81 ± 8	422 ± 9	5.2 ± 0.6	341 ± 7	0.0188 ± 0.0008
5' extension: 35 / Term loop 2: 35	178 ± 9	178 ± 8	1.00 ± 0.07	0 ± 5	0.0000 ± 0.0003
c					
Ideal	90 ± 5	21 000 ± 300	232 ± 13	20 900 ± 270	1
Handle loop: 15b / Term loop 1: 15a	100 ± 7	178 ± 6	1.77 ± 0.13	78 ± 5	0.0037 ± 0.0003
Handle loop: 25b / Term loop 1: 25a	92 ± 6	599 ± 12	6.5 ± 0.4	510 ± 11	0.0243 ± 0.0006
Handle loop: 35 / Term loop 1: 35	123 ± 5	5100 ± 50	41 ± 2	4980 ± 52	0.238 ± 0.004
Handle loop: 15b / Term loop 2: 15	67 ± 7	107 ± 8	1.6 ± 0.2	40 ± 7	0.0019 ± 0.0003
Handle loop: 25b / Term loop 2: 25	166 ± 8	359 ± 8	2.16 ± 0.11	193 ± 8	0.0092 ± 0.0004
Handle loop: 35 / Term loop 2: 35	307 ± 9	1015 ± 13	3.31 ± 0.11	710 ± 14	0.0339 ± 0.0008
Term loop 1: 15b / Term loop 2: 15	43 ± 6	114 ± 6	2.7 ± 0.4	71 ± 5	0.0034 ± 0.0002
Term loop 1: 25b / Term loop 2: 25	243 ± 6	42 ± 5	0.17 ± 0.02	-201 ± 3	-0.0096 ± 0.0002
Term loop 1: 35 / Term loop 2: 35	300 ± 8	103 ± 6	0.34 ± 0.02	-197 ± 7	-0.0094 ± 0.0003
Handle loop: 15a	318 ± 6	69 ± 5	0.22 ± 0.02	-249 ± 3	-0.0119 ± 0.0002
Handle loop: 25a	91 ± 5	155 ± 5	1.69 ± 0.11	63 ± 2	0.00303 ± 0.00010
Terminator loop 1: 15b	47 ± 5	143 ± 6	3.1 ± 0.4	96 ± 4	0.0046 ± 0.0002
Terminator loop 1: 25b	58 ± 5	107 ± 5	1.8 ± 0.2	49 ± 2	0.00234 ± 0.00012

Table C.2: Quantifying ON state, OFF state, fold change, and dynamic range for gRNA insert studies, 2 nM aTc.

Table C.2: Quantifying ON state, OFF state, fold change, and dynamic range for gRNA insert studies, 2 nM aTc (cont'd). ON = (cgRNA, no trigger) – AF; OFF = (cgRNA + cognate trigger) – AF; fold change = OFF/ON; dynamic range = OFF–ON; fractional dynamic range = [OFF–ON]/[ideal OFF – ideal ON]. Ideal values correspond to a standard gRNA for ideal ON and a no-target gRNA for ideal OFF. Autofluorescence values (AF) were 106 ± 10 (panel a), 85 ± 8 (panel b), and 87 ± 5 (panel c). Mean \pm estimated standard error (with uncertainty propagation) based on the mean single-cell fluorescence over 20,000 cells for each of $N = 3$ replicate wells.

cgRNA	ON	OFF	Fold Change	Dynamic Range	Fractional Dynamic Range
a					
Ideal 1	47 ± 15	22 600 ± 800	480 ± 150	22 500 ± 800	1
5' extension: 15	22 ± 10	125 ± 11	6 ± 3	103 ± 4	0.0046 ± 0.0002
5' extension: 25	22 ± 10	138 ± 10	6 ± 3	116 ± 3	0.0051 ± 0.0002
5' extension: 35	32 ± 11	83 ± 10	2.6 ± 1.0	52 ± 4	0.0023 ± 0.0002
Handle loop: 15b	50 ± 11	37 ± 10	0.7 ± 0.3	-13 ± 4	-0.0006 ± 0.0002
Handle loop: 25b	33 ± 11	90 ± 10	2.8 ± 1.0	57 ± 4	0.0025 ± 0.0002
Handle loop: 35	30 ± 11	230 ± 14	8 ± 3	199 ± 10	0.0089 ± 0.0005
Terminator loop 1: 15a	16 ± 10	67 ± 11	4 ± 3	51 ± 4	0.0023 ± 0.0002
Terminator loop 1: 25a	19 ± 10	64 ± 10	3 ± 2	45 ± 2	0.0020 ± 0.0001
Terminator loop 1: 35	21 ± 10	168 ± 10	8 ± 4	147 ± 3	0.0065 ± 0.0003
Terminator loop 2: 15	32 ± 10	25 ± 10	0.8 ± 0.4	-8 ± 3	-0.00034 ± 0.00015
Terminator loop 2: 25	56 ± 10	122 ± 11	2.2 ± 0.4	66 ± 4	0.0029 ± 0.0002
Terminator loop 2: 35	48 ± 10	55 ± 11	1.1 ± 0.3	6 ± 4	0.0003 ± 0.0002
b					
Ideal 2	64 ± 12	22 900 ± 1200	360 ± 70	22 800 ± 1200	1
5' extension: 15 / Handle loop: 15a	50 ± 6	197 ± 5	4.0 ± 0.5	148 ± 7	0.0065 ± 0.0005
5' extension: 25 / Handle loop: 25a	56 ± 3	529 ± 4	9.5 ± 0.5	473 ± 4	0.0207 ± 0.0011
5' extension: 35 / Handle loop: 35	40 ± 4	508 ± 3	12.6 ± 1.3	467 ± 4	0.0205 ± 0.0011
5' extension: 15 / Term loop 1: 15a	59 ± 3	270 ± 7	4.5 ± 0.2	211 ± 7	0.0092 ± 0.0006
5' extension: 25 / Term loop 1: 25	64 ± 3	326 ± 7	5.1 ± 0.3	263 ± 6	0.0115 ± 0.0007
5' extension: 35 / Term loop 1: 35	91 ± 3	476 ± 5	5.2 ± 0.2	385 ± 5	0.0169 ± 0.0009
5' extension: 15 / Term loop 2: 15	32 ± 4	163 ± 4	5.0 ± 0.6	131 ± 5	0.0057 ± 0.0004
5' extension: 25 / Term loop 2: 25	76 ± 2	318 ± 7	4.2 ± 0.2	242 ± 7	0.0106 ± 0.0007
5' extension: 35 / Term loop 2: 35	148 ± 3	187 ± 10	1.26 ± 0.07	39 ± 10	0.0017 ± 0.0005
c					
Ideal 3	50 ± 20	23 700 ± 400	500 ± 200	23 600 ± 400	1
Handle loop: 15b / Term loop 1: 15a	50 ± 20	110 ± 20	2.1 ± 0.8	57 ± 2	0.00240 ± 0.00011
Handle loop: 25b / Term loop 1: 25a	50 ± 20	450 ± 20	9 ± 3	398 ± 6	0.0168 ± 0.0004
Handle loop: 35 / Term loop 1: 35	90 ± 20	5600 ± 120	65 ± 13	5520 ± 120	0.234 ± 0.007
Handle loop: 15b / Term loop 2: 15	40 ± 20	60 ± 20	1.5 ± 0.7	20 ± 5	0.0008 ± 0.0002
Handle loop: 25b / Term loop 2: 25	130 ± 20	230 ± 20	1.8 ± 0.3	104 ± 15	0.0044 ± 0.0006
Handle loop: 35 / Term loop 2: 35	190 ± 20	630 ± 20	3.3 ± 0.3	435 ± 15	0.0184 ± 0.0007
Term loop 1: 15b / Term loop 2: 15	20 ± 20	80 ± 20	4 ± 4	61 ± 3	0.0026 ± 0.0002
Term loop 1: 25b / Term loop 2: 25	190 ± 20	30 ± 20	0.15 ± 0.09	-160 ± 7	-0.0068 ± 0.0003
Term loop 1: 35 / Term loop 2: 35	180 ± 20	70 ± 20	0.36 ± 0.10	-113 ± 5	-0.0048 ± 0.0002
Handle loop: 15a	180 ± 20	40 ± 20	0.20 ± 0.09	-142 ± 5	-0.0060 ± 0.0002
Handle loop: 25a	50 ± 20	80 ± 20	1.4 ± 0.5	23 ± 5	0.0010 ± 0.0002
Terminator loop 1: 15b	20 ± 20	90 ± 20	5 ± 5	71 ± 5	0.0030 ± 0.0002
Terminator loop 1: 25b	20 ± 20	60 ± 20	3 ± 3	36 ± 4	0.0015 ± 0.0002

Table C.3: Quantifying ON state, OFF state, fold change, and dynamic range for gRNA insert studies, 20 nM aTc.

Table C.3: Quantifying ON state, OFF state, fold change, and dynamic range for gRNA insert studies, 20 nM aTc (cont'd). ON = (cgRNA, no trigger) – AF; OFF = (cgRNA + cognate trigger) – AF; fold change = OFF/ON; dynamic range = OFF–ON; fractional dynamic range = [OFF–ON]/[ideal OFF – ideal ON]. Ideal values correspond to a standard gRNA for ideal ON and a no-target gRNA for ideal OFF. Autofluorescence values (AF) were 80 ± 10 (panel a), 68 ± 2 (panel b), and 80 ± 20 (panel c). Mean \pm estimated standard error (with uncertainty propagation) based on the mean single-cell fluorescence over 20,000 cells for each of $N = 3$ replicate wells.

cgRNA	ΔG_{cgRNA}	$\Delta G_{\text{trigger}}$	$\Delta G_{\text{cgRNA:trigger}}$	$\Delta\Delta G_{\text{hybridization}}$
5' extension: 15	-28.87	-25.55	-78.86	-24.44
5' extension: 25	-29.85	-30.95	-94.26	-33.46
5' extension: 35	-30.1	-31.75	-112.23	-50.38
Handle loop: 15a	-31.06	-25.63	-74.67	-17.98
Handle loop: 15b	-26.91	-27.08	-79.05	-25.06
Handle loop: 25a	-31.11	-28.38	-94.37	-34.88
Handle loop: 25b	-27.38	-28.86	-94.52	-38.28
Handle loop: 35	-32.81	-30.43	-113.93	-50.69
Terminator loop 1: 15a	-28.38	-25.52	-75.42	-21.52
Terminator loop 1: 15b	-27.48	-27.23	-77.23	-22.52
Terminator loop 1: 25a	-28.45	-26.93	-92.5	-37.12
Terminator loop 1: 25b	-27.66	-27.19	-92.78	-37.93
Terminator loop 1: 35	-28.62	-28.48	-110.13	-53.03
Terminator loop 2: 15	-27.72	-25.44	-66.31	-13.15
Terminator loop 2: 25	-27.98	-26.22	-84.32	-30.12
Terminator loop 2: 35	-27.89	-26.49	-98.1	-43.72
5' extension: 15 / Handle loop: 15a	-31.14	-29.19	-92.41	-32.08
5' extension: 25 / Handle loop: 25a	-32.18	-34.49	-127.51	-60.84
5' extension: 35 / Handle loop: 35	-34.25	-38.08	-165.03	-92.7
5' extension: 15 / Term loop 1: 15a	-28.46	-26.73	-93.08	-37.89
5' extension: 25 / Term loop 1: 25	-29.32	-32.78	-125.55	-63.45
5' extension: 35 / Term loop 1: 35	-29.8	-35.62	-161.14	-95.72
5' extension: 15 / Term loop 2: 15	-27.81	-28.84	-85.6	-28.95
5' extension: 25 / Term loop 2: 25	-29.04	-32.98	-119	-56.98
5' extension: 35 / Term loop 2: 35	-29.21	-37.63	-150.75	-83.91
Handle loop: 15b / Term loop 1: 15a	-26.46	-29.31	-92.84	-37.07
Handle loop: 25b / Termloop 1: 25a	-26.93	-35.73	-125.38	-62.72
Handle loop: 35 / Term loop 1: 35	-32.49	-40.09	-162.42	-89.84
Handle loop: 15b / Term loop 2: 15	-25.85	-31.51	-85.91	-28.55
Handle loop: 25b / Term loop 2: 25	-26.59	-35.49	-119.39	-57.31
Handle loop: 35 / Term loop 2: 35	-31.92	-39.23	-152.59	-81.44
Term loop 1: 15b / Term loop 2: 15	-26.44	-28.98	-82.29	-26.87
Term loop 1: 25b / Term loop 2: 25	-26.91	-33.38	-115.86	-55.57
Term loop 1: 35 / Term loop 2: 35	-27.75	-36.22	-146.99	-83.02

Table C.4: Free energy of cgRNA/trigger complexes and trigger hybridization for candidate cgRNAs with single and double inserts predicted via NUPACK analysis. $\Delta\Delta G$ values calculated using NUPACK analysis with RNA in 1 M Na⁺ at 37 °C,³⁸ $\Delta\Delta G_{\text{hybridization}} = \Delta G_{\text{cgRNA:trigger}} - [\Delta G_{\text{cgRNA}} + \Delta G_{\text{trigger}}]$.

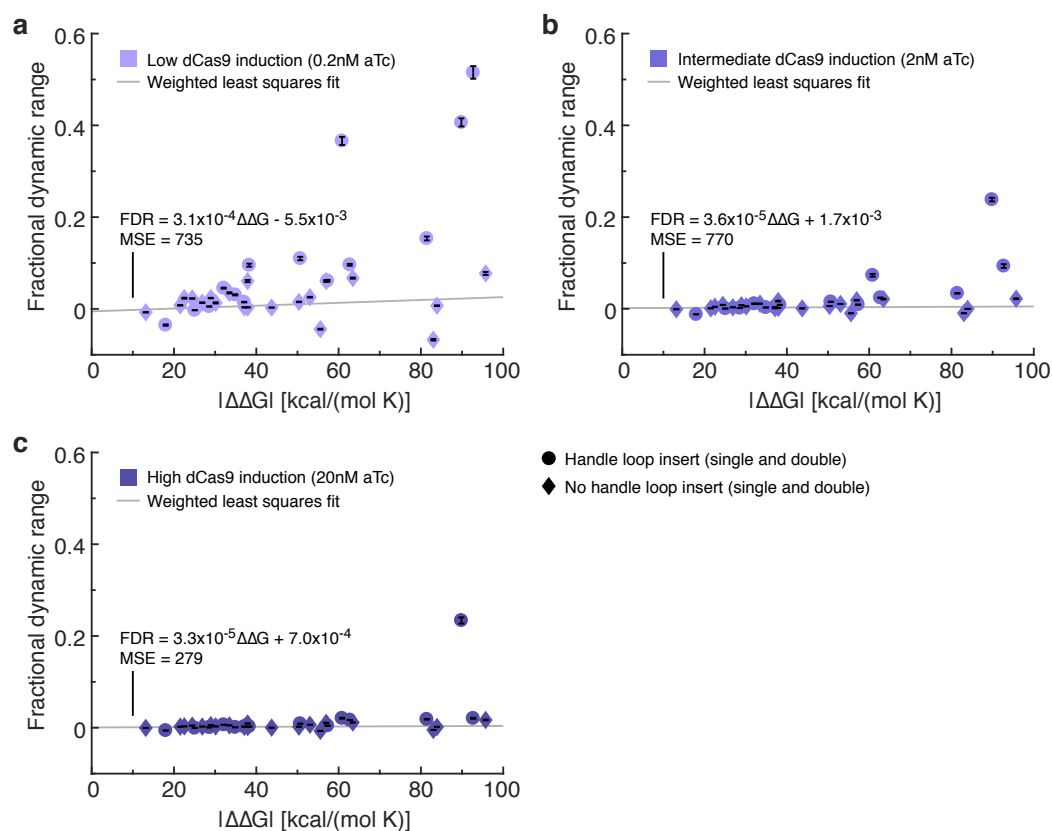


Figure C.1: Fractional dynamic range vs predicted $\Delta\Delta G$ of trigger binding for all single and double insert candidate cgRNAs. (a) 0.2 nM aTc induction of dCas9. (b) 2 nM aTc induction of dCas9. (c) 20 nM aTc induction of dCas9. Fractional dynamic range is higher for cgRNA:trigger pairs with high $|\Delta\Delta G|$, but is reduced with increased dCas9 induction. $\Delta\Delta G$ values calculated using NUPACK analysis (RNA in 1 M Na^+ at 37 °C,³⁸ $\Delta\Delta G = \Delta G_{\text{cgRNA:trigger}} - [\Delta G_{\text{cgRNA}} + \Delta G_{\text{trigger}}]$). Slope of fitted line and mean squared error (MSE) indicate a weaker effect of trigger as compared to analysis with handle loop insert containing candidate cgRNAs only (Figure 3.4). Fractional dynamic range: mean \pm estimated standard error based on $N = 3$ replicate wells with uncertainty propagation. Fitted lines calculated using least squares regression weighted by inverse estimate of variance of the mean.¹¹⁸

Appendix D

SUPPLEMENTARY FIGURES AND DATA FOR CHAPTER 4

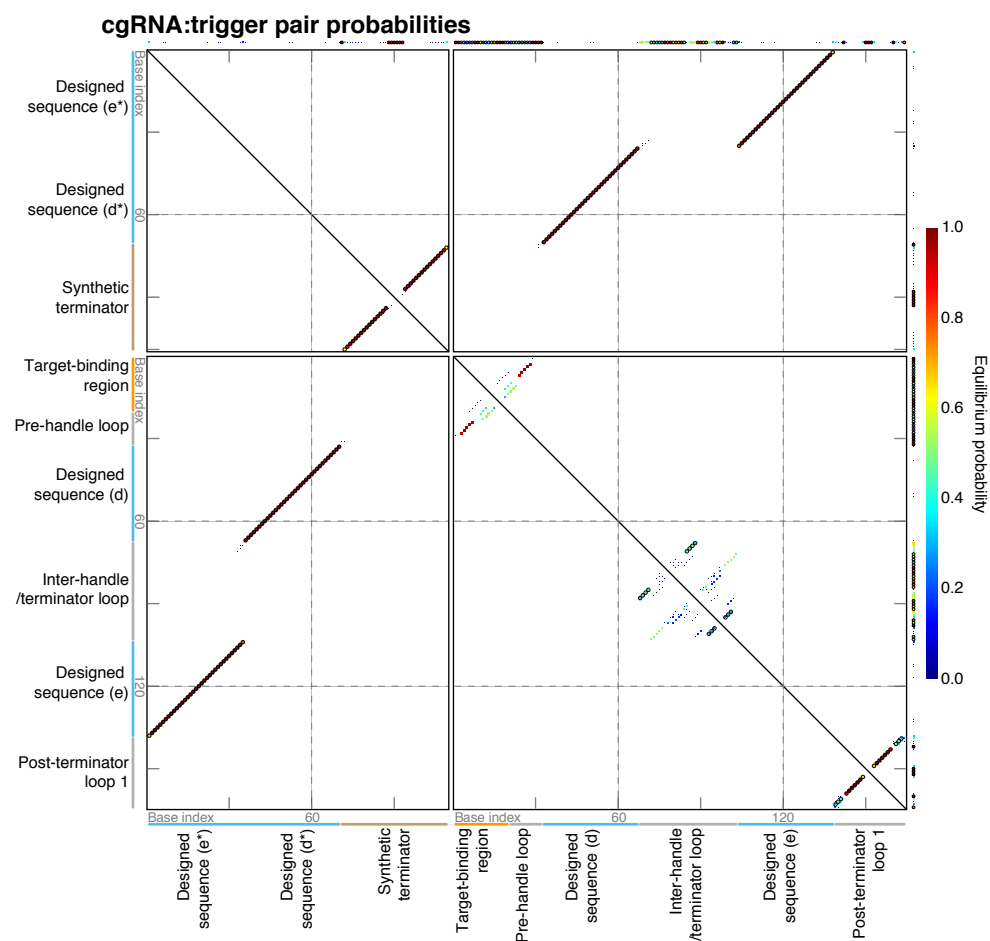


Figure D.1: Analysis of design quality by equilibrium pair probability for splinted switch cgRNA:trigger X_A duplex.^{34,35} Nucleotides shaded and scaled to indicate the probability of adopting the depicted base-pairing state at equilibrium. Pairing states in the target structure indicated with black circles. For this design, all on-target complexes are predicted to form with quantitative yield at the 10 nM target concentration, but some nucleotides have unwanted base-pairing interactions (circled pairs not shaded dark red, uncircled pairs with significant pair probability), notably the low-probability of the target constrained (orange) and dCas9 constrained (grey) sequence adopting their intended structure. For the cgRNA:trigger complex, constrained sequence was assigned the lowest weight ($w=0$) for design; here, the designed sequence appears to adopt the intended target structure with high probability, and as such, this design was selected for experimental characterization.

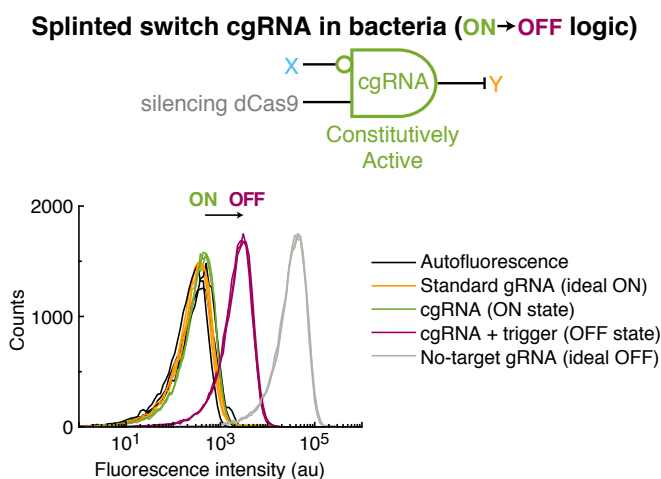


Figure D.2: Flow cytometry replicates for splinted switch ON state, OFF state, and conditional response in *E. coli*. Single-cell fluorescence intensities. Expression of RNA trigger X toggles the cgRNA from ON→OFF, leading to an increase in fluorescence. Induced expression (aTc) of silencing dCas9 and constitutive expression of sfGFP target gene Y and either: standard gRNA (ideal ON state), cgRNA (ON state), cgRNA + RNA trigger X (OFF state), or no-target gRNA that lacks target-binding region (ideal OFF state). Autofluorescence: cells with no sfGFP. Traces of the same color correspond to $N = 3$ replicate wells assayed on the same day (20,000 cells per well).

cgRNA	ON	OFF	Fold Change	Dynamic Range	Fractional Dynamic Range
Ideal	100 ± 40	35 450 ± 80	300 ± 100	35 350 ± 70	1
cgRNA A	150 ± 40	2270 ± 50	15 ± 4	2120 ± 30	0.0599 ± 0.0008
cgRNA B	140 ± 40	2450 ± 50	18 ± 5	2310 ± 30	0.0654 ± 0.0009
cgRNA C	160 ± 40	1320 ± 70	8 ± 2	1160 ± 60	0.033 ± 0.002

Table D.1: Quantifying ON state, OFF state, fold change, and dynamic range for splinted switch cgRNA in *E. coli*. Autofluorescence (AF) value was 3210 ± 40 . Ideal values correspond to a standard gRNA for ideal ON and a no-target gRNA for ideal OFF. Using silencing dCas9 in *E. coli*: fold change = OFF/ON, dynamic range = OFF–ON, fractional dynamic range = [OFF–ON]/[ideal OFF – ideal ON]. Mean ± estimated standard error (with uncertainty propagation) based on the mean single-cell fluorescence over 20,000 cells for each of $N = 3$ replicate wells.

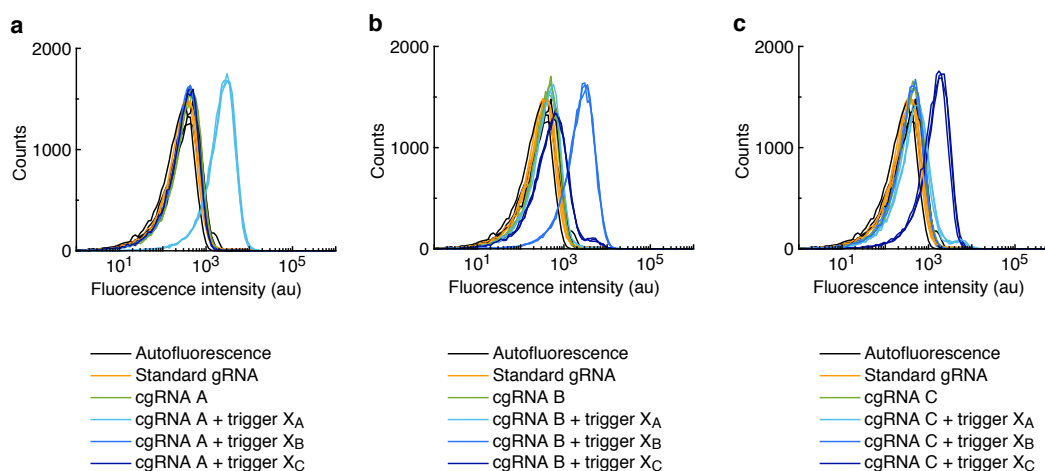


Figure D.3: Flow cytometry replicates for splinted switch orthogonal response in *E. coli*. (a) cgRNA A. (b) cgRNA B. (c) cgRNA C. Single-cell fluorescence intensities. Induced expression (aTc) of silencing dCas9 and constitutive expression of sfGFP target gene Y and either: standard gRNA, cgRNA without trigger, cgRNA + cognate trigger, or cgRNA + a noncognate trigger. Autofluorescence: cells with no sfGFP. Expression of the cognate RNA trigger (X_A for cgRNA A, X_B for cgRNA B, X_C for cgRNA C) toggles the cgRNA from ON→OFF, leading to an increase in fluorescence. Traces of the same color correspond to $N = 3$ replicate wells assayed on the same day (20,000 cells per well).

cgRNA	Trigger	Signal	Crosstalk
A	no trigger	150 ± 40	
A	A	2270 ± 50	1.00 ± 0.02
A	B	110 ± 40	-0.019 ± 0.003
A	C	110 ± 40	-0.021 ± 0.005
B	no trigger	140 ± 40	
B	A	190 ± 40	0.021 ± 0.006
B	B	2450 ± 50	1.00 ± 0.02
B	C	420 ± 40	0.122 ± 0.007
C	no trigger	160 ± 40	
C	A	380 ± 40	0.19 ± 0.02
C	B	150 ± 40	-0.007 ± 0.011
C	C	1320 ± 70	1.00 ± 0.07

Table D.2: Quantifying crosstalk for cognate and non-cognate splinted switch cgRNA/trigger pairs in *E. coli*. Autofluorescence (AF) value was 210 ± 40 . Mean ± estimated standard error (with uncertainty propagation) based on the mean single-cell fluorescence over 20,000 cells for each of $N = 3$ replicate wells.

Appendix E

SUPPLEMENTARY FIGURES AND DATA FOR CHAPTER 5

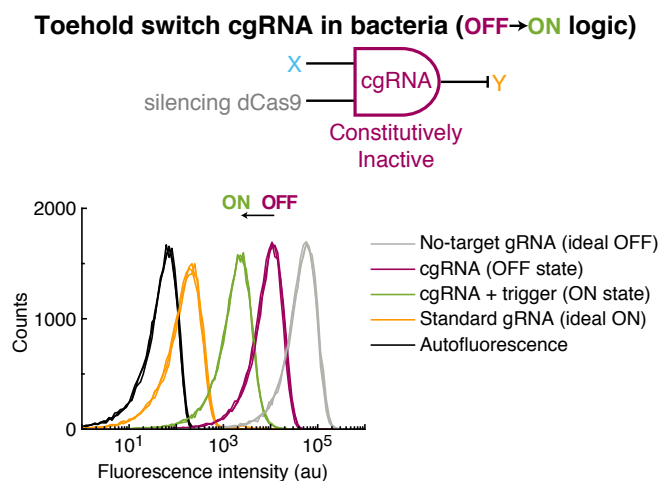


Figure E.1: Flow cytometry replicates for toehold switch ON state, OFF state, and conditional response in *E. coli*. Single-cell fluorescence intensities. Expression of RNA trigger X toggles the cgRNA from OFF→ON, leading to a decrease in fluorescence. Induced expression (aTc) of silencing dCas9 and constitutive expression of mRFP target gene Y and either: no-target gRNA that lacks target-binding region (ideal OFF state), cgRNA (OFF state), cgRNA + RNA trigger X (ON state), or standard gRNA (ideal ON state). Autofluorescence: cells with no mRFP. Traces of the same color correspond to $N = 3$ replicate wells assayed on the same day (20,000 cells per well).

cgRNA	ON	OFF	Fold Change	Dynamic Range	Fractional Dynamic Range
Ideal	340 ± 30	$102\,000 \pm 4000$	300 ± 30	$102\,000 \pm 4000$	1
cgRNA A	4400 ± 200	$18\,400 \pm 400$	4.2 ± 0.2	$14\,000 \pm 500$	0.138 ± 0.007
cgRNA B	$10\,200 \pm 400$	$16\,000 \pm 300$	1.57 ± 0.07	5800 ± 500	0.057 ± 0.005
cgRNA C	4890 ± 110	$15\,300 \pm 500$	3.13 ± 0.12	$10\,400 \pm 500$	0.102 ± 0.006

Table E.1: Quantifying ON state, OFF state, fold change, and dynamic range for toehold switch cgRNA in *E. coli*. Autofluorescence (AF) value was 33 ± 2 . Ideal values correspond to a standard gRNA for ideal ON and a no-target gRNA for ideal OFF. Using silencing dCas9 in *E. coli*: fold change = OFF/ON, dynamic range = OFF–ON, fractional dynamic range = [OFF–ON]/[ideal OFF – ideal ON]. Mean \pm estimated standard error (with uncertainty propagation) based on the mean single-cell fluorescence over 20,000 cells for each of $N = 3$ replicate wells.

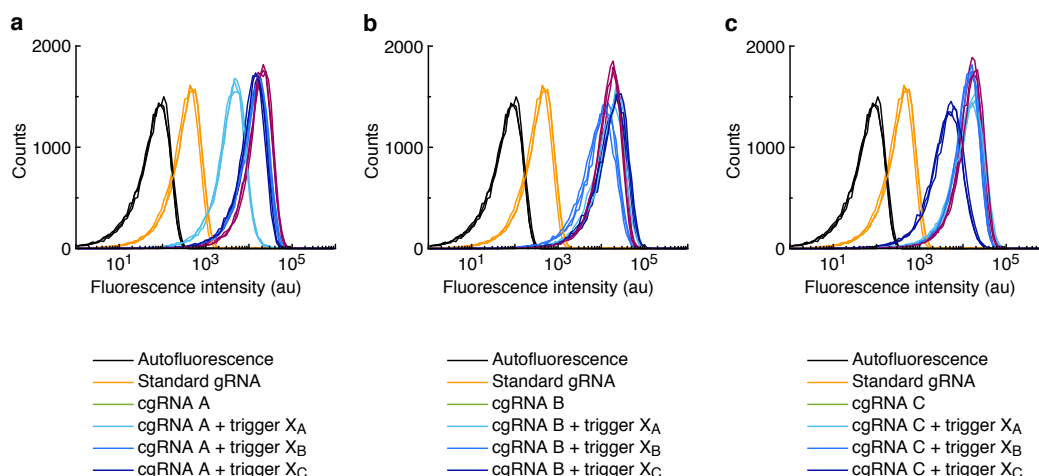


Figure E.2: Flow cytometry replicates for toehold switch orthogonal response in *E. coli*. Flow cytometry fluorescence assay shows selective activation of Toehold Switch cgRNA with expression of cognate RNA trigger. (a) cgRNA A. (b) cgRNA B. (c) cgRNA C. Single-cell fluorescence intensities. Induced expression (aTc) of silencing dCas9 and constitutive expression of mRFP target gene Y and either: standard gRNA, cgRNA without trigger, cgRNA + cognate trigger, or cgRNA + a noncognate trigger. Autofluorescence: cells with no mRFP. Expression of the cognate RNA trigger (X_A for cgRNA A, X_B for cgRNA B, X_C for cgRNA C) toggles the cgRNA from OFF \rightarrow ON, leading to decrease in fluorescence. Traces of the same color correspond to $N = 3$ replicate wells assayed on the same day (20,000 cells per well).

cgRNA	Trigger	Signal	Crosstalk
A	no trigger	18 400 \pm 400	
A	A	4400 \pm 200	1.00 \pm 0.05
A	B	14 100 \pm 300	0.31 \pm 0.04
A	C	12 800 \pm 400	0.40 \pm 0.05
B	no trigger	16 000 \pm 300	
B	A	17 500 \pm 900	-0.3 \pm 0.2
B	B	10 200 \pm 400	1.00 \pm 0.12
B	C	18 500 \pm 600	-0.43 \pm 0.12
C	no trigger	15 300 \pm 500	
C	A	14 000 \pm 500	0.12 \pm 0.07
C	B	13 000 \pm 60	0.22 \pm 0.05
C	C	4890 \pm 110	1.00 \pm 0.06

Table E.2: Quantifying crosstalk for cognate and non-cognate toehold switch cgRNA/trigger pairs in *E. coli*. Autofluorescence (AF) value was 33 ± 2 . Mean \pm estimated standard error (with uncertainty propagation) based on the mean single-cell fluorescence over 20,000 cells for each of $N = 3$ replicate wells.